



TITLE:

STRUCTURE AND PROPERTIES OF HOMOPOLYMER AND COPOLYMERS OF TRIFLUOROETHYLENE(Dissertation_全文)

AUTHOR(S):

Yagi, Toshiharu

CITATION:

Yagi, Toshiharu. STRUCTURE AND PROPERTIES OF HOMOPOLYMER AND COPOLYMERS OF TRIFLUOROETHYLENE. 京都大学, 1980, 工学博士

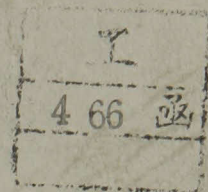
ISSUE DATE:

1980-01-23

URL:

<https://doi.org/10.14989/doctor.r4071>

RIGHT:



**STRUCTURE AND PROPERTIES
OF HOMOPOLYMER AND COPOLYMERS
OF TRIFLUOROETHYLENE**

TOSHIHARU YAGI

1979

**STRUCTURE AND PROPERTIES
OF HOMOPOLYMER AND COPOLYMERS
OF TRIFLUOROETHYLENE**



TOSHIHARU YAGI
1979

CONTENT

GENERAL INTRODUCTION	1
CHAPTER 1	
POLYMERIZATION OF TRIFLUOROETHYLENE, AND COPOLYMERIZATION OF TRIFLUOROETHYLENE WITH VINYLIDENE FLUORIDE, TETRAFLUOROETHYLENE, CHLOROTRIFLUOROETHYLENE AND HEXAFLUORO- PROPYLENE	13
1-1 Introduction	14
1-2 Polymerization of Homopolymer and Copolymer of Trifluoroethylene	14
1-3 Monomer Reactivity Ratios of Copolymer System	16
References	18
CHAPTER 2	
MICROSTRUCTURE OF POLY(TRIFLUOROETHYLENE) CHAIN: HIGH RESOLUTION FLUORINE-19 NMR AND MONTE CARLO SIMULATION	19
2-1 Introduction	20
2-2 High Resolution Fluorine-19 NMR Study	21
2-3 Change of Microstructure (Theoretical Treatment)	25
2-4 Reactivity Ratio of Head- and Tail-position of Trifluoroethylene Monomer	29
2-5 Application to Poly(vinylidene Fluoride)	33
References	37

CHAPTER 3	MICROSTRUCTURE OF TRIFLUOROETHYLENE COPOLYMERS WITH VINYLIDENE FLUORIDE, TETRAFLUOROETHYLENE, CHLOROTRIFLUOROETHYLENE AND HEXAFLUOROPROPYLENE: HIGH RESOLUTION FLUORINE-19 NMR MEASUREMENT	39
3-1	Introduction	40
3-2	Monomer Sequence Distribution	41
3-3	High Resolution Fluorine-19 NMR Study of Vinylidene Fluoride - Trifluoroethylene copolymers	46
3-3-1	NMR Assignment	46
3-3-2	Monomer Sequence Distribution, Estimated by NMR Results	59
	References	63
CHAPTER 4	CRYSTALLIZATION BEHAVIOR OF POLY(TRIFLUORO- ETHYLENE)	65
4-1	Introduction	66
4-2	Experimental	67
4-3	Electron Micrograph	68
4-4	Equilibrium Melting Temperature	72
4-5	Heat of Fusion	75
4-6	Surface Free Energy of Lamella	78
4-7	Crystallization Kinetics	79
4-8	Analysis of Crystallization Rate	82
	References	85

CHAPTER 5	CRYSTALLIZATION BEHAVIOR OF TRIFLUOROETHYLENE	
	COPOLYMERS: ISOMORPHISM REPLACEMENT	87
5-1	Introduction	88
5-2	Experimental	89
5-3	Melting Temperature of Copolymers	93
5-4	Trifluoroethylene-Vinylidene Fluoride Copolymer	94
5-4-1	Melting Temperature	94
5-4-2	Crystal Form	98
5-5	Trifluoroethylene - Tetrafluoroethylene Copolymers	105
5-6	Trifluoroethylene - Chlorotrifluoroethylene Copolymers	107
5-7	Trifluoroethylene - Hexafluoroethylene Copolymers	109
5-8	Theoretical Treatment of Isomorphism	109
5-9	Melting Temperature versus Polymers Composition	116
	References	118
CHAPTER 6	TRANSITIONS AND RELAXATIONS OF POLY(TRIFLUORO- ETHYLENE)	121
6-1	Introduction	122
6-2	Experimental	123
6-3	Experimental Results	126
6-3-1	Mechanical Relaxations	126
6-3-2	Dielectric Relaxations	126

6-4	Discussion	132
6-4-1	α -transition	132
6-4-2	β -transition	136
6-4-3	Effect of Cold Drawing	141
6-4-4	Effect of Copolymerization	141
6-4-5	Further Comment on Transition	142
6-4-6	Dipole Moment of Repeating Unit	142
6-4-7	Analysis of Dielectric Properties	145
	References	149

CHAPTER 7	TRANSITIONS AND RELAXATIONS OF VINYLIDENE FLUORIDE - TRIFLUOROETHYLENE COPOLYMERS	151
7-1	Introduction	152
7-2	Experimental	153
7-3	Vinylidene Fluoride Rich Copolymers	155
7-4	1 : 1 Copolymers	160
7-5	Transition Map	172
	References	175

CHAPTER 8	DIELECTRIC PROPERTIES OF TRIFLUOROETHYLENE COPOLYMERS	177
8-1	Introduction	178
8-2	Experimental	179
8-3	Dielectric Properties of Vinylidene Fluoride - Trifluoroethylene Copolymers	180

8-3-1	Magnitude of Dipole Moment	183
8-3-2	Position and Direction of Dipole	183
8-3-3	Freedom of Dipole Rotation	184
8-3-4	Crystal Form of Copolymer	186
8-4	Dielectric Properties of Trifluoroethylene Copolymers with Tetrafluoroethylene and Chlorotrifluoroethylene	188
8-5	Piezoelectricity of Trifluoroethylene - Vinylidene Fluoride Copolymers	191
	References	194
	GENERAL CONCLUSION	197
	LIST OF PAPERS	204
	LIST OF PRESENTATIONS	206
	ACKNOWLEDGEMENT	207

GENERAL INTRODUCTION

In science a fortuitous event serves as the genesis of an entirely new area of research. Thus the accidental discovery of poly(tetrafluoroethylene) (PTFE) by Plunkett in 1938 can be envisioned as marking the beginning of fluoropolymer chemistry.^{1,2} The discovery of PTFE, which is still the most chemical and thermal stable polymer known, led to a wide-spread search for other fluoropolymers possessing similar outstanding chemical and physical properties. Since then, many new fluoropolymers have been prepared, and much of these materials have been received attention widely in both chemical and physical aspects because of the superior or unique properties. Most of them, such as PTFE, poly(chlorotrifluoroethylene) (PCTFE), and the copolymer of tetrafluoroethylene (TFE) and hexafluoropropylene (HFP), are extremely stable and inert. Some of them prove the special properties as functionalized polymers. For example, poly(vinylidene fluoride) (PVdF) has drawn attention as a new transducer material due to their interesting piezoelectricity and pyroelectricity properties.³⁻⁶

The principle general value of studying the fluoropolymer is the great variability in properties that can be achieved. Not unexpectedly, a great deal of this research has been directed to synthesis and properties of fluorinated ethylene polymers varying fluorine content, i.e., PTFE, PCTFE, PVdF, and poly(vinyl fluoride) (PVF). Many works also have been directed to the copolymerization studies involving TFE, chlorotrifluoroethylene (CTFE), and vinylidene fluoride (VdF) in copolymer chain.

However, comparatively little research has been devoted to the synthesis, characterization, structure, and properties of polytrifluoroethylene (PTrFE) and trifluoroethylene (TrFE) copolymers. The reason for the lack of interests in PTrFE and TrFE-copolymers compared to other fluorinated ethylene polymers probably can be ascribed to two factors: (1) the lack of, or the difficulty in obtaining the TrFE-monomer and PTrFE polymer, and (2) the chemical and thermal unstabilities of PTrFE compared to PTFE and PCTFE. In early days, the main aim of fluoropolymer study is designed for chemically inert and themally stable polymers. Recently this situation has been changing because of seeking the new polymers having unique and special properties as a functionalized polymer. Therefore, it is of great interest and importance to studying properties of the homopolymer and many kinds of copolymers of this compound.

In this thesis, the preparation, structure, and properties of PTrFE, and the copolymers of TrFE with VdF, TFE, CTFE, and HFP are described. PTrFE is a tough, while solid polymer with high molecular weight and high crystallinity. Naylar and Lasoski⁷ reported the microstructure of PTrFE for the first time. However, they studied only the chemical shifts in the structure $-\text{CF}_2-\text{CFH}-\text{CF}_2-$ and $-\text{CFH}-\text{CF}_2-\text{CFH}-$, and gave no comments on the microstructure. Wilson⁸ predicated the presence of both head-to-head and tactic defects in the polymer chain. However, the NMR spectrum was not analyzed in detail. PTrFE is

classified as a highly crystalline polymer similar to other fluorinated ethylene polymers. However, the crystal form of PTrFE has not been established yet. There are some reports claiming that the crystal form is hexagonal and main chain takes helical conformation in crystal.^{9,10} A study on the crystallization behavior in PTrFE has not been reported at all. The melting temperature, heat of fusion, heat of entropy, morphology of crystal, surface free energy of lamella, and kinetic rate of the crystallization are very important parameters of crystallization, since bulk properties of solid polymers are largely effected by the transition from the amorphous to the crystalline state. Recently, Choy and coworker¹¹ reported the relaxation of PTrFE for the first time. However, the spectrum was not analyzed in detail. There exist still some problems as to the nature of transitions and relaxations in PTrFE because of its complicated solid state structure. For example, attempts to describe the crystallinity dependence on the transition peaks have not been successful.

Nothing has been reported on the copolymerization of TrFE with VdF, TFE, CTFE and HFP. These are new polymers in macromolecular field, and proved the unique and superior properties. The copolymers of both TrFE-VdF and TrFE-TFE are in crystalline state in whole range of polymer composition, and crystallized isomorphically. Especially, the TrFE-TFE copolymers show a linear melting temperature - polymer

composition relationships. However, not a single study has been reported on the isomorphism replacement theoretically in the base of thermodynamics yet. In the Flory's theory¹² of copolymer crystallization, it is assumed that in the crystallization of A and B units the crystal phase is composed entirely of A units, and B units are excluded from the crystal phase and remained in the amorphous phase. Therefore, this theory can not be applied to the isomorphism replacement.

The dielectric constant ϵ' of the TrFE-VdF and TrFE-TFE copolymers does not change linearly with polymer composition, but takes maximum at the middle point of polymer composition. Especially, the value of ϵ' of the 1 : 1 TrFE-VdF copolymer is about 15 (1 kHz and 22°C), and about 1.8 times larger than that of PVdF. PVdF has been distinguished among the crystalline polymers by a high dielectric constant as $\epsilon' = 8.5$ (1 kHz and 22°C).

Recently, PVdF has drawn attention as a new transducer material because of their interesting piezoelectricity and pyroelectricity.^{4,5} There are many reports which are claiming that these properties are closely correlated with the existence of an oriented dipole structure in crystal.^{5,13} Therefore, the high ϵ' material⁵ are desirable for these purposes.

It was mentioned that the high value of the dielectric constant of semicrystalline polymer depends on (1) the magnitude of dipole moment of repeating units, (2) the position and

direction of dipole with respect to the chain backbone, (3) the freedom of the dipole rotation in the electric field, and (4) the crystal form of polymer, i.e., a possibility of a spontaneous polarization in crystal.

In this thesis, studies, on synthesis, microstructure, crystallization behavior and molecular transitions of the homopolymer and some kinds of the copolymers of TrFE performed by the present author since 1975, are described in the following eight chapters.

In chapter 1, the polymerization of PTrFE and the copolymerizations of TrFE with VdF, TFE, CTFE, and HFP are described. The monomer reactivity ratios of these copolymers obtained from the Fineman and Ross method¹⁴ are also reported.

In chapter 2, the microstructure and the reactivity ratios of head- and tail-position of TrFE-monomer and VdF-monomer are described. The microstructure of PTrFE molecule is investigated by high resolution fluorine-19 NMR measurement. The assignment of NMR peaks is based on empirical method.¹⁵ The estimation of backward-added monomer units and their distribution in the polymer chain is made by applying the Monte Carlo simulation to NMR data. The distribution of the backward-added monomer units can be obtained from the reactivity ratios of the head- and tail-position of monomer. It is evident that only the assignment of NMR peaks is not sufficient to estimate the microstructure of polymer. For instance, the sequences of the

tail-to-head addition is detected as a head-to-tail addition in the NMR spectrum. The NMR spectrum reflects only a limited local structure.

In chapter 3, the microstructure and comonomer sequence distribution of the TrFE copolymers with VdF, TFE, CTFE and HFP are described. The normalized monomer-diad and -triad fractions as a function of polymer composition are obtained from the comonomer-sequence distribution theory suggested by Ito and Yamashita.¹⁶ The microstructure of these copolymers is examined by means of high resolution fluorine-19 NMR. The assignment of NMR peaks is also based on empirical method.¹⁵ In the TrFE-VdF copolymer system, the normalized monomer diad fraction as a function of polymer composition is also obtained from the NMR line-intensity relationships, and compared to the results of the calculated ones.

In chapter 4, the crystallization behavior of PTrFE molecule is described. This chapter deals primarily with the crystal morphology, the equilibrium melting temperature, the heat of fusion and entropy, the surface free energy of lamellar crystal, and the crystallization rate of PTrFE polymer. The crystal morphology is observed by means of electron microscope. Sample is prepared by replication method. The equilibrium melting temperature is determined by the Hoffman and Weeks plot.¹⁷ The heat of fusion is obtained from the depression of the melting temperature by changing the volume fractions of diluent,

or by changing the fraction of second component in the copolymer.^{12,18} The surface free energy of lamellar crystal is determined graphically by the plot of melting temperature versus reciprocal lamellar thickness. The lamellar thickness of crystal is estimated by use of small angle x-ray diffraction measurement. The crystallization kinetic is studied by means of calorimetric method using the Avrami equation.²⁰

In chapter 5, the crystallization behaviors of the TrFE copolymers with VdF, TFE, CTFE and HFP are described. The crystal properties of these copolymers are investigated by use of DSC, x-ray diffraction and infrared measurements. This chapter deals with the theory of isomorphism replacement on the base of thermodynamics. The theoretical result is compared to the experimental one obtained by DSC study of the TrFE-TFE copolymer system.

In chapter 6, the transitions and relaxations of PTrFE are described. The mechanical relaxation measurements are carried out in the region of -150 to 100°C and various frequencies up to 110 Hz. The influence of crystallinity, molecular weight, cold drawing, and copolymerization on mechanical properties are discussed. The dielectric properties are measured in the region of -150 to 100°C and various frequencies up to 300 kHz. For the evaluation of the dielectric properties of PTrFE molecule, the Froelich-Kirkwood theory²⁰ is employed.

In chapter 7, the transition and relaxation behaviors of

the TrFE-VdF copolymers are described. These are also examined by means of mechanical and dielectric measurements as well as those PTrFE molecule, in the region of -150 to 100 °C and at various frequencies. This study deals with the 1 : 1 TrFE-VdF copolymers and VdF-rich copolymers. The glass-to-rubber transition of the 1 : 1 TrFE-VdF copolymer is determined by means of thermal expansion measurement.

In chapter 8, the dielectric properties of the TrFE copolymers with VdF, TFE and CTFE are described. The dielectric properties of the TrFE-VdF copolymers are discussed in terms of (1) the magnitude of dipole moment of repeating units , (2) the position and direction of dipole with respect to the chain backbone, (3) the freedom of the dipole rotation, and (4) the crystal form of the TrFE-VdF copolymers.

In the end, conclusion of the respective chapters is summarized with particular emphasis on the fundamental studies of PTrFE, the TrFE-VdF copolymers and the TrFE-TFE copolymers. And several points necessary for further detailed investigation and possibilities of practical applications are also described.

REFERENCES

1. P.J. Plunkett, U.S. Patent 2,230,654 (1941).
2. W.E. Hanford and R.M. Joyce, J. Amer. Chem. Soc., 68, 2082 (1946).
3. H. Kawai, Japan J. Appl. Phys., 8, 975 (1969).
4. E. Fukada and S. Takahashi, Japan J. Appl. Phys, 8, 960 (1969).
5. R. Hayakawa and Y. Wada, Advances in Polymer Science, 11, 1 (1971).
6. Y. Wada and R. Hayakawa, Japan J. Appl. Phys., 15, 2041 (1976).
7. R.E. Naylor, Jr., and S.W. Lasoski, Jr., J. Polym. Sci., 44, 1 (1960).
8. C.W. Wilson, paper presented at 155 National ACS Meeting, San Francisco, California, 1968. Division of Fluorine Chemistry.
9. E.L. Galperin and Yu.V. Strogalin, Vysokomolekul. Soedin.,, , , Soedin., 7, 16 (1965); Polymer Sci. (USSR) (English transl.), 7, 16 (1965).
10. R.R. Kolda and J.B. Lando, J. Macromol. Sci., -Phys., B11 (1), 21 (1975).
11. C.L. Choy, T.K. Tse, S.M. Tsui and B.S. Hsu, Polymer, 16, 501 (1975).
12. P.J. Flory, "Principle of Polymer Chemistry", Cornell Univ. Press, New York, 1953.

13. K. Nakanura and Y. Wada, J. Polym. Sci., Part-2, 9, 161 (1971).
14. M. Fineman and S.D. Ross, J. Polym. Sci., 5, 259 (1950).
15. C.W. Wilson, III and E.R. Santee, Jr., J. Polym. Sci., Part C, No. 8, 97 (1965).
16. K. Ito and Y. Yamashita, J. Polym. Sci., Part A, 3, 2165 (1965).
17. J.D. Hoffman and J.J. Weeks, J. Res. Natl. Bur. Stand., 66A, 13 (1962).
18. L. Manderkern, "Crystallization of Polymers", McGraw-Hill, New York, 1964.
19. J.I. Lauritzen, Jr., and J.D. Hoffman, J. Res. Natl. Bur. Stand., 64A, 73 (1960).
20. H. Froelich, "Theory of Dielectrics", Oxford Univ. Press, 1958.

CHAPTER *1*

POLYMERIZATION OF TRIFLUOROETHYLENE,
AND COPOLYMERIZATION OF TRIFLUOROETHYLENE
WITH VINYLIDENE FLUORIDE, TETRAFLUOROETHYLENE,
CHLOROTRIFLUOROETHYLENE AND HEXAFLUOROPROPYLENE

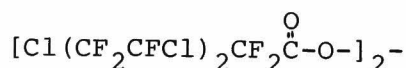
1-1 INTRODUCTION

In this chapter, polymerization of trifluoroethylene [TrFE, $\text{CF}_2=\text{CFH}$], and copolymerization of TrFE with vinylidene fluoride [VdF, $\text{CF}_2=\text{CH}_2$], tetrafluoroethylene [TFE, $\text{CF}_2=\text{CF}_2$], chlorotrifluoroethylene [CTFE, $\text{CF}_2=\text{CFCl}$], and hexafluoropropylene [HFP, $\text{CF}_2=\text{CFCF}_3$] are described. TrFE monomer polymerizes so readily, and has a tendency to form high polymer.¹ Any of methods used for polymerizing the fluorinated ethylene monomers may be used for this monomer. The boiling point of this monomer is -51°C .

TrFE can be copolymerized with all of the fluorinated ethylene monomers.¹ However, copolymerization of TrFE with some fluorinated ethylene monomers has not been reported yet.¹ In this chapter, monomer reactivity ratios obtained from the Fineman and Ross method² are described.

1-2 POLYMERIZATION OF HOMOPOLYMER AND COPOLYMERS OF TRFE

Polytrifluoroethylene [PTrFE, $-(\text{CF}_2-\text{CFH})_n-$], and the copolymers of TrFE with VdF, TFE, CTFE and HFP were prepared by the bulk polymerization at 22°C using 3,5,6-trichloroperfluorohexanoyl peroxide as initiator.



The polymerization was stopped at a low conversion, under 20%, so as to estimate the exact polymer composition. The polymer

composition of these copolymers was determined by carbon element analysis. Carbon element analysis was undertaken with a Yanako C,H,N-Corder, type-2. Figure 1 shows the variation in copolymer composition with the composition of the monomer feed for TrFE-VdF, TrFE-TFE, TrFE-CTFE, and TrFE-HFP copolymer systems.

Among these TrFE-copolymers, PTrFE, all of the TrFE-VdF copolymers, 0-17 mol% TFE copolymers, 0-51 mol% CTFE copolymers,

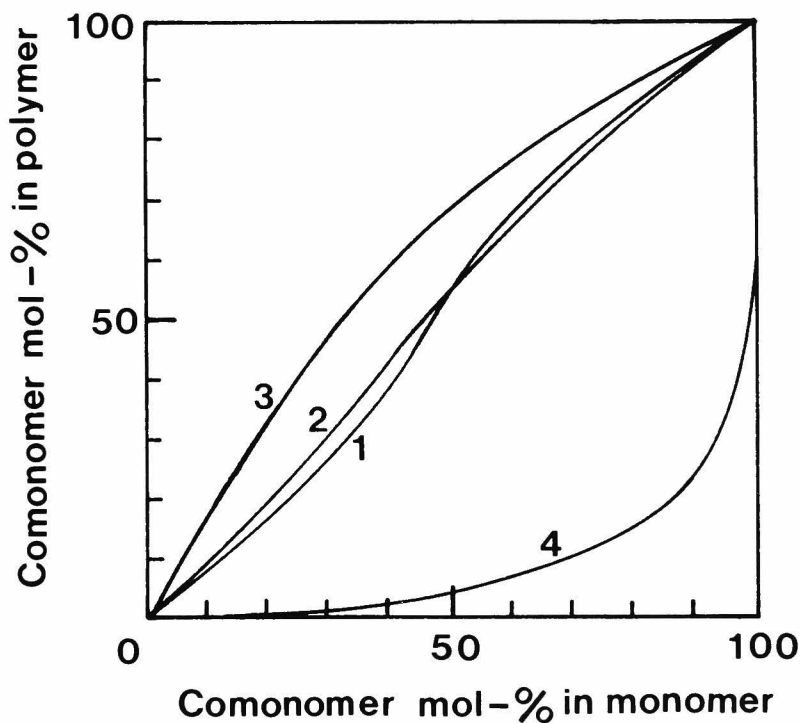


Figure 1. Relationship between polymer and monomer composition for the copolymerization of TrFE with VdF, TFE, CTFE, and HFP: 1, TrFE-VdF; 2, TrFE-TFE; 3, TrFE-CTFE; and 4, TrFE-HFP.

and TrFE-HFP copolymers in the range of polymer composition studied here are soluble in many kinds of solvent, such as acetone, methylethylketone, and dimethylformamide.

1-3 MONOMER REACTIVITY RATIOS

The monomer reactivity ratios (r_A and r_B) for the copolymerization of TrFE with VdF, TFE, CTFE, and HFP were obtained from the copolymer compositions using the Fineman and Ross method.² The results are tabulated in Table I. The reactivity ratio is a measure of the preference of a given radical for its own monomer rather than the comonomer. If $r_A > 1$ a radical P_A prefers to add monomer M_A , whereas if $r_B < 1$ a radical P_A prefers to add monomer M_B . The condition $r_A r_B = 1$ is defined

Table I. List of monomer reactivity ratios (r_A and r_B) for copolymerization of TrFE with VdF, TFE, CTFE, and HFP, at 22 °C.

System	r_A (TrFE)	r_B (comonomer)
TrFE-VdF	0.5	0.7
TrFE-TFE	0.75	0.95
TrFE-CTFE	0.5	2.0
TrFE-HFP	20.0	0.01

as an "ideal copolymerization", and gives a random copolymer. The condition $r_A r_B = 0$ implies that each of the radicals P_A and P_B can only react with the opposite monomer and leads to an alternating copolymer. The case in which r_A and r_B are both greater than 1 implies that the monomers tend to homopolymerize simultaneously, and leads to a block copolymer. Most monomers pairs usually copolymerize with reactivity ratios given by $0 < r_A r_B < 1$. Therefore, it is speculated that the copolymers of TrFE-VdF, TrFE-TFE, TrFE-CTFE, and TrFE-HFP are in random structure.

REFERENCES

1. L.A. Wall, "Fluoropolymer", Wiley-Interscience, 1972.
2. M. Fineman and F.M. Ross, J. Polym. Sci., 5, 259 (1950).

CHAPTER 2

MICROSTRUCTURE OF POLY(TRIFLUOROETHYLENE) CHAIN:
HIGH RESOLUTION FLUORINE-19 NMR AND MONTE CARLO
SIMULATION

2-1 INTRODUCTION

Since the high-resolution fluorine-19 NMR study was made by Freguson on vinylidene fluoride (VdF) - hexafluoropropylene copolymers and by Naylor and Lasoski on poly(vinylidene fluoride) (PVdF), there have been published in literature a number of ^{19}F NMR studies¹⁻¹⁵ on the microstructure of fluorinated polymers. The ^{19}F NMR is effective for studying the microstructure of fluorinated polymers, since the fluorine chemical shifts are so large compared with those of proton. In the series of fluorinated ethylene polymers from poly(vinyl fluoride) (PVF) to poly(trifluoroethylene) (PTrFE), the microstructure of PVF^{4,10} and PVdF^{1,3,4,10} have been studied in detail by many authors, while that of PTrFE,^{1,7} by only a few. The first work on PTrFE was that of Naylor and Lasoski.¹ They studied the chemical shifts in the structure $-\text{CF}_2-\text{CFH}-\text{CF}_2-$ and $-\text{CFH}-\text{CF}_2-\text{CFH}-$, but gave no comments on microstructure. The work of Wilson indicated the presence of both head-to-tail and head-to-head linkages and tacticity defects in the PTrFE chain.⁷

On the other hand, Tedder and his coworkers^{16,17} studied the reactivity ratios of head- and tail-positions of vinyl fluoride (VF), VdF, and trifluoroethylene (TrFE) to methyl radical ($\text{CH}_3\cdot$) and fluorinated methyl radicals ($\text{CFH}_2\cdot$, $\text{CF}_2\text{H}\cdot$ and $\text{CF}_3\cdot$), in the gaseous state at a high temperature. They reported that the regularity of reaction position decreased in the order, VdF, VF, and TrFE.

The purpose of this chapter is, first, to assign the ^{19}F

NMR peaks of PTrFE and, second to estimate the amount of backward-added monomer units and their distribution in the polymer chain by applying Monte Carlo simulation to NMR data. This distribution is represented by reactivity ratios of the head- and tail-positions in the monomer. Only the assignment of NMR peaks and comparison of their intensity ratios are not sufficient to estimate the microstructure. For instance, the long sequence of the tail-to-head addition is also detected as a head-to-tail addition in the NMR spectrum. The NMR spectrum reflects only a limited local structure.

2-2 HIGH RESOLUTION FLUORINE-19 NMR STUDY

Figure 1 shows the 56.45 MHz high resolution fluorine-19 NMR spectrum of PTrFE in the $-\text{CF}_2-$ region. The spectrum was measured with a Hitachi-Perkin-Elmer R-20B spectrometer at 35 °C in acetone, using benzotrifluoride (BTF) as an internal reference. In the figure, the main peaks are designated as H, I, and J (in the order of increasing magnetic field). The magnetic field scale is given in parts per million (ppm) upfield from an BTF internal resonance. The chemical shifts are expressed by adding 63.7 ppm to each original values.

Let us consider the polymerization mechanism of TrFE. If the addition of the monomer $\text{CFH}=\text{CF}_2$ to growing chain end occurs in either a forward or backward manner to form a new end $---\text{CFH}-\text{CF}_2\cdot$ or $---\text{CF}_2\text{CFH}\cdot$, respectively, the following four

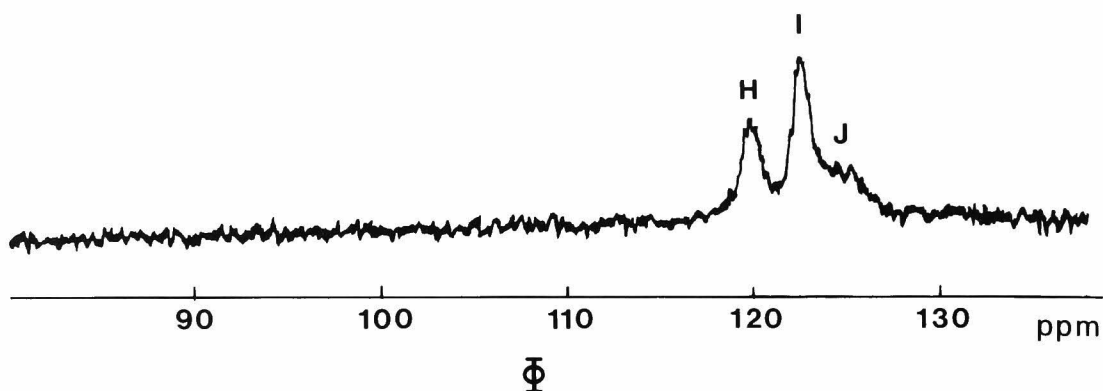


Figure 1. High-resolution fluorine-19 NMR spectrum of PTrFE at 56.45 MHz and 35 °C in acetone. BTF is the internal reference and the chemical shifts are expressed by adding 63.6 ppm to each original value.

types of microstructure will be generated as a part of a chain consisting of one central $-\text{CF}_2-$ group and its two front and rear groups.

- | | |
|---------|---|
| st. (1) | $-\text{CF}_2-\text{CFH}-\text{CF}_2-\text{CFH}-\text{CF}_2-$ |
| st. (2) | $-\text{CFH}-\text{CFH}-\text{CF}_2-\text{CFH}-\text{CF}_2-$ |
| st. (3) | $-\text{CF}_2-\text{CFH}-\text{CF}_2-\text{CF}_2-\text{CFH}-$ |
| st. (4) | $-\text{CFH}-\text{CFH}-\text{CF}_2-\text{CF}_2-\text{CFH}-$ |

If there is no backward addition, the resulting chain should contain only st. (1). The st. (2), (3), and (4) originate from backward-added monomer units, apart from their content and dis-

tribution. As a typical example, let us consider three polymer segments.

segment (a) $\text{-CFH-CF}_2\text{-CFH-CF}_2\text{-CFH-CF}_2\text{-CF}_2\text{-CFH-CFH-CF}_2\text{-CFH-CF}_2\text{-}$

segment (b) $\text{-CFH-CF}_2\text{-CFH-CF}_2\text{-CF}_2\text{-CFH-CF}_2\text{-CFH-CFH-CF}_2\text{-CFH-CF}_2\text{-}$

segment (c) $\text{-CFH-CF}_2\text{-CFH-CF}_2\text{-CF}_2\text{-CFH-CFH-CF}_2\text{-CF}_2\text{-CFH-CFH-CF}_2\text{-}$

Segment (a) has one backward-added monomer unit as underlined, and segment (b) and (c) have two, but with different distributions. It is obvious that an atomic sequence including a central $\text{-CF}_2\text{-}$ group has one of the four microstructures st. (1), (2), (3), and (4) mentioned above. As shown in Figure 1, there are three peaks H, I, and J in ^{19}F NMR spectrum of PTrFE, while the number of microstructures which may correspond to these is four. This suggests that one of the three peaks should correspond to two structures. Taking into account the empirical rule of ^{19}F NMR concerning the relation between chemical shifts and the microstructure⁴, we may expect that four NMR peaks in $\text{-CF}_2\text{-}$ region will align in the order of st. (1), (2), (3), and (4), from low to high magnetic field. Therefore, peak H must be derived from difficult to conceive that these peaks are derived from two st-alone or from st. (3) and (4), respectively. However, it is hard to from conceive that these peak are derived from two structural components. The st. (2), though resembling st. (1) up to the first neighbors of the central $\text{-CF}_2\text{-}$, can not be expected to give the same effect on the ^{19}F NMR chemical shift.⁴ Thus,

Table I. Chemical shifts of carbon triad structure in $-\text{CF}_2-$ region.

Structure	Chemical shift ^a (ppm)	Magnetic field strength (MHz)
$-\text{CH}_2-\text{CF}_2-\text{CH}_2-$	13.3 ^b	30
$-\text{CH}_2-\text{CF}_2-\text{CF}_2-$	36.6 ^b	30
$-\text{CFH}-\text{CF}_2-\text{CFH}-$	38.3 ^b	30
$-\text{CH}_2-\text{CF}_2-\text{CH}_2-$	14.3 ^c	40
$-\text{CF}_2-\text{CF}_2-\text{CF}_2-$	38.4 ^c	40
$-\text{CFH}-\text{CF}_2-\text{CF}_2-$	41.3 ^c	40

^aChemical shifts from trifluoroacetic acid.

^bData taken from ref. 1.

^cData taken from ref. 2.

peak H is tentatively assigned to st. (1). In the same way, peak J is assigned to st. (4). Accordingly, it is expected that peak I is derived from both st. (2) and (3). Table I shows the effect on the ^{19}F NMR chemical shift of $-\text{CH}_2-\text{CF}_2-\text{CH}_2-$, $-\text{CH}_2-\text{CF}_2-\text{CF}_2-$, $-\text{CFH}-\text{CF}_2-\text{CFH}-$, and $-\text{CFH}-\text{CF}_2-\text{CF}_2-$.^{1,2} Considering the difference in the measured magnetic field strength (30 MHz and 40 MHz), it may be expected that the effect on the chemical shift of the $-\text{CFH}-\text{CF}_2-\text{CFH}-$ relative to $-\text{CH}_2-\text{CF}_2-\text{CF}_2-$ is similar, in magnitude, to that of $-\text{CFH}-\text{CF}_2-\text{CF}_2-$. Accordingly, it is ex-

Table II. ^{19}F NMR chemical shifts of PTrFE molecule in $-\text{CF}_2-$ region.

Peak	Chemical shifts ^a (ppm)	Structure	Intensity ^b ratio
H	119.6	$-\text{CF}_2-\text{CFH}-\text{CF}_2-\text{CFH}-\text{CF}_2-$	0.3
I	122.7	$-\text{CFH}-\text{CFH}-\text{CF}_2-\text{CFH}-\text{CF}_2-$	0.5 ^c
J	125.9	$-\text{CF}_2-\text{CFH}-\text{CF}_2-\text{CF}_2-\text{CFH}-$ $-\text{CFH}-\text{CFH}-\text{CF}_2-\text{CF}_2-\text{CFH}-$	0.2

^aThe magnetic field scale is given in parts per million (ppm) upfield from an internal BTF resonance. The chemical shifts are expressed by adding 63.7 ppm to each original values.

^bCalculated from areas and normalized to unity.

^cPeak I is composed of two components; this value is expressed by the sum of two components.

pected that two st. (2) and (3) have the same effect on the ^{19}F NMR chemical shift as the central $-\text{CF}_2-$ group, since they have a common second neighbor structure. Thus, it was decided that both peaks of st. (2) and (3) overlap in the NMR spectrum and are observed as peak I. These results are summarized in Table II.

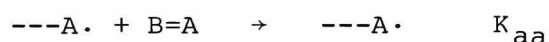
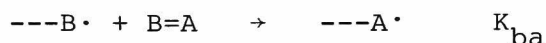
2-3 CHANGE OF MICROSTRUCTURE

Let us denote an unsymmetrical monomer as $\text{B}=\text{A}$, where A represents the head-position and B the tail-position. In the case of PTrFE, the symbol A is CF_2 and B is CFH. There are two pro-

pagating radicals, ---A· and ---B·, and two reaction positions, A and B, in the monomer. In this report, we adopt the copolymerization theory of the conventional terminal model.¹⁸ Denote the kinetic constant by K_{bb} , for the propagating reaction,



Similarly, three other kinetic constants K_{ba} , K_{ab} and K_{aa} are defined for these reactions,



Now, we put $K_{aa}/K_{ba}=x$ and $K_{bb}/K_{ba}=y$, then the parameters x and y represent the relative reactivity ratios of head- and tail-position of unsymmetrical monomer. We represent by $P(BB)$ the probability that a propagating radical ---B· is attached to an A-position and a radical ---B· is again generated. In a similar way, $P(BA)$, $P(AB)$, and $P(AA)$ are defined. Thus, $P(BB)$, $P(BA)$, $P(AB)$, and $P(AA)$ are given by,

$$P(BB) = \frac{K_{bb}(\text{---B}\cdot)(M)}{K_{bb}(\text{---B}\cdot)(M) + K_{ba}(\text{---B}\cdot)(M)} = \frac{y}{y + 1} \quad (1)$$

$$P(BA) = 1 - P(BB) = \frac{1}{y + 1} \quad (2)$$

$$P(AB) = \frac{K_{ab}(\text{---A}\cdot)(M)}{K_{aa}(\text{---A}\cdot)(M) + K_{ab}(\text{---A}\cdot)(M)} = \frac{1}{x + 1} \quad (3)$$

$$P(AA) = 1 - P(AB) = \frac{1}{x + 1} \quad (4)$$

where (M) is the concentration of the monomer, and ($---B\cdot$) and ($---A\cdot$), that of the propagating radicals. If the parameters x and y are determined, we can calculate the relative intensity of each peak in NMR. We simulated many polymers, actually 289 polymers, changing both parameters x and y , in equations (1), (2), (3) and (4), and calculated the intensity of the four possible sequences of 5 letters having A at the middle, as well as the amount of backward added monomer units $-A-B-$.

Figure 2 shows the change in the percentage of forward-added monomer units when numerical values of the two parameters x and y are varied from 0.01 to 100. The degree of polymerization of each polymer was 10000. This range of parameters x and y will cover most cases of practical interest. The percentage of forward-added monomer units becomes large when the parameter x takes on a high value and parameter y , a small value, respectively. On the contrary, this percentage becomes small when x takes on a small value and y , a high value, respectively. Many polymers, having the same amount of forward-added monomer units but different distributions, are derived from combinations of parameters x and y . If both x and y are greater than unity, the microstructure becomes bloky, while x and y are close to unity, it becomes random. When x and y are less than unity, the microstructure becomes alternate.

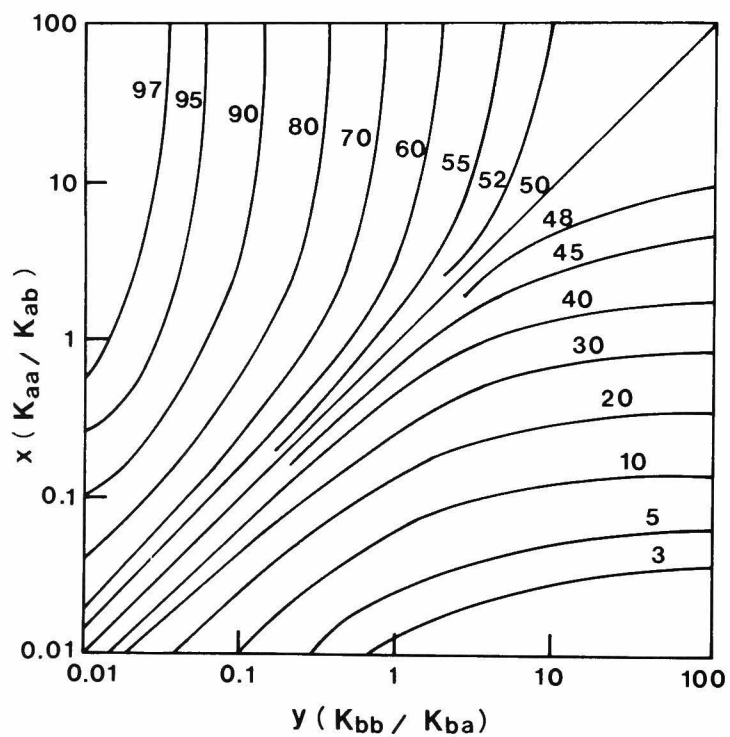


Figure 2. Chnge in the percentage of forward-added monomer-units when the parameters x and y change from 0.01 to 100, respectively. The values of the percentage of forward-added monomer-units are indicated on the diagram.

For example, when both x and y are 100, the percentage of forward-added monomer units is 50 % as shown in Figure 2, and they are distributed blockishly. When x and y are unity, the percentage of forward-added monomer units is 50 %, but they are distributed randomly; when x and y are 0.01, the percentage of forward-added monomer units is again 50 % and these units are distributed alternately. These changes in microstructures are reflected by the intensity of the NMR peaks. Figure 3 shows the change in the fraction of four local microstructures -A-B-A-B-A-, -B-B-A-B-A-, -A-B-A-A-B- and -B-B-A-A-B- when the parameter x ($=y$) changes from 0.01 to 100, for which the percentage of forward-added monomer units is assumed to be 50 %.

2-4 REACTIVITY RATIO OF HEAD- AND TAIL-POSITIONS

We have estimated the microstructure of PTrFE from the standpoint of backward-added monomer units and their distributions in the polymer chain by comparing the polymerized PTrFE with the computer simulated polymers, with respect to the intensity of each peak appearing in the NMR spectrum, i.e., the fraction of each structure which contains 5 carbon atoms along the polymer chain with a $-\text{CF}_2-$ group as the central group. The intensity ratio of polymerized PTrFE is listed in Table II. We select from the simulated 289 polymers one polymer which shows the best fit to this PTrFE. In this way, we found that the

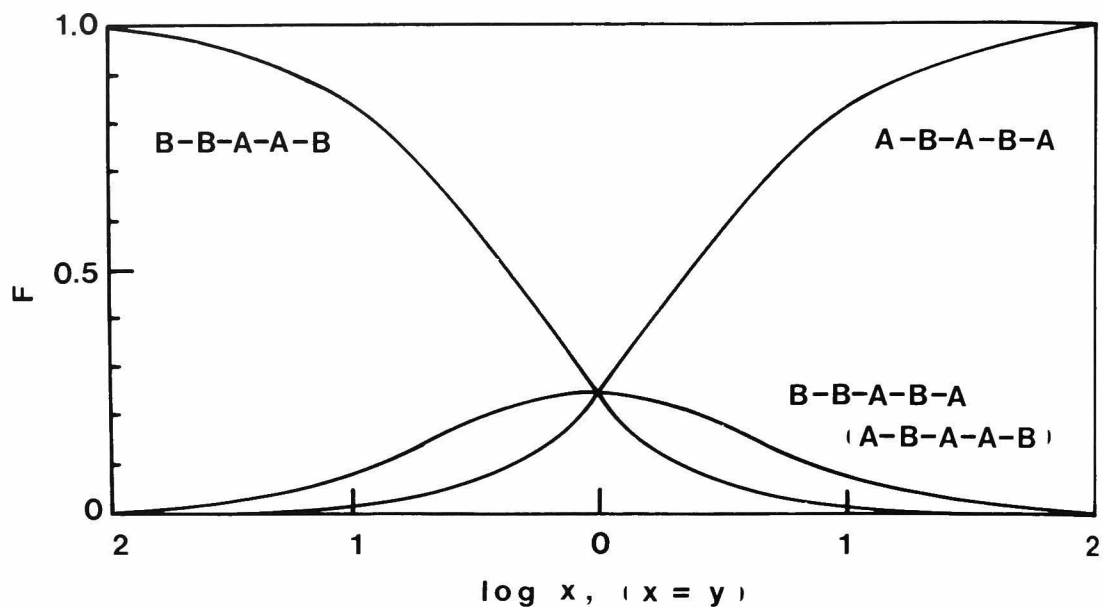


Figure 3. Change in the fraction of four local structures when the parameter x ($=y$) changes from 0.01 to 100; i.e., the percentage of the forward-added monomer-units is assumed to be 50%. The curves -B-B-A-B-A- and -A-B-A-A-B- overlap.

percentage of backward-added monomer units in PTrFE chain polymerized at 22 °C was 50%, and the parameters x and y were 1.33 and 1.33, respectively. Accordingly, denoting the CFH-position and CF_2 -position in TrFE ($\text{CFH}=\text{CF}_2$) as B and A, respectively, we estimated the reactivity ratio of B and A to the $\text{---CF}_2\cdot$ radical as $B/A = 1/0.75$ and that to the $\text{---CFH}\cdot$ radical as $1/1.33$. The TrFE monomer is thought to be polymerized in a random state; i.e., there is no difference between head- and tail-position in the adding reactions. This irregularity of reactivity in TrFE-monomer was also reported

Table III. Reactivity ratio of tail- and head-positions (B/A) of TrFE monomer.

Radical	Reaction temp., (°C)	B/A
---CF ₂ -CFH·	22	1/1.33
---CFH-CF ₂ ·	22	1/0.75
CH ₃ ·	150	1/7.27 ^a
CFH ₂ ·	164	1/2.04 ^b
CF ₂ H·	164	1/1.07 ^b
CF ₃ ·	164	1/0.50 ^b

^aData taken from ref 16.

^bData taken from ref 17.

by Tedder and coworkers^{16,17} in the study of fluoroethylenes, and by Ishigure and coworkers¹⁵ in the study of TrFE-isobutylene copolymers.

Table III shows the reactivity ratios of head- and tail-positions of TrFE to two propagating radicals (---CFH-CF₂· and ---CF₂CFH·), methyl radical (CH₃·) and fluorinated methyl radicals (CFH₂·, CF₂H· and CF₃·), at various temperatures. From the similarity in molecular structures, we may conclude that the reactivity of the propagating radical ---CH₂· is similar to that of the intermediate radical of CH₃· and CFH₂·, furthermore, that the reactivity of ---CFH· is similar to

that of $\text{CFH}_2\cdot$ and $\text{CF}_2\text{H}\cdot$. Finally, the reactivity of $---\text{CF}_2\cdot$ is similar to that of $\text{CF}_2\text{H}\cdot$ and $\text{CF}_3\cdot$. Thus, there is a good agreement in the reactivity ratios of the reacting positions of TrFE to each corresponding radical, although there are many differences in the reaction system, as shown in Table III. In Figure 4, the generated polymer chains of PTrFE formed under the above conditions are shown. The symbol 0 and 1 represent the forward-added and backward-added monomer units, respectively.

```

10100000100000011001011010011110000000011111101011011101010000010000010
111010001101000000001001111101001001101000001111101011110111110010000
01010111101000011111111010001101111111001000000111011100000001010000
111010000111110001010011011111101100000110010111000111110111010010011
1100010011101000101011101101111011000100000110001001100000011111001001
00111110000011101111101100111010100111100000011000110001111011111011
0100001100000100100101000001000100110011001111100001010000100011100010
111111000110100100011010011111011100101111000110001110000000000000101
000010110010111110100101101100001111101101111101010011100000010010100
10011001110111001110000010111100010000001100001001001111110111111110

```

Figure 4. Schematic diagram of PTrFE molecules. The symbol 0 and 1 represent forward-added and backward-added monomer units, respectively.

2-5 APPLICATION TO PVdF

The PVdF polymer is also studied in same manner as PTrFE polymer. The preparation of PVdF is described in chapter 1. The ^{19}F NMR spectrum of PVdF in $-\text{CF}_2-$ region, measured in dimethylformamide at 35 °C, is shown in Figure 5. The detail work of Wilson^{3,4} showed that the peaks (designated A, C, F and G, from low to high magnetic field) observed in PVdF were associated with structures of $-\text{CF}_2-\text{CH}_2-\text{CF}_2-\text{CH}_2-\text{CF}_2-$, $-\text{CH}_2-\text{CH}_2-\text{CF}_2-\text{CH}_2-\text{CF}_2-$, $-\text{CF}_2-\text{CH}_2-\text{CF}_2-\text{CF}_2-\text{CH}_2-$, and $-\text{CH}_2-\text{CH}_2-\text{CF}_2-\text{CF}_2-\text{CH}_2-$, respectively. The chemical shifts and carbon pentad structures are listed in Tavle IV.

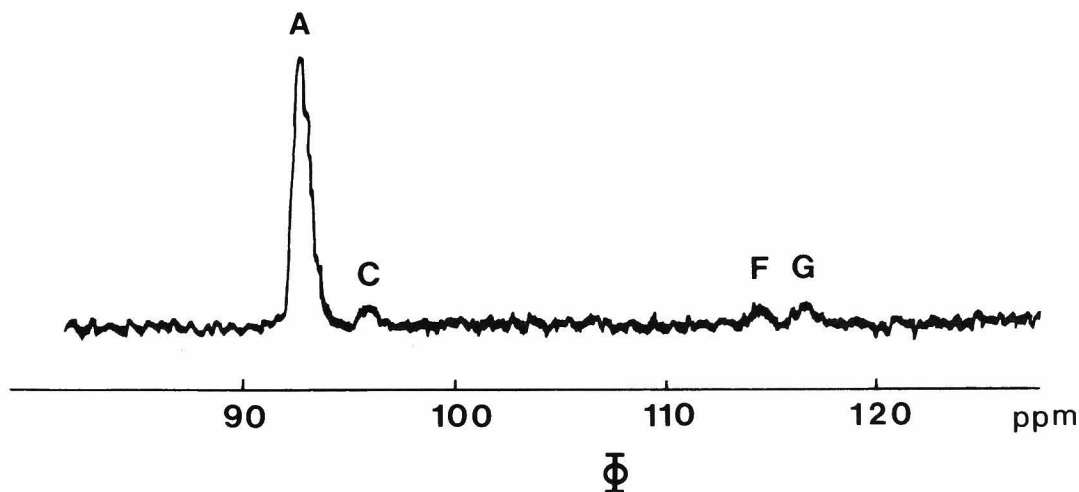


Figure 5. High-resolution fluorine-19 NMR spectrum of PVdF at 56.45 MHz and 35 °C in dimethylformamide. BTF is the internal reference and the chemical shifts are expressed by adding 63.6 ppm to each original values.

Table IV. ^{19}F NMR chemical shifts of PVdF molecule in $-\text{CF}_2-$ region.

Peak	Chemical shifts ^a (ppm)	Structure	Intensity ^b ratio
A	92.7	$-\text{CF}_2-\text{CH}_2-\text{CF}_2-\text{CH}_2-\text{CF}_2-$	0.82
C	95.9	$-\text{CH}_2-\text{CH}_2-\text{CF}_2-\text{CH}_2-\text{CF}_2-$	0.06
F	114.7	$-\text{CF}_2-\text{CH}_2-\text{CF}_2-\text{CF}_2-\text{CH}_2-$	0.06
G	117.0	$-\text{CH}_2-\text{CH}_2-\text{CF}_2-\text{CF}_2-\text{CH}_2-$	0.06

^aThe magnetic field scale is given in parts per million (ppm) upfield from an internal BTF resonance. The chemical shifts are expressed by adding 63.7 ppm to each original values.

^bCalculated from peak area and normalized to unity.

In same manner as PTrFE molecule, we estimated that the percentage of backward-added monomer-units in PVdF chain polymerized at 22 °C was 7%, and the parameters x and y were 50 and 0.075, respectively. Accordingly, denoting the CH_2 -position and CF_2 -position as B and A, respectively, we estimated the reactivity ratio of B and A to the $---\text{CF}_2\cdot$ radical as $B/A = 1/0.02$ and that to the $---\text{CH}_2\cdot$ radical as $1/0.05$. These results indicated that the VdF-monomer reacted to radicals from tail position in high regularity independent of radical sorts. This regularity of reactivity in VdF monomer agreed well with the study on fluoroethylenes by Tedder and coworkers.^{16, 17} Table V shows the reactivity ratios of head- and tail-position of

Table V. Reactivity ratio of tail- and head-positions (B/A) of VdF monomer.

Radical	Reaction temp., (°C)	B/A
---CF ₂ -CH ₂ ·	22	1/0.075
---CH ₂ -CF ₂ ·	22	1/0.02
CH ₃ ·	150	1/0.013 ^a
CFH ₂ ·	164	1/0.15 ^b
CF ₂ H·	164	1/0.15 ^b
CF ₃ ·	164	1/0.03 ^b

^aData taken from ref 16.

^bData taken from ref 17.

[illegible]

Figure 6. Schematic diagram of PVdF molecules. The symbol o and l represent forward-added and backward-added monomer units, respectively.

VdF monomer to some of radicals.

In Figure 6, the generated polymer chains of PVdF formed under the above condition are also shown. The symbol 0 and 1 represent the forward-added and backward-added monomer units, respectively.

In conclusion, it is seen that the reactivity of VdF-monomer is quite different from TrFE-monomer. The VdF-monomer is thought to be polymerized in high regularity compared with TrFE-monomer.

This method may be applied to other polymers consisting of unsymmetry olefins.

REFERENCES

1. R.E. Naylor, Jr. and S.W. Lasoski, Jr., J. Polym. Sci., 44, 1 (1960).
2. R.C. Freguson, J. Amer. Chem. Soc., 82, 2418 (1960).
3. C.W. Wilson, III, J. Polym. Sci., 56, S12 (1962).
4. C.W. Wilson, III and E.R. Santee, Jr., J. Polym. Sci., Part C, 8, 97 (1965).
5. A.S. Shashkov, F.A. Galil-Ogly, and A.S. Novikov, Vysokomol. Soedin., 8, 267 (1966).
6. D.D. Lawson and J.D. Ingham, J. Polym. Sci., Part B, 6, 181 (1968).
7. C.W. Wilson, paper presented at 155th National ACS Meeting, San Francisco, California, 1968, Division of Fluorine Chemistry.
8. K. Ishigure and Y. Tabata, Macromolecules, 3, 450 (1970).
9. K. Ishigure, Y. Tabata and K. Oshima, polym. J., 2, 321 (1971).
10. Von Manfred Goerltz, R. Minke, W. Trautverter and G. Weisgerber, Angew. Macromol. Chem., 29/30, 137 (1973).
11. K. Ishigure, Y. Tabata and K. Oshima, Macromolecules, 6, 584 (1973).
12. K. Ishigure, Y. tabata and K. Oshima, Macromolecules, 8, 177 (1975).
13. K. Ishigure, H. Ohashi, Y Tabata and K. Oshima, Macromolecules, 9, 290 (1976).

14. G. Kojima, H. Wachi, and Y. Tabata, J. Polym. Sci., 14, 1317 (1976).
15. K. Ishigure, H. Ohashi, Y. Tabata and K. Oshima, Macromolecules, 10, 567 (1977).
16. J.M. Tedder, J.C. Walton and K.D.R. Winton, Chem. Commun., , , , 1046 (1971).
17. J.P. Sloan, J.M. Tedder and J.C. Walton J. Chem. Soc., Perkin, 11, 1846 (1975).
18. F.R. Mayo and F.M Lewis, J. Amer. Chem. Soc., 66, 1594 (1944).

CHAPTER 3

MICROSTRUCTURE OF TRIFLUOROETHYLENE COPOLYMERS
WITH VINYLIDENE FLUORIDE, TETRAFLUOROETHYLENE,
CHLOROTRIFLUOROETHYLENE AND HEXAFLUOROPROPYLENE:
HIGH RESOLUTION FLUORINE-19 NMR MEASUREMENT

3-1 INTRODUCTION

Microstructure and comonomer sequence distribution are of central importance in the study of copolymerization. It has been shown by many authors¹⁻¹⁵ that ^{19}F NMR is very useful for studying the microstructure of fluorine containing homopolymers and copolymers, since the fluorine chemical shifts are so large compared with those of proton. On the other hand, theories to characterize the comonomer sequence distribution in copolymer have been given by many authors¹⁶⁻²⁸, all of whom applied a stationary process.

By using 56.45 MHz magnetic field strength NMR, we can study the presence of the carbon-pentad sequence (one containing 5 carbon atoms along the polymer chain) in the $-\text{CF}_2-$ region. In chapter II, we dealt with the microstructure of polytrifluoroethylene (PTrFE) with regard to the head-to-tail (H-T), head-to head (H-H), tail-to-tail (T-T), and tail-to-head (T-H) structures using ^{19}F NMR and a Monte Carlo simulation, and found that the amount of the normal H-T structure is very small in a polymer chain.¹⁵

The purposes of this chapter are , first, to obtain the normalized monomer-diad and -triad fractions as a function of polymer composition from numerical calculation using the comonomer-sequence distribution theory suggested by Ito and Yamashita,²⁷ and second, to examine the microstructure by high resolution fluorine-19 NMR.

3-2 MONOMER SEQUENCE DISTRIBUTION

Ito and Yamashita^{2,7} developed a theory to characterize the copolymer composition and microstructure by applying the statistical stationary process given by Coleman and Fox.^{2,4} They treated three models in a copolymerization system, in which the last one, two, or three monomer units in a propagating polymer radical affect the probability of monomer addition (terminal, penultimated, and pen-penultimate models). From these three models we adopted the terminal model to obtain the normalized fraction of monomer-diad and -triad as a function of polymer composition. For this system the conditional probabilities are given by

$$\begin{aligned}P_{AA} &= r_A / (1 + r_A F) \\P_{AB} &= 1 / (1 + r_A F) \\P_{BA} &= 1 / (1 + r_B / F) \\P_{BB} &= (r_B / F) / (1 + r_B / F)\end{aligned}\tag{1}$$

where r_A and r_B are monomer reactivity ratios and F is the ratio of initial monomer fraction. The fractions $F(A)$ and $F(B)$ are given by

$$F(A) = P_{BA} / (P_{AB} + P_{BA})$$

$$F(B) = P_{AB} / (P_{AB} + P_{BA}) \quad (2)$$

$$F(A) + F(B) = 1$$

Substitution of equation 1 into equation 2 yields the Mayo-Lewis equation.²⁹ The fractions of monomer diads [F(AA), F(AB), F(BA), and F(BB)] are given by

$$\begin{aligned} F(AA) &= P_{BA} P_{AA} / (P_{AB} + P_{BA}) \\ F(AB) &= F(BA) = P_{AB} P_{BA} / (P_{AB} + P_{BA}) \\ F(BB) &= P_{AB} P_{BB} / (P_{AB} + P_{BA}) \\ F(AA) + F(AB) + F(BA) + F(BB) &= 1 \end{aligned} \quad (3)$$

The fractions of monomer triads [F(AAA), F(AAB), F(ABA), F(ABB), F(BAA), F(BAB), F(BBA), and F(BBB)] are given by

$$\begin{aligned} F(AAA) &= P_{BA} P_{AA} P_{AA} / (P_{AB} + P_{BA}) \\ F(AAB) &= F(BAA) = P_{AB} P_{AA} P_{BA} / (P_{AB} + P_{BA}) \\ F(ABA) &= P_{BA} P_{BA} P_{AB} / (P_{AB} + P_{BA}) \\ F(BAB) &= P_{AB} P_{AB} P_{BA} / (P_{AB} + P_{BA}) \\ F(BBA) &= F(ABB) = P_{AB} P_{BA} P_{BB} / (P_{AB} + P_{BA}) \end{aligned} \quad (4)$$

$$F(BBB) = P_{AB}P_{BB}P_{BB}/(P_{AB} + P_{BA})$$

$$F(AAA) + F(AAB) + F(ABA) + F(ABB) + F(BAB) + F(BBA) +$$

$$F(BAA) + F(BBB) = 1$$

Figures 1, 2, 3, and 4 show the normalized fractions of monomer diad as a function of polymer composition, calculated by using equations 1 and 3, for the TrFE-VdF, TrFE-TFE, TrFE-CTFE, and TrFE-HFP copolymer systems, respectively. In the figures, $F(\overline{AB})$ means $F(AB) + F(BA)$. It may be expected that the randomness of monomer distribution in copolymer chain will be most remarkable at 50 mol% copolymer for TrFE-VdF, at 50 mol% copolymer for TrFE-TFE, at 30 mol% copolymer for TrFE-CTFE, and at 98 mol% copolymer for TrFE-HFP copolymer. Figure 5 shows the normalized fractions of monomer triad as a function of polymer composition, calculated by using equation 1 and 4, for the TrFE-VdF copolymer system. In the figure, $F(\overline{AAB})$ and $F(\overline{BBA})$ mean $F(AAB) + F(BAA)$, and $F(BBA) + F(ABB)$, respectively.

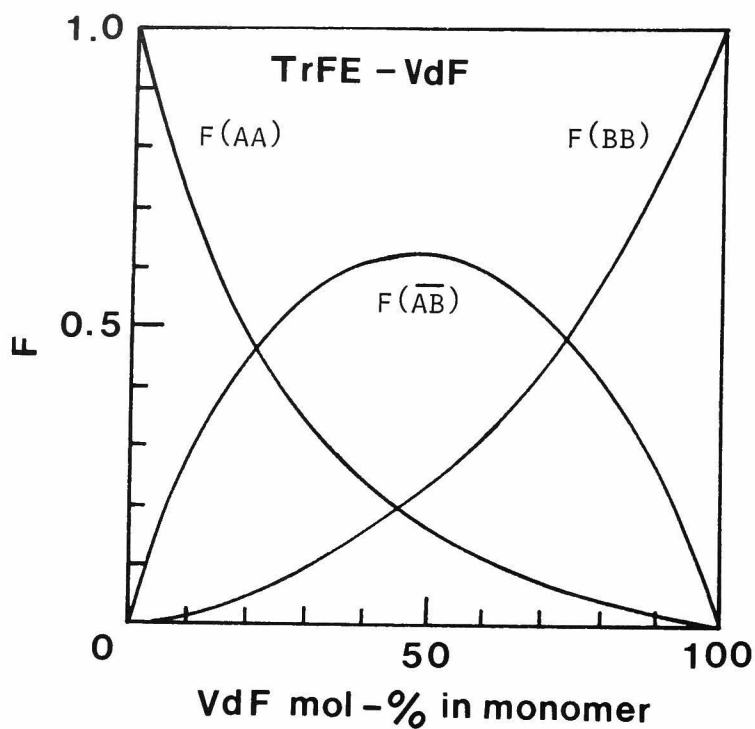


Figure 1. Normalized fractions of monomer diad as a function of polymer composition for TrFE-VdF copolymer system. $F(\overline{AB})$ means $F(AB) + F(BA)$.

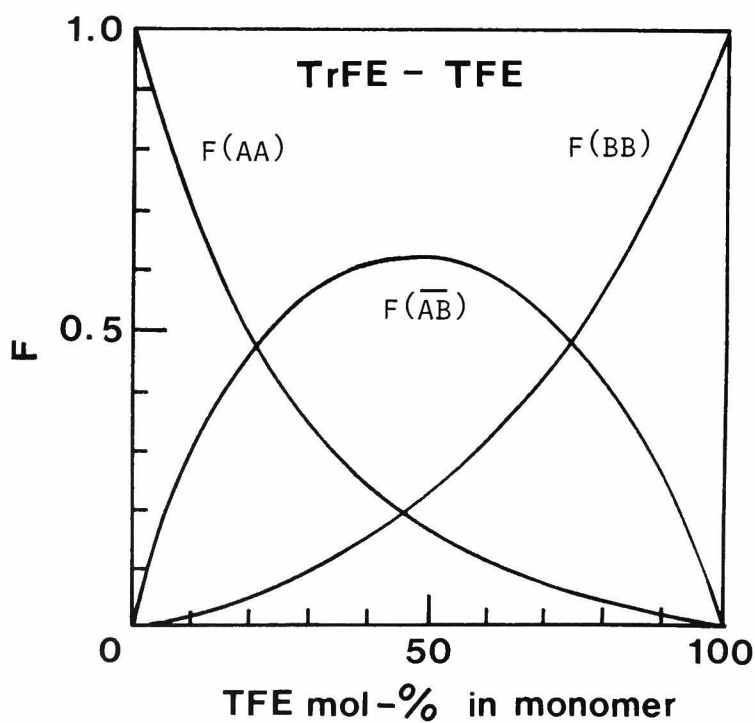


Figure 2. Normalized fraction of monomer diads as a function of polymer composition for TrFE-TFE copolymer system. $F(\overline{AB})$ means $F(AB) + F(BA)$.

Figure 3. Normalized fraction of monomer diads as a function of polymer composition for TrFE-CTFE copolymer system. $F(\overline{AB})$ means $F(AB) + F(BA)$.

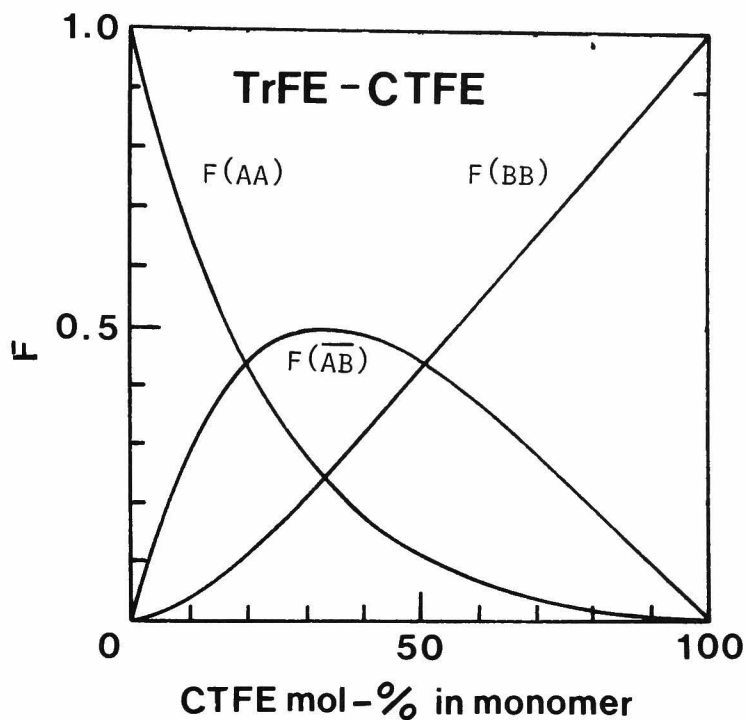
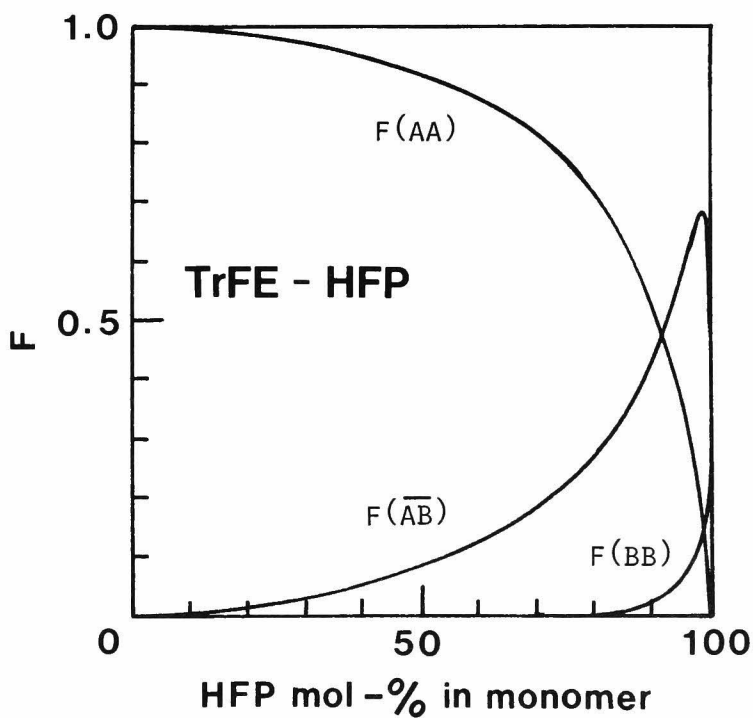


Figure 4. Normalized fraction of monomer diads as a function of polymer composition for TrFE-HFP copolymer system. $F(\overline{AB})$ means $F(AB) + F(BA)$.



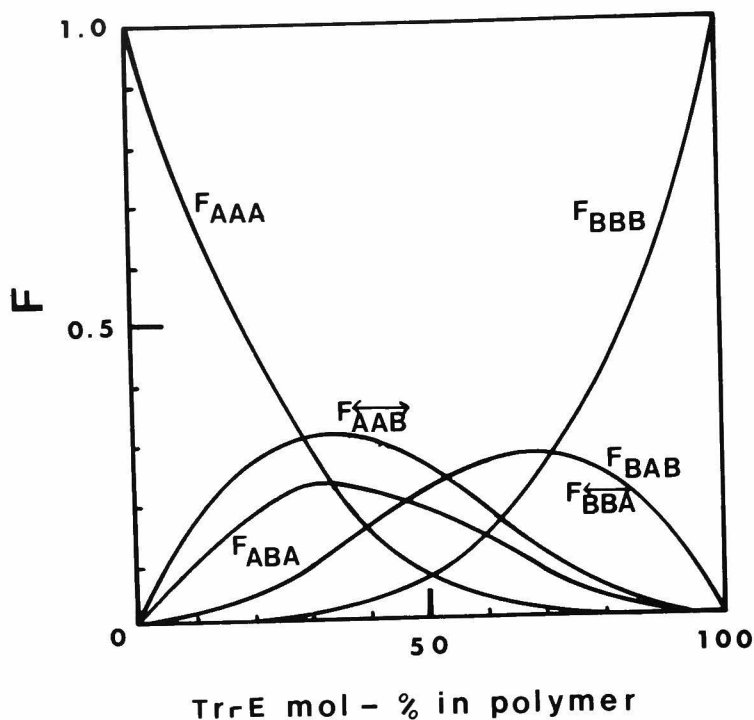


Figure 5. Normalized fractions of monomer triad as a function of polymer composition for TrFE-VdF copolymer system. $F(\overline{AAB})$ and $F(\overline{BAA})$ mean $F(AAB) + F(BAA)$ and $F(BAA) + F(ABB)$, respectively.

3-3 HIGH RESOLUTION FLUORINE-19 NMR STUDY OF TRFE-VdF COPOLYMERS

3-3-1 NMR ASSIGNMENT

Figure 6 shows the high resolution fluorine-19 NMR spectra of the TrFE-VdF copolymers in $-CF_2-$ region. ^{19}F NMR spectra were measured with a Hitachi-Perkin-Elmer R-20B spectrometer at 35 °C in acetone for PTrFE and TrFE-VdF copolymers, and in dimethylformamide for PVdF, using benzotrifluoride as the internal reference. Figures 6(a) and 6(e) show the NMR spectra of PVdF and PTrFE homopolymers. Figures 6(b) and 6(c) show those of VdF-rich copolymers. Figure 6(d) shows those of the 1 : 1

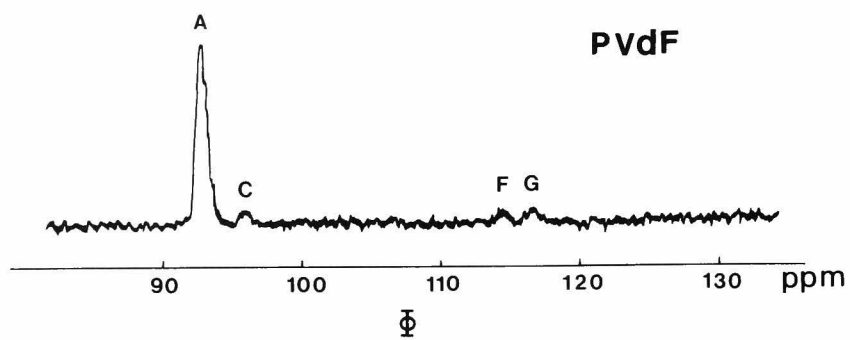
Table I. Microstructures of carbon-pentad sequences with a $-\text{CF}_2-$ group at their center in TrFE-VdF copolymer.

Structure no.	Structure
st. (1)	$-\text{CF}_2-\text{CH}_2-\text{CF}_2-\text{CH}_2-\text{CF}_2-$
st. (2)	$-\text{CH}_2-\text{CH}_2-\text{CF}_2-\text{CH}_2-\text{CF}_2-$
st. (3)	$-\text{CF}_2-\text{CH}_2-\text{CF}_2-\text{CF}_2-\text{CH}_2-$
st. (4)	$-\text{CH}_2-\text{CH}_2-\text{CF}_2-\text{CF}_2-\text{CH}_2-$
st. (5)	$-\text{CF}_2-\text{CFH}-\text{CF}_2-\text{CFH}-\text{CF}_2-$
st. (6)	$-\text{CFH}-\text{CFH}-\text{CF}_2-\text{CFH}-\text{CF}_2-$
st. (7)	$-\text{CF}_2-\text{CFH}-\text{CF}_2-\text{CF}_2-\text{CFH}-$
st. (8)	$-\text{CFH}-\text{CFH}-\text{CF}_2-\text{CF}_2-\text{CFH}-$
st. (9)	$-\text{CH}_2-\text{CFH}-\text{CF}_2-\text{CF}_2-\text{CFH}-$
st. (10)	$-\text{CH}_2-\text{CFH}-\text{CF}_2-\text{CFH}-\text{CF}_2-$
st. (11)	$-\text{CFH}-\text{CH}_2-\text{CF}_2-\text{CH}_2-\text{CF}_2-$
st. (12)	$-\text{CFH}-\text{CH}_2-\text{CF}_2-\text{CF}_2-\text{CH}_2-$
st. (13)	$-\text{CH}_2-\text{CH}_2-\text{CF}_2-\text{CFH}-\text{CF}_2-$
st. (14)	$-\text{CFH}-\text{CH}_2-\text{CF}_2-\text{CFH}-\text{CF}_2-$
st. (15)	$-\text{CF}_2-\text{CH}_2-\text{CF}_2-\text{CFH}-\text{CF}_2-$
st. (16)	$-\text{CH}_2-\text{CH}_2-\text{CF}_2-\text{CF}_2-\text{CFH}-$
st. (17)	$-\text{CFH}-\text{CH}_2-\text{CF}_2-\text{CF}_2-\text{CFH}-$
st. (18)	$-\text{CF}_2-\text{CH}_2-\text{CF}_2-\text{CF}_2-\text{CFH}-$
st. (19)	$-\text{CH}_2-\text{CFH}-\text{CF}_2-\text{CH}_2-\text{CF}_2-$
st. (20)	$-\text{CFH}-\text{CFH}-\text{CF}_2-\text{CH}_2-\text{CF}_2-$
st. (21)	$-\text{CH}_2-\text{CFH}-\text{CF}_2-\text{CF}_2-\text{CH}_2-$
st. (22)	$-\text{CFH}-\text{CFH}-\text{CF}_2-\text{CF}_2-\text{CH}_2-$
st. (23)	$-\text{CF}_2-\text{CFH}-\text{CF}_2-\text{CF}_2-\text{CH}_2-$

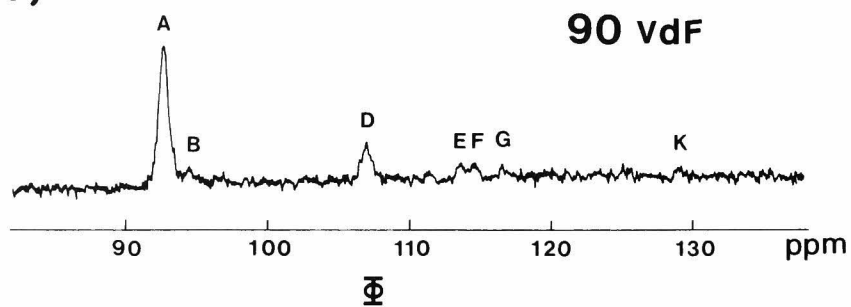
TrFE-VdF copolymers. The polymer compositions of samples are indicated on the figures, The main resonance peaks are designated as A, B, C, D, E, F, G, H, I, J, and K (in the order of increasing magnetic field strength). The magnetic field scale is given in parts per million (ppm). The chemical shifts are expressed by the addition of 63.7 ppm to each original values.

There are 23 microstructures of carbon pentad sequence which have a $-\text{CF}_2-$ group at their center in the TrFE-VdF copolymer system, as shown in Table I. If all of these structures

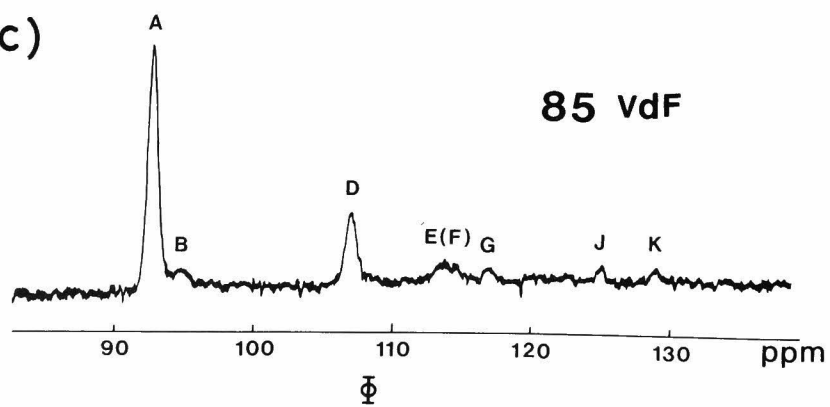
(a)



(b)



(c)



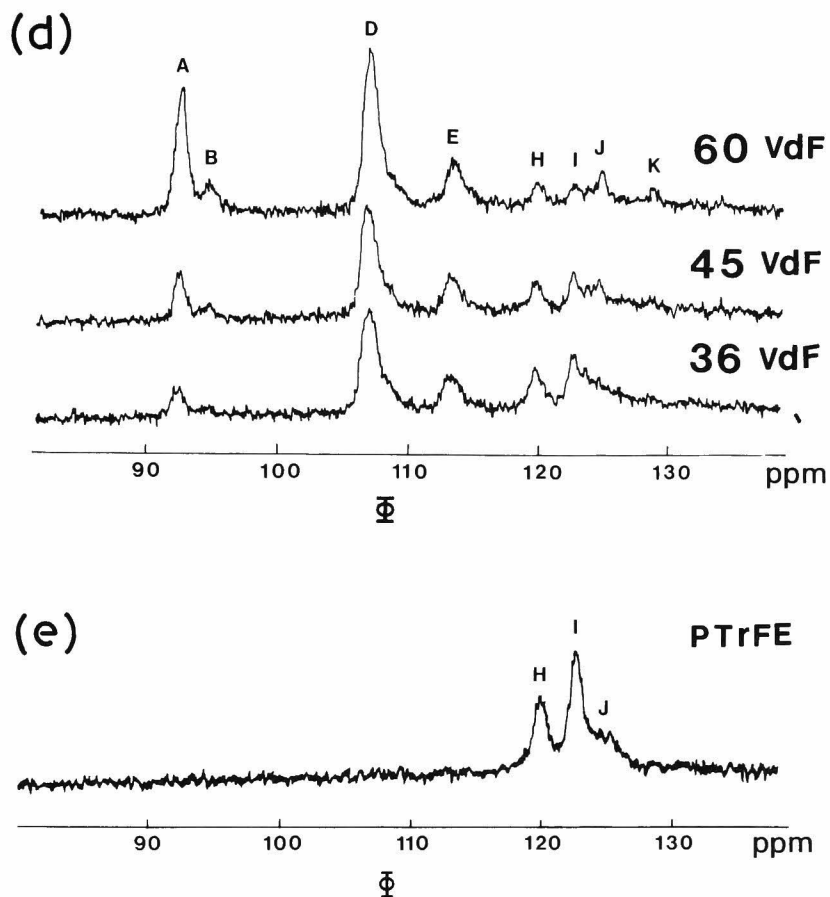


Figure 6. High-resolution fluorine-19 NMR spectra of PVdF, TrFE-VdF copolymers and PTrFE in $-\text{CF}_2^-$ region at 56.45 MHz and at 35 °C in dimethylformamide for PVdF, and in acetone for TrFE-VdF copolymers and PTrFE. Benzotrifluoride is the internal reference. The chemical shifts are expressed by the addition of 63.7 ppm to each original values.

actually exist in the copolymer chain, then 23 peaks corresponding to them will be observed in the spectra. However, only 11 peaks were observed in the spectra, so it is conceivable that some of the structures shown in Table I do not actually exist in the copolymer and/or some of the 23 peaks overlap each other.

Comparing the NMR spectra of TrFE-VdF copolymers, peaks A, C, F, G, H, I, and J are derived from homopolymer of both PVdF and PTrFE, while peaks B, D, E, and K are characteristic of TrFE-VdF copolymer sequences.

We take the following factors into account in making the spectral assignments.

- 1) The experimental law^{2,4} of ^{19}F NMR that the chemical shifts of the central $-\text{CF}_2-$ group are affected when the first or second neighbor is substituted by $-\text{CFH}-$ or $-\text{CF}_2-$ (from $-\text{CH}_2-$). If the first neighbor is $-\text{CF}_2-$, then the central $-\text{CF}_2-$ peak shifts upfield by 9.5 ppm, independently of other groups. On the other hand, substitution of a second group by $-\text{CF}_2-$ shifts the central $-\text{CF}_2-$ peak downfield by 2.5 ppm, again independently of other groups.
- 2) ^{19}F NMR studies^{1,2,3,4} of fluorinated homopolymers and copolymers.

In addition, we take following definition to TrFE monomer. Supposing that CH_2 is the tail and CF_2 is the head in VdF, and that CFH is the tail and CF_2 is the head in TrFE, we represent forward addition, which is defined as the addition of a monomer at the tail-position to any propagating radical, by the symbol (N), and the backward addition, which is defined as the

addition of a monomer at the head-position to a propagating radical, by symbol (B).

PVdF: The ^{19}F NMR spectrum of PVdF in $-\text{CF}_2-$ region is shown in Figure 6(a). The detail work of Wilson^{3,4} showed that the peaks observed in PVdF were associated with structures st. (1), (2), (3), and (4) in Table I. The chemical shifts and carbon pentad structures are listed in Table II.

PTrFE: The ^{19}F NMR spectrum of PTrFE is shown in Figure 6(e). We assigned peaks H, I, and J as follow: peak H corresponds to st. (15), peak I to st. (6) and (7), and peak J to st. (8), in Table I. The detail process was described in chapter 2. The results are also listed in Table II.

90 MOL% VdF COPOLYMER: The ^{19}F NMR spectrum of 90 mol% VdF copolymer in $-\text{CF}_2-$ region is shown in Figure 6(b). As the content of TrFE monomer units is only 10 mol%, the microstructure of this sample is thought to resemble to that of PVdF. In the spectrum, seven peaks (A, B, D, E, F, G and K) are observed. Among these peaks, peaks A, B, F and G surely correspond to those of PVdF. The chemical shift of peak B is 94.8 ppm and slightly different from peak C. The chemical shift of peak C (95.9 ppm) accurately corresponds to st. (2) in Table II. We will consider the reason for this difference between peak B and C. Peaks D, F and K are surely originated from the TrFE-VdF copolymer sequence. Among these peaks, peak D is very large.

We made the following assumptions in order to assign these new peaks to the microstructure of 90 mol% VdF copolymer.

Table II . Chemical shift assignment of ^{19}F NMR peaks in PTrFE, TrFE-VdF copolymers, and PVdF.

Peak	Chemical shift (ppm)	Structure
A	92.7	$-\text{CF}_2-\text{CH}_2-\text{CF}_2-\text{CH}_2-\text{CF}_2-$
B	94.8	$-\text{CFH}-\text{CH}_2-\text{CF}_2-\text{CH}_2-\text{CF}_2-$
C	95.9	$-\text{CH}_2-\text{CH}_2-\text{CF}_2-\text{CH}_2-\text{CF}_2-$
D	107.1	$-\text{CF}_2-\text{CFH}-\text{CF}_2-\text{CH}_2-\text{CF}_2-$
E	113.4	$-\text{CF}_2-\text{CH}_2-\text{CF}_2-\text{CF}_2-\text{CFH}-$
F	114.7	$-\text{CF}_2-\text{CH}_2-\text{CF}_2-\text{CF}_2-\text{CH}_2-$
G	117.0	$-\text{CH}_2-\text{CH}_2-\text{CF}_2-\text{CF}_2-\text{CH}_2-$
H	119.6	$-\text{CF}_2-\text{CFH}-\text{CF}_2-\text{CFH}-\text{CF}_2-$
I	122.7	$-\text{CFH}-\text{CFH}-\text{CF}_2-\text{CFH}-\text{CF}_2-$ $-\text{CF}_2-\text{CFH}-\text{CF}_2-\text{CF}_2-\text{CFH}-$
J	125.9	$-\text{CH}_2-\text{CF}_2-\text{CF}_2-\text{CFH}-\text{CH}_2-$ $-\text{CH}_2-\text{CF}_2-\text{CF}_2-\text{CFH}-\text{CF}_2-$
K	128.8	$-\text{CH}_2-\text{CF}_2-\text{CF}_2-\text{CFH}-\text{CH}_2-$

- 1) There is no TrFE-TrFE sequence, only one TrFE-monomer exists in the monomer-triad sequence. This assumption is justified by the normalized monomer-diad and-triad sequence distributions shown in Figures 1 and 5.
- 2) The end of last VdF-monomer of the propagating radical to which a TrFE-monomer attaches is usually in the head-position.
- 3) There is 7% of backward-added VdF-monomers in the long sequence of VdF-monomers, in the same manner as found for PVdF molecules.
- 4) When the last monomer of the propagating radical is TrFE, then the VdF-monomer is ordinarily added to this radical from the tail-position. This assumption is justified by the result that the VdF-monomer has a tendency to add radicals from the tail-position independent of radical species. Table III shows the reactivity ratio of CH_2 to CF_2 of VdF-monomer onto the radical^{31, 32}.

The above assumptions lead to the following polymer segments;

segment (1): VdF(N)-VdF(N)-VdF(N)-VdF(B)-VdF(N)-VdF(N)-VdF(N)

segment (2): VdF(N)-VdF(N)-VdF(N)-TrFE(N)-VdF(N)-VdF(N)-VdF(N)

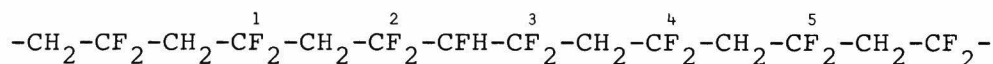
segment (3): VdF(N)-VdF(N)-VdF(N)-TrFE(B)-VdF(N)-VdF(N)-VdF(N)

Segment (1) contains one backward-added VdF-monomer in the sequence. Segment (2) contains one forward-added TrFE-monomer in the VdF(N) sequence. Segment (3) contains one backward-added TrFE-monomer in the VdF(N) sequence. The microstructure of segment (1) is the same as that of PVdF.

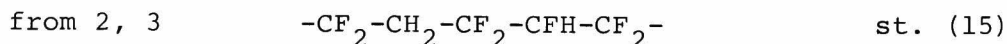
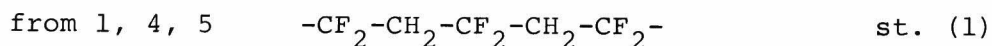
Table III. Reactivity ratio of CH_2 -position to CF_2 -position of VdF ($\text{CH}_2=\text{CF}_2$) onto radical. These are reproduced from the data by Tedder and coworkers^{31,31}.

Radical	Reactivity ratio
$\text{CH}_3\cdot$	1/0.179
$\text{CFH}_2\cdot$	1/0.44
$\text{CF}_2\text{H}\cdot$	1/0.15
$\text{CF}_3\cdot$	1/0.03
$\text{C}_3\text{F}_7\cdot$	1/0.009

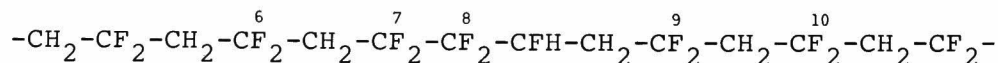
The microstructure of segment (2) is



Carbon-pentad structures with a central $-\text{CF}_2-$ group are as follows.



The microstructure of segment (3) is



Carbon-pentad structures with a central $-\text{CF}_2-$ group are as follows.

from 6, 10	$-\text{CF}_2-\text{CH}_2-\text{CF}_2-\text{CH}_2-\text{CF}_2-$	st. (1)
from 7	$-\text{CF}_2-\text{CH}_2-\text{CF}_2-\text{CH}_2-\text{CFH}-$	st. (18)
from 8	$-\text{CH}_2-\text{CF}_2-\text{CF}_2-\text{CFH}-\text{CH}_2-$	st. (21)
from 9	$-\text{CFH}-\text{CH}_2-\text{CF}_2-\text{CH}_2-\text{CF}_2-$	st. (11)

Structures (15), (18), (21), and (11) appear only in this sample, noting PVdF. These four structures must be correspond to four peaks B, D, E, and K.

Judging from the experimental law of ^{19}F NMR, the chemical shift of st. (11) is at the center of the shifts of st. (1) and (2). As there is no clear peak at 95.9 ppm for st. (2), it is certainly possible to consider that peak B is coupling with peak C. Peak B thus corresponds to st. (11). The real chemical shift position of st. (11) must be on the slightly downfield side of 94.8 ppm.

Judging from the ^{19}F NMR experimental law, the chemical shift of st. (21) must be on the upfield side of the shifts of st. (8). The peak for st. (8) is 125.9 ppm; it was named peak J. There is only one peak (peak K) on the upfield side of peak J. Thus this peak K observed at 128.8 ppm corresponds to st. (21).

The st. (18) resembles st. (3). Judging from the experimental law, the chemical shift of st. (18) is a little downfield of peak F. Peak E is at 113.4 ppm, where two peaks (peak E and F) are slightly overlapping. Peak E definitely corresponds to st. (18).

In the same manner, using the experimental law, st. (15)

must appear at upfield of st. (2) and at downfield of st. (18). Only peak D can correspond to st. (15). Structure (15) must be observed as peak D in the ^{19}F NMR spectrum.

From the assumptions for the microstructure of 90 mol% VdF copolymer, it is expected that the amounts of st. (2), (3), and (4) will be equal. Furthermore, st. (11), (18), and (21) must be present in equal amounts. Comparing the fractions of these structures in NMR spectrum, it was found that they agreed well. This result indicates the correctness of the chemical shifts assignments to peak B, D, E, and K. The results are listed in Table II.

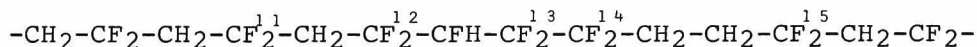
85 MOL% VdF COPOLYMER: The ^{19}F NMR spectrum of 85 : 15 VdF-TrFE is shown in Figure 6(c). The microstructure of this sample is thought to resemble that of 90 mol% VdF copolymer. Only peak J is new in the NMR spectrum of this sample as compared with that of 90 mol% VdF copolymer. Peak J is observed at 125.9 ppm and appears at the same position as st. (8). Structure (8) results from a TrFE-TrFE-TrFE sequence of PTrFE homopolymers. As is obvious from the copolymer composition, which is shown in Figure 5, the amount of TrFE-TrFE-TrFE sequence in this sample is not great. The content of TrFE in this sample is only 15 mol% and the fraction of TrFE-TrFE-TrFE sequence is 0. Therefore, it is difficult to consider that peak J corresponds to st. (8). Furthermore, if st. (8) actually exists in this sample, then peaks of st. (6) and (7) must be observed in the NMR spectrum along with the peak of st. (8). But, there are no such peaks in NMR spectrum,

as is seen in Figure 6(c). So we judged that the peak J is not derived from st. (8) but from a structure whose microstructure is similar to st. (8). From Table I, we can select st. (23) as the most likely structure for peak J. Structure (23) can be derived from VdF(N)-TrFE(B)-VdF(B) or VdF(N)-TrFE(B)-TrFE(B) sequences. The fraction of VdF-TrFE-VdF is 0.13, while that of VdF-TrFE-TrFE is 0 (see Figure 5). So peak J surely derives from the VdF-TrFE-VdF sequence.

Applying the assumption used for the polymer segment of 90 mol% VdF copolymer, the polymer segment which newly appeared in this sample can be described as follow;

segment (4): VdF(N)-VdF(N)-VdF(N)-TrFE(B)-VdF(B)-VdF(N)-VdF(N)

The microstructure of segment (4) is



Carbon-pentad structures with a central $-\text{CF}_2-$ group are as follow:

from 11	$-\text{CF}_2-\text{CH}_2-\text{CF}_2-\text{CH}_2-\text{CF}_2-$	st. (1)
from 12	$-\text{CF}_2-\text{CH}_2-\text{CF}_2-\text{CF}_2-\text{CFH}-$	st. (18)
from 13	$-\text{CF}_2-\text{CFH}-\text{CF}_2-\text{CF}_2-\text{CH}_2-$	st. (23)
from 14	$-\text{CH}_2-\text{CH}_2-\text{CF}_2-\text{CFH}-\text{CF}_2-$	st. (13)
from 15	$-\text{CH}_2-\text{CH}_2-\text{CF}_2-\text{CH}_2-\text{CF}_2-$	st. (2)

If st. (23) really exists in the 85 : 15 VdF-TrFE copolymer chain, then st. (2), (13), and (18) must give NMR signal in the same manner as st. (23). Among these four structures, st. (2) and (18) are observed as peaks B and E, respectively. And st.(13)

is observed as the shoulder of peak D at 109.1 ppm. Comparing intensity ratios of these peaks, it was found that they agreed well. Thus, we judged that peak J corresponded to st. (23).

1:1 TrFE-VdF COPOLYMERS: Figure 6(c) shows the ^{19}F NMR spectra of samples. The molar ratios of these copolymers are close to unity. The NMR spectra of these copolymers resemble one another. There are 8 peaks (A, B, D, E, F, G, H, I, J, and K) in the spectra of these three samples. These peaks were already observed in PVdF, VdF-rich copolymer and PTrFE, and were assigned as listed in Table II. As noted above, these assignments are based on only the limited polymer segments of these polymers [segments (1), (2), (3), and (4)]. The existence of other carbon-pentad structures having $-\text{CF}_2-$ group at their centers can be presumed in these samples, because the VdF-TrFE copolymer systems have a random configuration and the existence of the 23 kinds of structures listed in Table I can be presumed. We have judged that the structures which are not apparent in the NMR spectrum are very minor and practically do not exist in the copolymer chain.

The main feature of the spectra of these copolymers is peak D. Peak D is assigned to st. (15): this microstructure is derived from $\text{VdF(N)}-\text{VdF(N)}-\text{TrFE(N)}$, $\text{VdF(N)}-\text{TrFE(N)}-\text{VdF(N)}$, $\text{TrFE(N)}-\text{TrFE(N)}-\text{VdF(N)}$, and $\text{TrFE(N)}-\text{VdF(N)}-\text{TrFE(N)}$. These 4 monomer-triad sequences consist of head-to-tail structures of VdF-TrFE

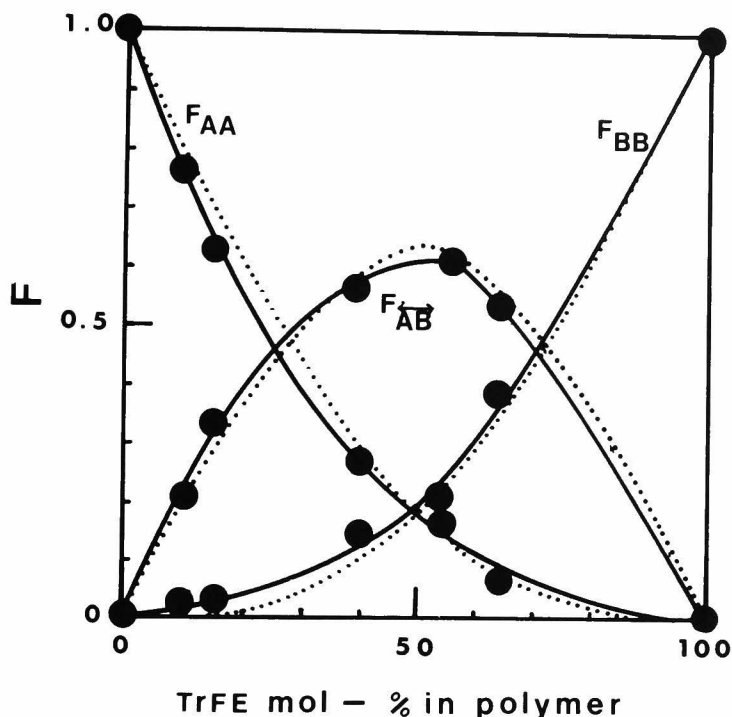


Figure 7. Normalized fractions of monomer diad as a function of polymer composition for the TrFE-VdF copolymer system: (—), calculated by simply measuring the ratios of the integral intensities of the respective peaks; (.....), calculated by equations 1 and 3. Symbols A and B represent VdF and TrFE, respectively.

or TrFE-VdF sequences. The chemical shifts and assignment of the peaks are summarized in Table II.

3-3-2 MONOMER SEQUENCE DISTRIBUTION: ^{19}F NMR

The monomer-diad fractions of TrFE-VdF copolymers as a function of polymer composition are shown by solid lines in

in Figure 7. These are obtained by simply determining the ratios of the integrated intensities of the respective peaks in NMR spectra. It may be expected from the figure that the TrFE-VdF copolymer system is in random configuration. The broken lines in the figure are obtained from the calculation using by equations 1 and 3. These lines agree well with the experimental curves estimated by NMR data. This results indicate the accuracy of the monomer reactivity ratios (r_A and r_B).

The normalized fractions of monomer-diad, consisting of head-to-tail structure in TrFE-TrFE, TrFE-VdF, and VdF-VdF sequences, as a function of polymer composition are shown in Figure 8. These are also obtained from the intensities of respective NMR peaks. The broken lines in the figure represent the monomer-diad sequence distribution curves containing H-T, H-H, T-T and T-H sequences. As is seen from the figure, the amount of H-T structure in the VdF-VdF sequence is very large and that in TrFE-TrFE sequence is very small. However, the amount of H-T structure in TrFE-VdF sequence is rather abundant. This result indicates that the TrFE-monomer reacts to $---CH_2CF_2\cdot$ propagating radical from the tail-position with a considerably high probability. However, such a behavior is considered to be a unique phenomenon. For example, Tedder and coworkers^{31, 32} studied the reactivities of TrFE-monomer with respect to reacting positions (head- or tail-position) to methyl radical ($CH_3\cdot$) and fluorinated

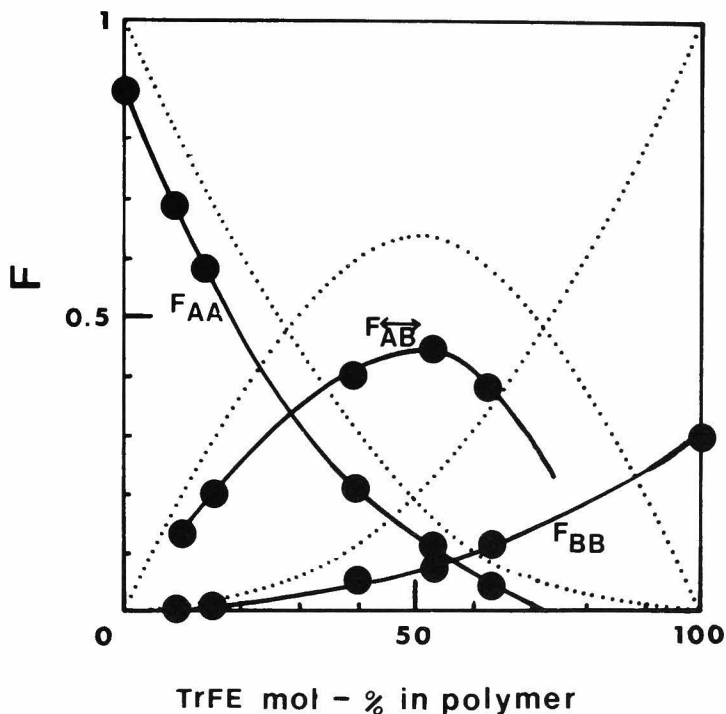


Figure 8. Normalized fractions of monomer diad, consisted of head-to-tail structure in TrFE-TrFE, TrFE-VdF, and VdF-VdF sequences, as a function of polymer composition for TrFE-VdF copolymer system (—); and normalized monomer-diad fractions containing head-to-tail, head-to-head, tail-to-tail, and tail-to-head structures (.....). These data are obtained from simply measuring the peak areas. Symbols A and B represent VdF and TrFE, respectively.

methyl radicals ($\text{CFH}_2\cdot$, $\text{CF}_2\text{H}\cdot$ and $\text{CF}_3\cdot$), in the gaseous state and at high temperature, and showed that the regularity of reacting position of TrFE-monomer was very low. Ishigure and co-workers¹⁴ also reported the abnormal reactivity of TrFE-monomer by a high resolution fluorine-19 NMR study of TrFE-isobutylene

copolymers. Furthermore, high-resolution fluorine-19 NMR and simulation studies of PTrFE¹⁵ indicated that the TrFE-monomer had a tendency to be polymerized in a random state with respect to the reacting position of monomer; i.e., there was no distinct difference between head- and tail-position in adding reaction.

REFERENCES

1. R.E. Naylor, Jr., and S.W. Lasoski, Jr., J. Polym. Sci., 44, 1 (1960).
2. R.C. Freguson, J. Amer. Chem. Soc., 82, 2418 (1960).
3. C.W. Wilson, III, J. Polym. Sci., 56, S12 (1962).
4. C.W. Wilson, III, and E.R. Santee, Jr., J. Polym. Sci., Part C, 8, 97 (1965).
5. A.S. Shashkov, F.A. Galil-Ogly and A.S. Novikov, Vysokomol. Soedin., 8, 267 (1966).
6. D.D. Lawson and J.D. Ingham, J. Polym. Sci., Part B, 6, 181 (1968).
7. K. Ishigure and Y. Tabata, Macromolecules, 3, 450 (1970).
8. K. Ishigure, Y. Tabata and K. Oshima, Polym. J., 2, 321 (1971).
9. Von Manfred Goerltz, R. Minke, W. Trautverter and G. Weisgerber, Angew. Makromol. Chem., 29/30, 137 (1973).
10. K. Ishigure, Y. Tabata and K. Oshima, Macromolecules, 6, 584 (1973).
11. K. Ishigure, Y. Tabata and K. Oshima, Macromolecules, 8, 177 (1976).
12. K. Ishigure, H. Ohashi, Y. Tabata and K. Oshima, Macromolecules, 9, 290 (1976).
13. G. Kojima, H. Wachi, K. Ishigure and Y. Tabata, J. Polym. Sci., 14, 1317 (1976).
14. K. Ishigure, H. Ohashi, Y. Tabata and K. Oshima,

- Macromolecules, 10, 567 (1977).
15. T. Yagi, Polym. J., 11, 353 (1979).
 16. T. Alfrey, Jr., and G. Goldfinger, J. Chem. Phys., 12, 205 (1944).
 17. T. Alfrey, Jr., and G. Goldfinger, J. Chem. Phys., 12, 322 (1944).
 18. F.T. Wall, J. Amer. Chem. Soc., 66, 2050 (1944).
 19. E. Merz, T. Alfrey, Jr., and G. Goldfinger, J. Polym. Sci., 1, 74 (1946).
 20. G. Goldfinger and T. Kane, J. Polym. Sci., 3, 462 (1948).
 21. R. Miller and L.E. Nielsen, J. Polym. Sci., 46, 303 (1960).
 22. F.P. Price, J. Chem. Phys., 36, 209 (1962).
 23. H.K. Frensdorff and R. Pariser, J. Chem. Phys., 39, 2303 (1963).
 24. B.D. Coleman and T.G. Fox, J. Polym. Sci., A1, 3183 (1963).
 25. H.J. Harwood and W.M. Ritchey, J. Polym. Sci., B2, 601 (1964).
 26. T. Fueno and J. Furukawa, J. Polym. Sci., A2, 3681 (1964).
 27. K. Ito and Y. Yamashita, J. Polym. Sci., A3, 2165 (1965).
 28. C.W. Pyun, J. Polym. Sci., A2, 8, 1111 (1970).
 29. M. Finemann and S.D. Ross, J. Polym. Sci., 5, 259 (1950).
 30. F.R. Mayo and F.M. Lewis, J. Amer. Chem. Soc., 66, 1594 (1944).
 31. J.M. Tedder, J.C. Walton and K.D.R. Winton, Chem. Comm., 1046 (1971).
 32. J.P. Sloan, J.M. Tedder and J.C. Walton, J.C.S. Perkin, 11, 1846 (1975).

CHAPTER 4

CRYSTALLIZATION BEHAVIOR OF POLY(TRIFLUOROETHYLENE)



4-1 INTRODUCTION

In chapters 1 and 2, we have reported the preparation and microstructure of poly(trifluoroethylene) [PTrFE, $-(\text{CF}_2\text{-CFH})_n$], and found that the amount of abnormal head-to-head, tail-to-tail, and tail-to-head linkages in polymer chain was very large.¹

In this chapter, we will concern with the crystallization behavior of PTrFE polymer. The heat of fusion is an extremely important thermodynamic property of semicrystalline polymers. Many papers have presented data on the heat of fusion for fluorinated-ethylene polymers; for example, the heat of fusion is 1920 cal/mol for poly(ethylene)² [PE, $-(\text{CH}_2\text{-CH}_2)_n$], 1800 cal/mol for poly(vinyl fluoride)³ [PVF, $-(\text{CFH-CH}_2)_n$], 1435 cal/mol or 1400 cal/mol for poly(vinylidene fluoride)^{4,5} [PVdF, $-(\text{CF}_2\text{-CH}_2)_n$], 1370 cal/mol for poly(tetrafluoroethylene)⁶ [PTFE, $-(\text{CF}_2\text{-CF}_2)_n$], and 1200 cal/mol for poly(chlorotrifluoroethylene)⁷ [PCTFE, $-(\text{CF}_2\text{-CFCl})_n$]. However, data on PTrFE are lacking in the literature.

The heat of fusion can be obtained from the depression of melting temperature (T_m) by changing the volume fraction of diluent or by changing the fractions of second component in the copolymer.^{8,9}

The investigations of the kinetic and mechanism of the crystallization is also very important, since bulk properties of polymers are largely affected by the transition from amorphous to crystal state. The dilatometric and calorimetric

methods are the main techniques for studying the crystallization rate of polymer. In this study, the calorimetric method was employed.

The purpose of this chapter is concerned with crystallization behavior of PTrFE. This study deals with the crystal morphology, the equilibrium melting temperature, the heat of fusion, the surface free energy, and crystallization rate of PTrFE polymer.

4-2 EXPERIMENTAL

The preparation of both PTrFE and trifluoroethylene (TrFE) - chlorotrifluoroethylene (CTFE) copolymers are described in chapter 1.

The intrinsic viscosity of PTrFE polymer in dimethylformamide (DMF) was found to be 2.2 dl/g at 30 °C.

The polymer-diluent mixture was prepared by adding, in a glass tube, PTrFE polymer to desired amount of diluent dimethylacetamide (DMAc). After sealing the tube, the tubes were heated to about 270 °C in slot-bath for at least 5 hours to ensure homogenous solution, and then quenched to room temperature.

Thermal analysis was performed with a differential scanning calorimeter (Perkin-Elmer DSC-2). Aluminium pan was used as a specimen container and each specimen weight was about 10 mg. The temperature calibration was based on indium, thin,

and lead standard.

For the study of the morphology of PTrFE crystal, the electron microscope (Hitachi, model H-500) was used. The isothermally crystallized sample was measured. PTrFE polymer was maintained at 250 °C for 30 min. to ensure complete melting of the crystal before cooled at 1.25 °C/min to crystallization temperature, T_c . Sample was isothermally crystallized at 185 °C for 5 hours, and then cooled to room temperature at 1.25 °C/min. And then, sample was fractured at liquid nitrogen temperature. The fractured surface was prepared by replication method.

The lamellar thickness of samples was estimated by small angle x-ray diffraction method with a Rigaku-Denki diffractometer. These specimens of the different lamellar thickness were prepared by changing time and temperature of annealing process.

4-3 ELECTRON MICROSCOPE

Figure 1 shows electron micrograph of fractured PTrFE crystal. The sample was annealed for 5 hours at 185 °C in order to grow the crystal enough. These electron micrographs show the distinct lamellar spherulites character. The lamellar thickness of this polymer was estimated to be about 600 Å. This indicates that the PTrFE crystal is not consisted of extended chain but of fold one.

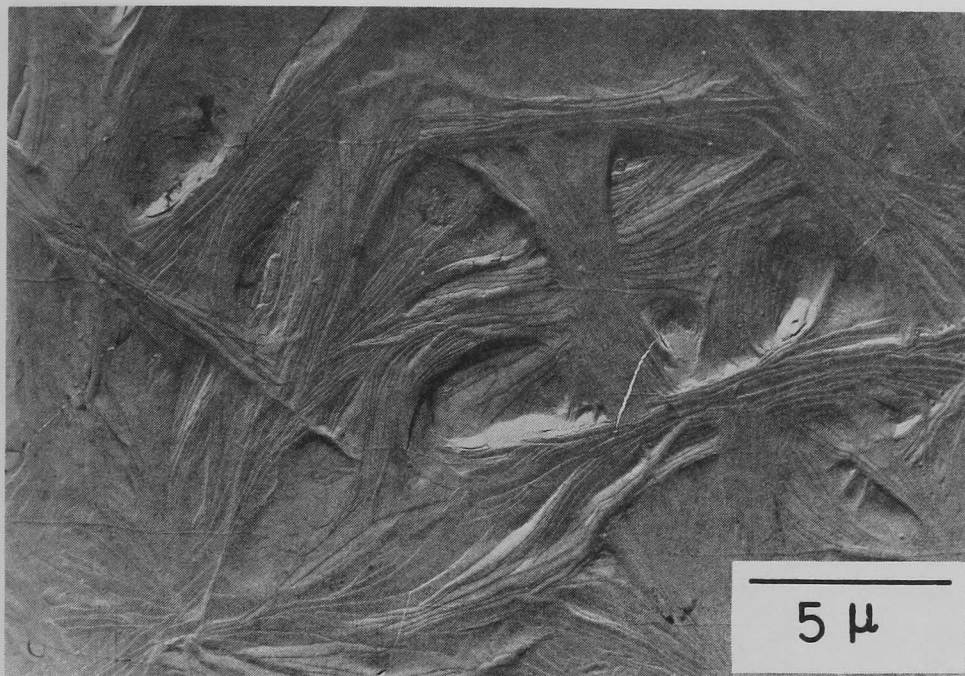


Figure 1(a). The electron micrograph of replica of fractured PTrFE polymer. Spherulites can be seen. Sample was annealed for 5 hours at 185 °C.

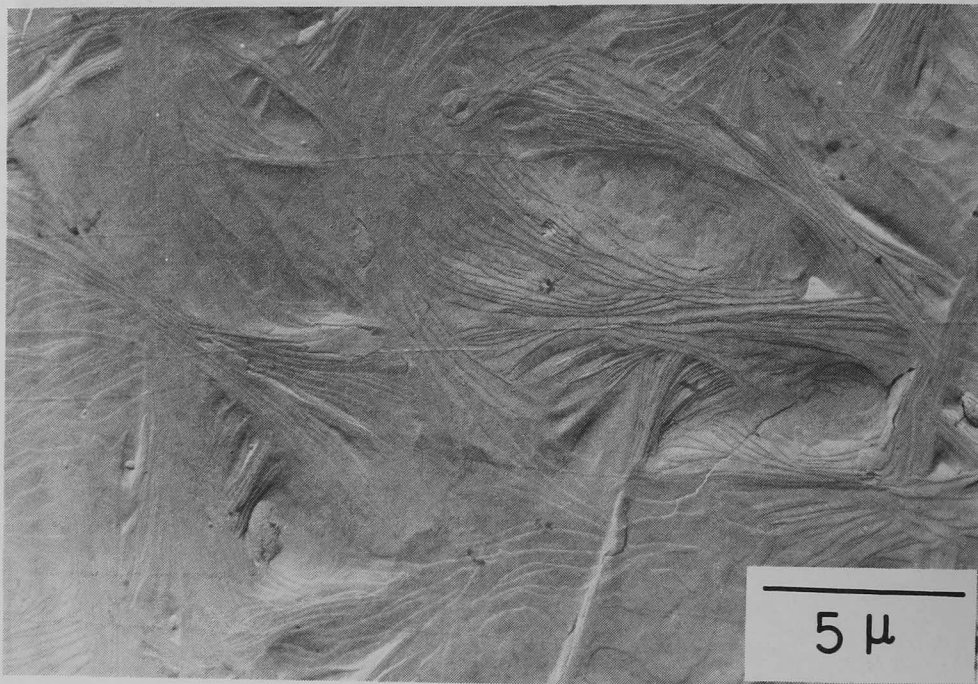


Figure 1(b). The electron micrograph of replica of fractured PTrFE polymer. Spherulites can be seen. Sample was annealed for 5 hours at 185 °C.

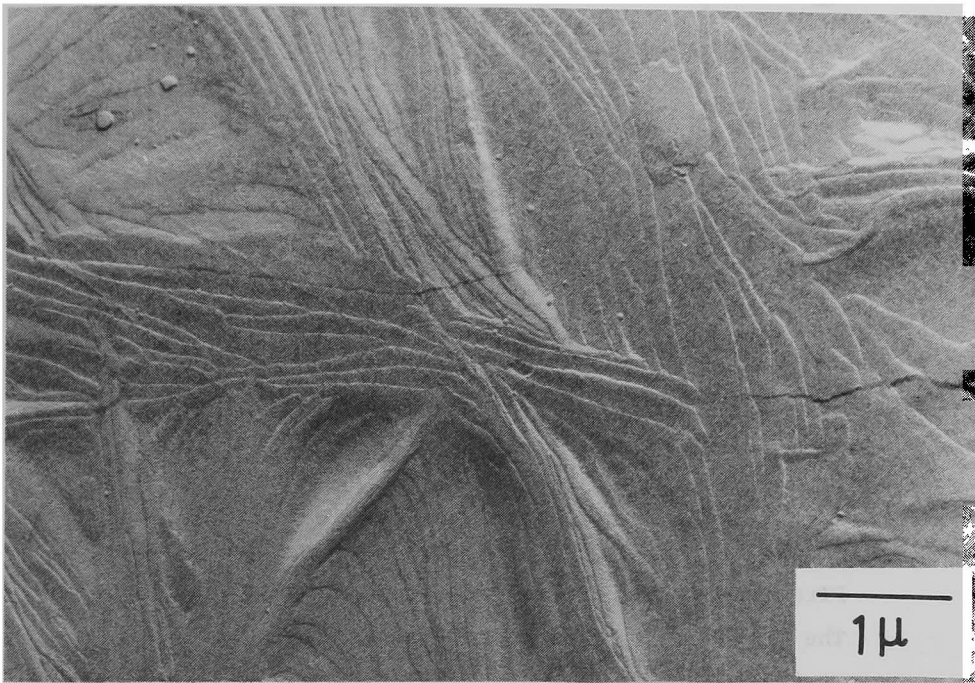


Figure 1(c). The electron micrograph of replica of fractured PTrFE polymer. Lamellar crystal can be seen. Sample was annealed for 5 hours.

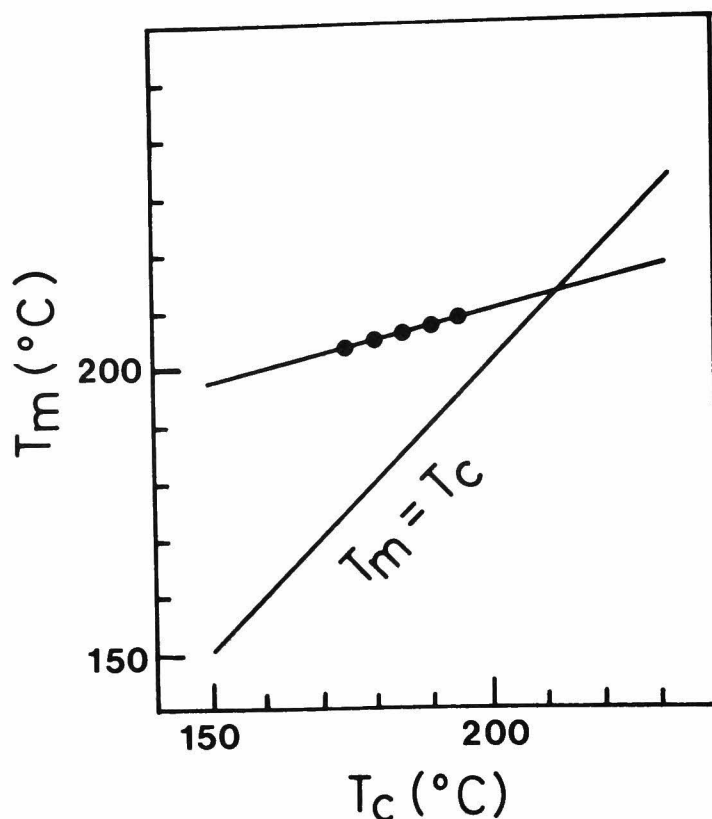


Figure 2. A plot of the melting temperature T_m of PTrFE versus the crystallization temperature T_c . The T_m versus T_c line intersects the line $T_m = T_c$ at 213 °C.

4-4 EQUILIBRIUM MELTING TEMPERATURE

Figure 2 shows a plot of the crystallization temperature, T_c , versus observed melting temperature, T_m , for PTrFE polymer; i.e., a Hoffman-Week plot.¹⁰ A linear relationship is observed between T_c and T_m . The value of an equilibrium melting point, T_m^0 , can be obtained by a linear extrapolation of the apparent melting temperature. The T_c versus T_m line

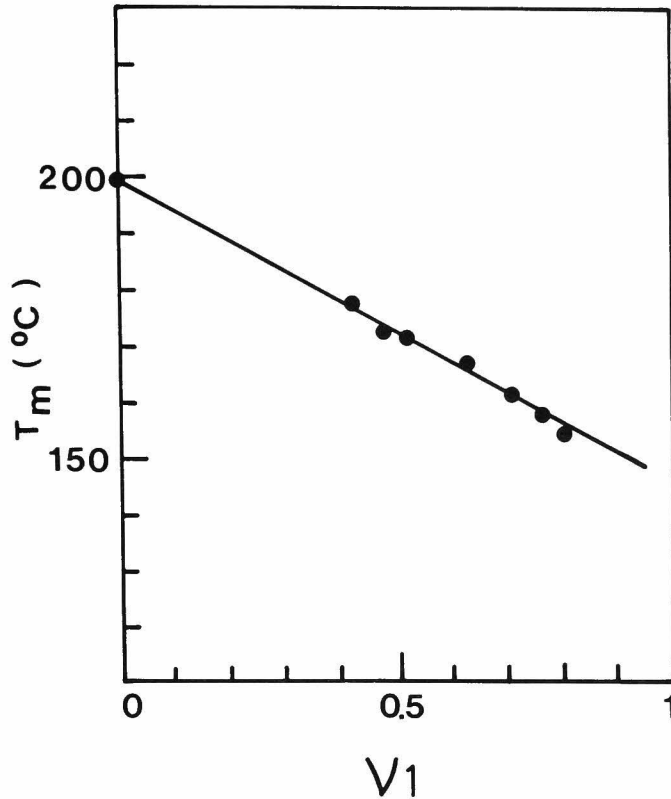


Figure 3. Dependence of the melting temperature T_m of PTrFE with volume fraction V of dimethylacetamide.

intersects with the $T_m = T_c$ line at 213 °C.

Assuming that the crystal is perfect and the heating process used in the melting temperature determination does not disturb the nature of crystal, the depression in the melting temperature of the crystal resulting from its finite size is represented by¹⁰

$$T_m^\circ - T_m = \phi (T_m^\circ - T_c) \quad (1)$$

where ϕ is the stability parameter which depends on crystal thickness. Equation 1 indicates that T_m should be a linear

function of T_c , and ϕ constrained to lie between 0 and 1. The condition $\phi = 0$ represents the maximum stability and $\phi = 1$ represents the inherent unstability. The ϕ value of PTrFE is found to be about 0.26 using eq 1. This value suggests that the PTrFE crystal should be fairly stable. Nishi and Wang¹¹ reported comparable value of PVDF as $\phi = 0.2$. Comparing the ϕ value of PTrFE with that of PVdF, there is not much difference, and, neither for other polymers.¹⁰

Figure 3 shows change of melting temperature T_m with diluent. The data for DMAc as diluent are well represented by a straight line. Extrapolation of this line to zero diluent concentration yield $T_m = 199$ °C. This value is roughly 14° below compared with the equilibrium melting temperature T_m° .

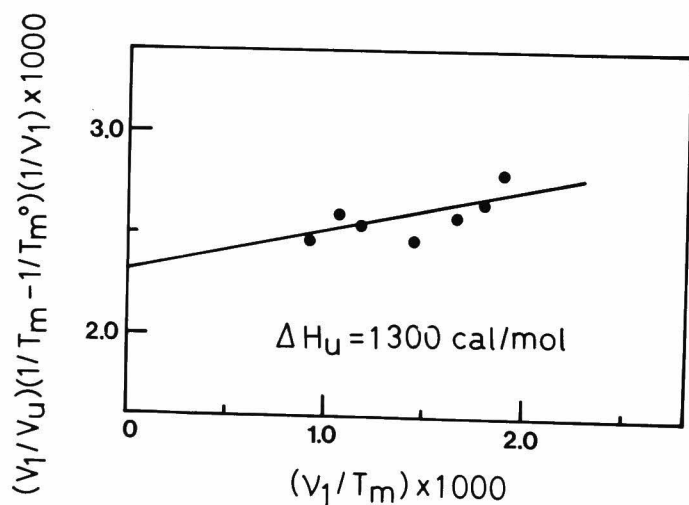


Figure 4. A plot of the quantity $(1/T_m - T_m^\circ)/v_1$ versus v_1/T_m for the PTrFE-dimethylacetamide system.

4-5 HEAT OF FUSION

The heat of fusion, ΔH_u , can be obtained from the depression of melting temperature by varying the volume fraction of diluent,^{8,9}

$$1/T_m - 1/T_m^\circ = (R/\Delta H_u) (V_u/V_1) [v_1 - (BV_1/RT_m)v_1^2] \quad (2)$$

where T_m° is the melting temperature of undiluent polymer, T_m the melting temperature of polymer-diluent system, R the gaseous constant, ΔH_u the heat of fusion, V_u the molar volume of polymer repeating unit, V_1 the molar volume of the diluent, v_1 the volume fraction of diluent, and B the interaction parameter.

Figure 4 shows a plot of the quantity $(1/T_m - 1/T_m^\circ)/V_1$ versus V_1/T_m for the PTrFE-DMA system. From the straight line, the ΔH_u of PTrFE was found to be about 1300 cal/mol. Since the equilibrium melting temperature, T_m° , is 213 °C, the equilibrium melting entropy, ΔS_u , was calculated as 2.75 eu/mol.

The heat of fusion can be also obtained by polymer composition - melting temperature relation in copolymer,^{8,9}

$$1/T_m - 1/T_m^\circ = -(R/\Delta H_u) \ln x_a \quad (3)$$

where x_a is the molar fraction of in a copolymer. Figure 5 shows a plot of $1/T_m$ versus $\ln x_a$ in TrFE-CTFE system. The ΔH_u is calculated as 1050 cal/mol using equation 3. This value is a little small compared with diluent method. In

general, the heat of fusion obtained by copolymerization method shows small value compared with diluent method.⁹ It is mentioned that the ΔH_u obtained from the diluent method is more accuracy compared with the copolymer method, since the value of ΔH_u changes with the kinds of comonomer.⁹ In our study both diluent and copolymer methods agree fairly well.

The values of ΔH_u and ΔS_u of PTrFE are very similar to those of PCTFE, whose chemical structure differs from PTrFE in that only a hydrogen atom is substituted by a chlorine atom: the values of ΔH_u and ΔS_u of PCTFE are 1200 cal/mol and 2.49 eu/mol, respectively.

The values of T_m , T_m° , ΔH_u , and ΔS_u of PTrFE are tabulated in Table I, together with those of other fluorinated ethylene polymers.^{2,3,5,6,12-14} As seen from the table, the values of ΔH_u and ΔS_u decrease with increasing the number of fluorine atom in the repeating unit of fluorinated ethylene polymers.

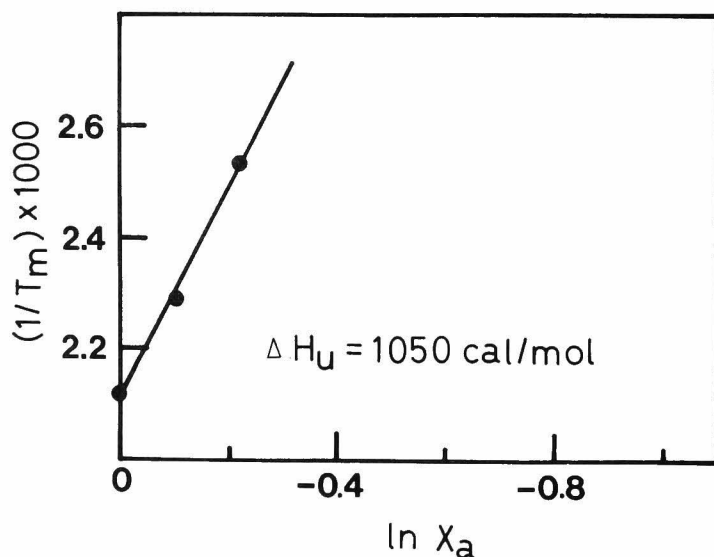


Figure 5. A plot of the $1/T_m$ versus X_a for the TrFE-CTFE copolymer system.

Table I. Comparison of the thermodynamic parameters of fluorinated ethylene polymers.

Polymer	T_m , °C	T_m^o , °C	ΔH_u , cal/mol	ΔS_u , eu/mol	σ_e , erg/cm ²
PE ^{a, b}		143	1710	5.78	57
PVF ^c	200		1800	3.80	
PVdF ^{d, e}	178	210	1425	3.16	65
PTrFE	199	213	1300	2.75	54
PTFE ^f	330		1370	2.27	
PCTFE ^b	218	221	1200	2.49	37

^aData of Broadhurst.³

^bData of Hoffman.^{14, 15}

^cData of Sapper.⁴

^dData of Welch.⁶

^eData of Mancarella.¹⁶

^fData of Starkweather.⁷

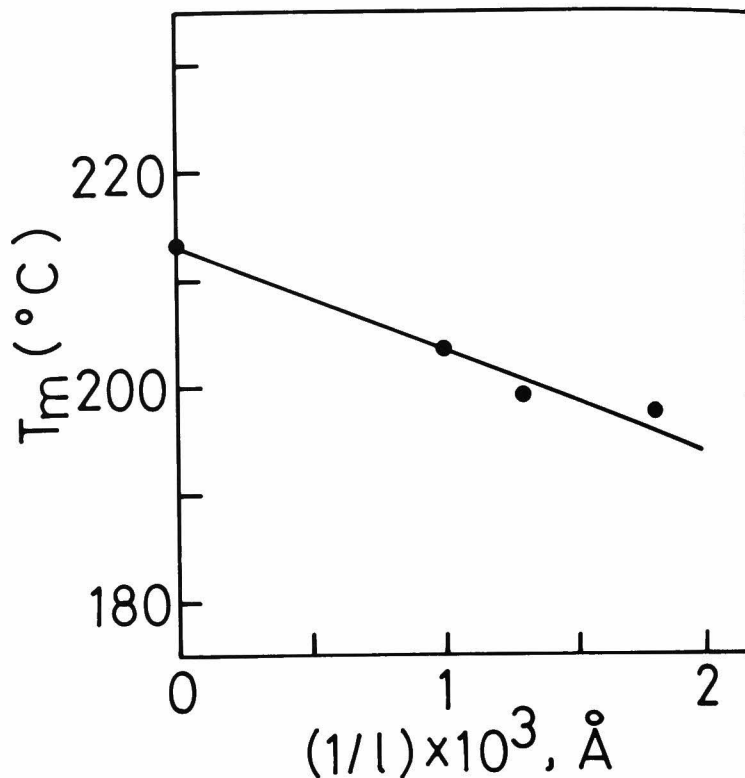


Figure 6. A plot of T_m versus reciprocal lamellar thickness.

4-6 SURFACE FREE ENERGY OF LAMELLA

According to Hoffman^{10,15,16} the surface free energy of lamella, σ_e , is given by

$$T_m = T_m^\circ (1 - 2\sigma_e / \Delta H_u \ell) \quad (4)$$

where ℓ is the lamella thickness, T_m° the equilibrium melting temperature, and ΔH_u the heat of fusion. The values of ΔH_u and T_m° are 1300 cal/mol and 213°C, respectively, as mentioned above.

Figure 6 shows a plot of the melting temperature versus the reciprocal lamella thickness. The lamella thickness was estimated by small angle x-ray diffraction method. As seen from

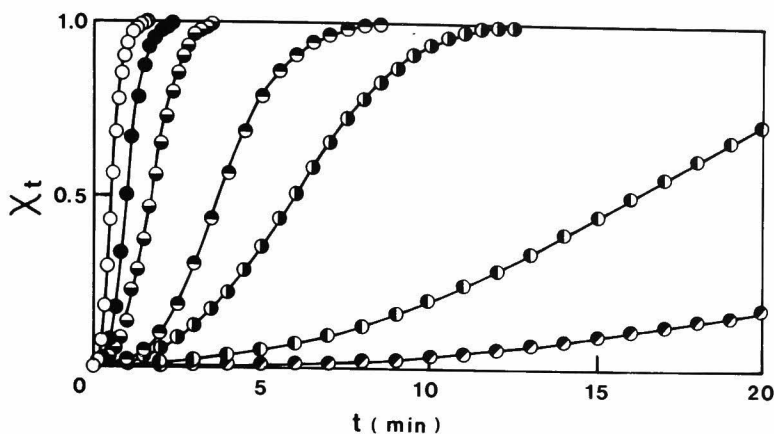


Figure 7. Change of crystallinity X_t of PTrFE with isothermal crystallization time t , at various crystallization temperature: \circ , 453.0 °C; \bullet , 454.0 °C; \circ , 455.0 °C; \bullet , 456.0 °C; \bullet , 457.0 °C; \bullet , 458.0 °C; and \bullet , 459.0 °C.

the figure, the plot of T_m versus $1/l$ is linear, and the intercept at $1/l = 0$ gives the equilibrium melting temperature. The value of 1.2 Kcal/mol for σ_e was obtained from the slope of this line.

4-7 CRYSTALLIZATION KINETICS

Figure 7 shows change of the crystallinity of PTrFE polymer with isothermal crystallization time, at various crystallization temperatures. From these curves the half time of conversion, $t_{1/2}$, has been determined at various crystallization temperature, T_c . Figure 8 shows a plot of $t_{1/2}$ versus T_c . The slope changes at 457 K.

The kinetics of isothermal crystallization of polymers can be analyzed by means of the well-known Avrami equation,^{10,17}

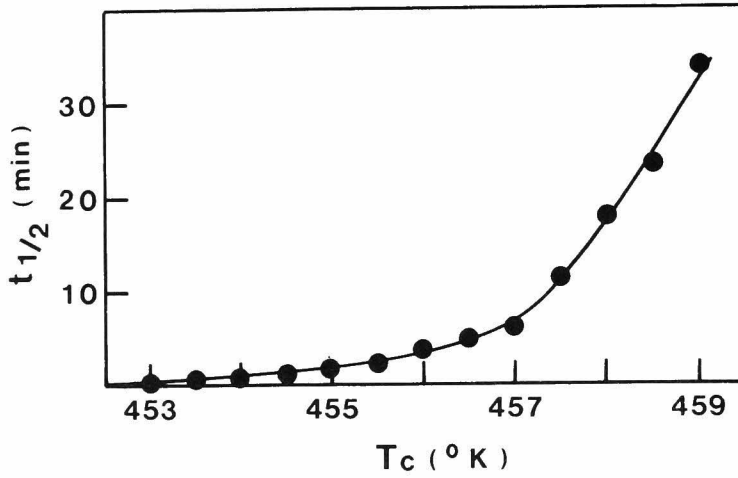


Figure 8. A plot of crystallization half time $t_{1/2}$ of PTrFE versus crystallization temperature T_c .

$$(1 - X_t) = \exp(-Zt^n) \quad (5)$$

The double logarithmic form of equation 5 is given by

$$\log[-\ln(1 - X_t)] = n \log(t) + \ln(Z) \quad (6)$$

where X_t is the weight fraction of crystallized polymer at time t , Z the rate constant, and n the Avrami exponent. Figure 9 shows Avrami plots of PTrFE at various crystallization temperatures..... As seen from the figure, the crystallization kinetics of PTrFE obeys the Avrami equation. The exponent changes with the crystallization temperature. The average value of n is found to be about 2.7. From equation 6, the kinetic constant Z is

$$Z = \ln(2/t_{1/2}^n) \quad (7)$$

The crystallization parameters of PTrFE polymer crystallized at each temperature are tabulated in Table II.

Table II. Crystallization parameters for PTrFE.

$T_c^{a)}$ (°C)	$n^{b)}$	$t_{1/2}^{c)}$ (min)	$z^{d)}$ (min ⁻ⁿ)
453.0	2.5	0.56	2.95
453.5	2.8	0.70	1.88
454.0	3.1	1.03	0.63
454.5	3.1	1.41	0.245
455.0	2.7	1.70	0.165
455.5	2.6	2.40	0.0712
456.0	2.8	3.80	0.0165
456.5	2.6	5.0	0.0106
457.0	2.5	6.0	7.86×10^{-3}
457.5	2.7	11.5	9.48×10^{-4}
458.0	2.8	16.0	2.95×10^{-4}
458.5	2.5	23.5	2.59×10^{-4}
459.0	2.5	34.0	1.03×10^{-4}

a) T_c , the crystallization temperature.

b) n , the Avrami exponent.

c) $t_{1/2}$, the half-time of conversion.

d) z , the kinetic rate constant.

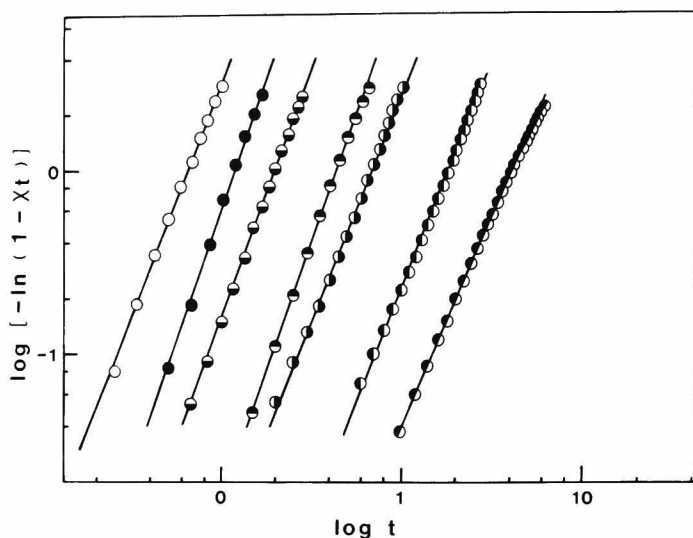


Figure 9. An Avrami plot for PTrFE at various crystallization temperature: ○ , 453.0 °C; ● , 454.0 °C; ◐ , 455.0 °C; ◑ , 456.0 °C; ◒ , 457.0 °C; ◓ , 458.0 °C; and ◔ , 459.0 °C.

4-8 ANALYSIS OF CRYSTALLIZATION RATE

According to the theoretical treatment of coherent surface nucleation in chain fold polymer, given by Hoffman and Lauritzen^{13,17}, the free energy of formation of a nucleus of critical dimensions, $\Delta\phi^*$, may be expressed to a good approximation by

$$\Delta\phi^* = 4b\sigma\sigma_e/\Delta f_v \quad (8)$$

where σ and σ_e are the surface free energies per unit area of the surface parallel and perpendicular, respectively, to the molecular chain direction, and Δf_v the Gibb's free energy difference between the liquid and the crystal. The Δf_v is given by¹³

$$\Delta f_v = \Delta H_u (\Delta T / T_m^\circ) \quad (9)$$

where ΔH_u is the heat of fusion, T_m° the equilibrium melting temperature, and $\Delta T = T_m^\circ - T_m$, the degree of the supercooling.

According to the kinetic theory,^{18,19} the rate of overall crystallization may be expressed by

$$\frac{1}{n} \log Z + \frac{\Delta F^*}{2.3kT_c} = A_n - \frac{\Delta \phi^*}{2.3kT_c} \quad (10)$$

where k is the Boltzmann constant, Z the rate constant in the Avrami equation, and ΔF^* the activation energy for the transport process at interface. By the combination of eq 8, 9, and 10

$$\frac{1}{n} \log Z + \frac{\Delta F^*}{2.3kT_c} = A_n - \frac{4b_o \sigma \sigma_e T_m^\circ}{2.3k\Delta H_u T_c \Delta T} \quad (11)$$

ΔF^* can be obtained by the WLF equation²⁰,

$$\Delta F^* = F_{WLF} = \frac{C_1 T_c}{C_2 + T_c - T_g} \quad (12)$$

where C_1 and C_2 are constant, respectively, equal to 4.12 Kcal/mol and 51.6 deg, which were derived from the universal WLF constants. Figure 10 shows a plot of $(1/n) \log Z$ versus $(T_m^\circ / T_c \Delta T)$ for PTrFE. It was calculated using equation 11 the values of σ and σ_e are 7.3 and 54 erg/cm² (0.24 and 0.79 Kcal/mol), respectively. The value of σ_e obtained from calorimetric method is considerably in good agreement with that of the small angle x-ray diffraction method ($\sigma_e = 1.2$ Kcal/mol). The value of σ_e of PTrFE crystal is also tabulated in Table I

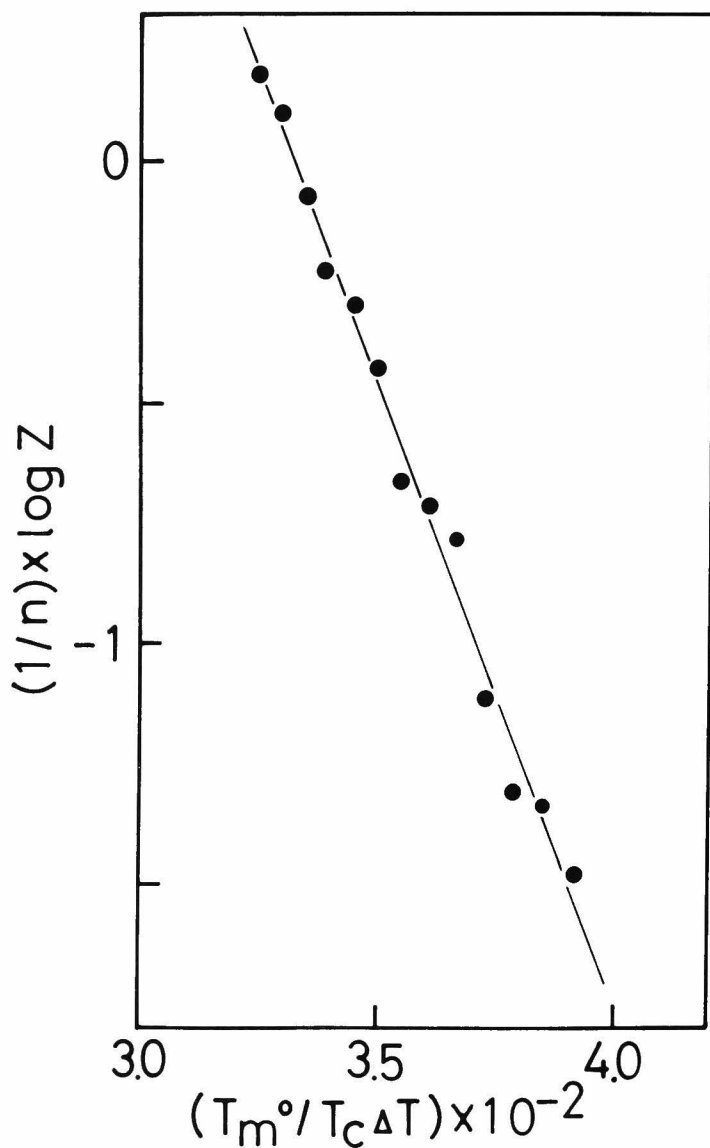


Figure 10. A plot of $(1/n)\log Z$ versus $(T_m^0/T_c\Delta T)$ for PTrFE.

together with that of other fluorinated ethylene polymers.

It is of great interesting to note that the crystals of other fluorinated ethylene polymers also yield comparably values for

σ_e .

REFERENCES

1. T. Yagi, Polym. J., 11, 353 (1979).
2. M.G. Broadhurst, J. Res. Natl. Bur. Stand., 67A, 233 (1963).
3. D.I. Sapper, J. Polym. Sci., 43, 383 (1960).
4. K. Nakagawa, and Y. Ishida, J. Polym. Sci., Phys. Ed., 11, 2153 (1973).
5. G.J. Welch, J. Polym. Sci., Phys. Ed., 14, 1683 (1976).
6. H.W. Starkweather, Jr., and R.H. Boyd, J. Phys. Chem., 64, 410 (1960).
7. A.M. Bueche, J. Amer. Chem. Soc., 74, 65 (1952).
8. P.J. Flory, "Principles of Polymer Chemistry", Cornell Univ. Press, Ithaca, N.Y., 1953.
9. L. Mandelkern, "Crystallization of Polymers", McGraw-Hill, New York, 1964.
10. J.D. Hoffman and J.J. Weeks, J. Res. Natl. Bur. Stand., 66A, 13 (1962).
11. T. Nishi, and T.T. Wang, Macromolecules, 8, 909 (1975).
12. J.D. Hoffman, and J.J. Weeks, J. Chem. Phys., 37, 1723 (1962).
13. J.D. Hoffman, SPE Trans., 4, 315 (1964).
14. C. Mancarella, and E. Martuscelli, Polymer, 18, 1240 (1977).
15. B. Wunderrich, "Macromolecular Physics, Volume 2", Academic Press, 1976.

16. J.I. Lauritzen and J.D. Hoffman, J. Chem. Phys., 31, 1680 (1959).
17. D. Turnbull and J.C. Fisher, J. Chem. Phys., 17, 71 (1949).
18. M.L. Williams, R.F. Landel, and J.D. Ferry, J. Amer. Chem. Soc., 77, 3701 (1955).

CHAPTER 5

CRYSTALLIZATION BEHAVIOR OF TRIFLUOROETHYLENE COPOLYMERS:
ISOMORPHISM REPLACEMENT

5-1 INTRODUCTION

Since Edger and Hill¹ first reported isomorphism behavior with hexamethylene adipamide and terephthalamide copolymers, isomorphism phenomena in macromolecular field have been studied by many authors.¹⁻¹⁴ Usually in binary copolymerization system, the introduction of the second component brings about a reduction in melting point and reduction in crystallinity and increase in solubility. In Flory's theory of copolymer crystallization,¹⁵ it is assumed that in the copolymerization of A and B units the crystal phase is composed entirely of A units, and B units are excluded from the crystal phase and remained in amorphous phase. In this system, as the preferential ordering of copolymer chains is required for crystallization, then the melting point reduction is occurs as a necessary cosequence. In these circumstances melting point - polymer composition curve shows a minimum point at the intermediate ranges of composition. However, several system have been reported in which the melting point-polymer composition curve shows a linear or nearly so without minimum point. In these system, B units are able to pack A crystal without appreciable distortion. The term isomorphous replacement was used to described this phenomenon. It has become widely accepted as a criterion for isomorphous replacement to use a melting point-polymer composition relationship. However, Tranter⁷ has shown that this criterion is not valid for

isomorphism replacement in polyamide. As a result of x-ray diffraction study, he concluded that in a truth isomorphism the lattice parameters and crystallinity should be independent of copolymer composition.

Recently, a theory of copolymer crystallization reveals, on which crystal contains a small concentration of comonomer units.¹⁶⁻¹⁸ Analysis of lattice data of random copolymer crystal confirms the model that the intermolecular distance increases linearly with increasing of concentration of the comonomer units.

In chapter 5, the crystallization behavior of polytrifluoroethylene (PTrFE) was described.¹⁹ The purpose of this chapter is concerned with determination of the crystallization behavior of trifluoroethylene (TrFE) copolymers with vinylidene fluoride (VdF), tetrafluoroethylene (TFE), chlorotrifluoroethylene (CTFE), and hexafluoropropylene (HFP). The details of the experimental results by DSC, x-ray and infrared measurements, and a theory of random copolymer crystallization which shows a isomorphism replacement, will be discussed.

5-2 EXPERIMENTAL

The preparation and microstructure of the TrFE-copolymers with VdF, TFE, CTFE and HFP were described in chapter 1 and 3. List of samples are tabulated in Table I for the TrFE-VdF copolymers, in Table II for the TrFE-TFE copolymers, in Table III for the TrFE-CTFE copolymers, and in Table IV for the TrFE-HFP

Table I. List of sample for the TrFE-VdF copolymers.

Sample no.	VdF mol-% in copolymer	Melting point (°C)	
		As polymerized	Heat pressed ^a
A-1	0	198.3	199.4
A-2	12.5	185.5	185.0
A-3	30	171.6	172.5
A-4	36	167.6	165.7
A-5	44	161.6	163.8
A-6	54	161.6	160.2
A-7	60	155.5	155.2
A-8	63	158.5	160.8
A-9	85	149.6	146.7
A-10	90	142.1	146.7
A-11	98	159.3	159.9
A-12	100	176.1	175.8

^aCooling rate is about 50 °C/min.

Thermal analysis was performed with a differential scanning calirimeter (Perkin-Elmer DSC-2) at a heating rate of 10 °C/min.... Aluminum pan was used as the specimen container and specimen weight was about 10 mg. The temperature calibration was based on indium, tin and lead standard.

Wide angle x-ray diffraction profiles were obtained with a

Table II. List of samples for the TrFE-TFE copolymers.

Sample no.	TFE mol-% in copolymer	Melting point (°C)	
		As polymerized	Heat pressed ^a
B-1	12	214.2	214.4
B-2	17	232.6	225.6
B-3	38	252.5	250.2
B-4	49	275.8	273.0
B-5	77	309.2	307.8
B-6	100	335.7	330.8

^aCooling rate is about 50 °C/min.

Rigaku-Denkin diffractometer. The specimens used for x-ray diffraction measurements were heat-pressed sheets of which the cooling rate was about 50 °C/min. The degrees of the crystallinity were also estimated by x-ray diffraction method.

Infra-red spectra were recorded on a Japan-Spectroscopic IR-G Spectrometer. The specimen films were prepared by heat-pressed method.

Table III. List of samples for the TrFE-CTFE copolymers.

Sample no.	CTFE mol-% in copolymer	Melting point (°C)	
		As polymerized	Heat pressed ^a
C-1	9	163.2	164.2
C-2	18	122.0	122.0
C-3	34	114.8	117.6
C-4	51	132.2	130.0
C-5	71	159.8	160.8
C-6	89	195.2	196.2
C-7	100	215.3	213.5

^aCooling rate is about 50 °C/min.

Table IV. List of samples for the TrFE-HFP copolymers.

Sample no.	HFP mol-% in copolymer	Melting point (°C)	
		As polymerized	Heat pressed ^a
D-1	1	179.1	183.1
D-2	3	148.3	156.0
D-3	9	-	-
D-4	28	-	-

^aCooling rate is about 50 °C/min.

5-3 MELTING TEMPERATURES OF COPOLYMERS

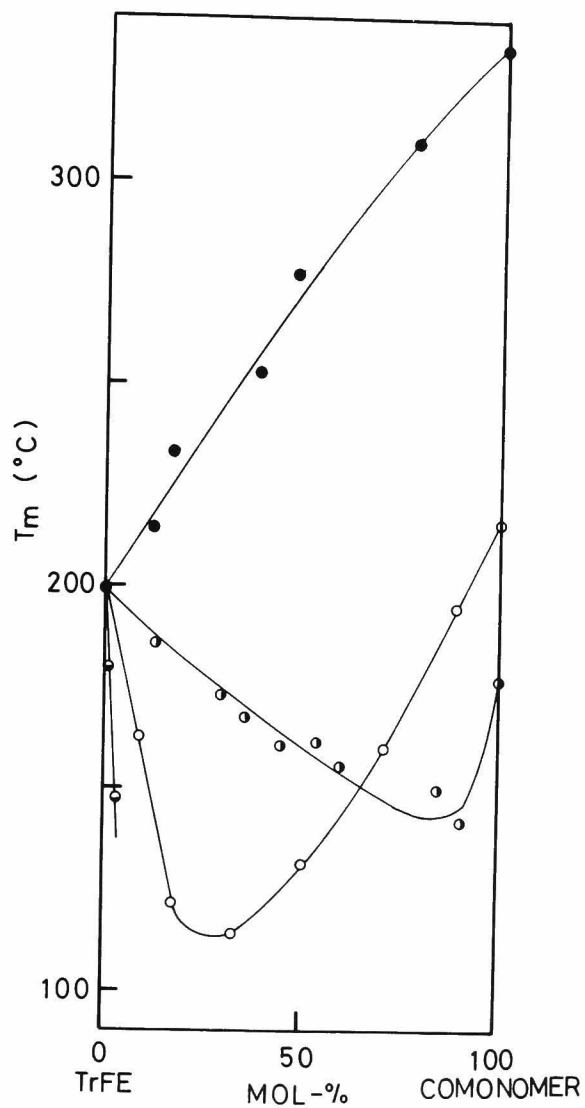


Figure 1. Change of melting temperature T_m with polymer composition: \bullet , TrFE-VdF; \bullet , TrFE-TFE; \circ , TrFE-CTFE; and \bullet , TrFE-HFP.

The melting temperature T_m in both original powder and heat pressed sheet are tabulated in Table I for the TrFE-VdF copolymers, in Table II for the TrFE-TFE copolymers, in Table III for the TrFE-CTFE copolymers and in Table IV for the TrFE-HFP copolymers.

Figure 1 shows the change of T_m with polymer composition for these copolymers.

5-4 TrFE-VdF COPOLYMERS

5-4-1 MELTING TEMPERATURE

Figure 2 shows DSC curves of the TrFE-VdF copolymers. As seen from the figure, the double endothermic peaks (designated T_m and T_m') are observed in VdF-rich copolymers in the region of 54 to 90 mol-% VdF content; T_m is the primary melting temperature which observed at high temperature side, and T_m' the secondary melting temperature observed at lower temperature side. The peak-area ratio of T_m to T_m' is about 8 : 1 at 85 mol-% VdF content.

As is obvious from Figure 2, the endothermic peak of primary melting was observed clearly in whole range of polymer compositions. These results indicate that the TrFE-VdF copolymers are in crystalline state in whole range of polymer compositions. In most random copolymer systems, the introduction of second component usually brings about a reduction in crystallinity.¹⁵

Figure 3 shows the change of melting temperature with polymer composition (data are reproduced from Figure 2). The T_m

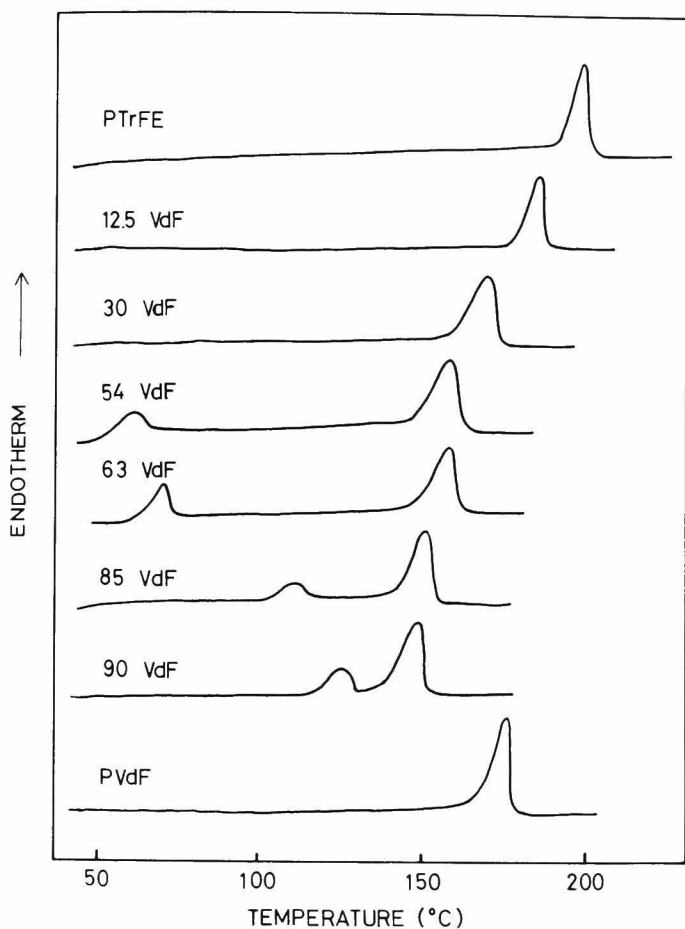


Figure 2. DSC thermograms of TrFE-VdF copolymers.

versus polymer composition curve takes a minimum point at 90 mol-% VdF content. On the other hand, T_m' appears at about 50 mol-% VdF content, the shifts to upper temperature side linearly with increasing VdF content. The extrapolation of the T_m' versus polymer composition curve to 100% VdF gives T_m of PVdF.

It is generally recognized that two endotherms, appear in DSC measurement, arise from two different sources: one is due

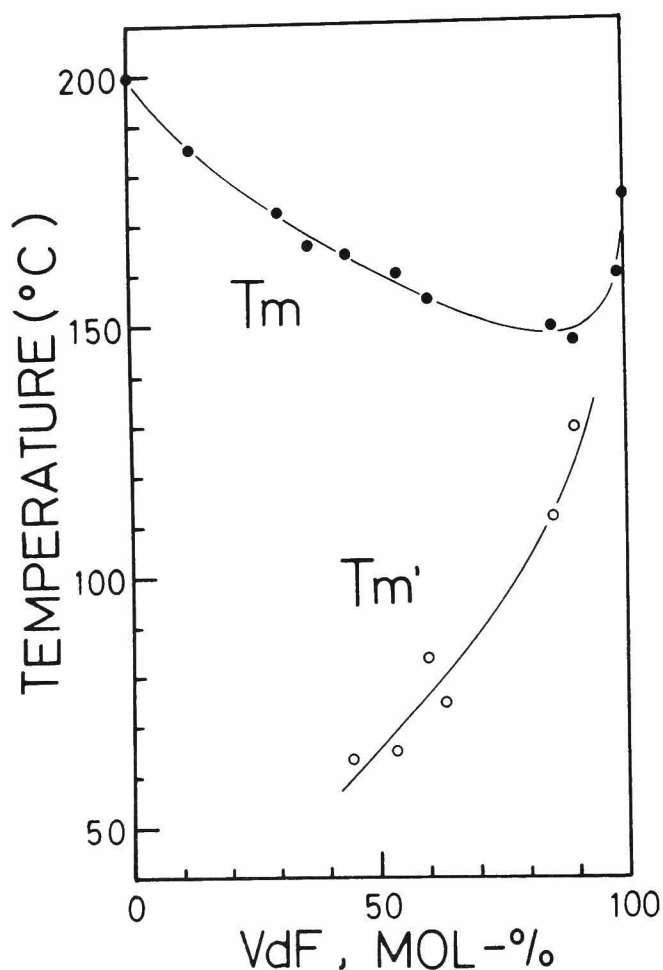


Figure 3. Change of melting temperature, T_m and T_m' , with polymer composition for TrFE-VdF copolymers.

to thermal history of the sample, and the other a common origin in polymer.^{20,21} Examples of thermal history are the recrystallization during cooling after annealing, and the additional crystallization during the DSC measurement. An example of the common origin is a solid phase transition in crystal, a partially melt of crystal phase, or a melting of the crystal phase of polymer which has two crystal phase originally.

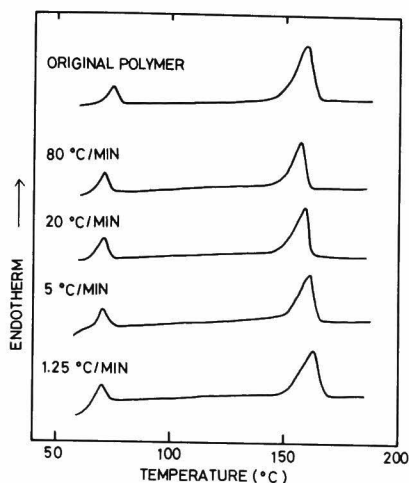


Figure 4. Effect of heating rate on DSC thermograms of sample A-8 (63 mol% VdF).

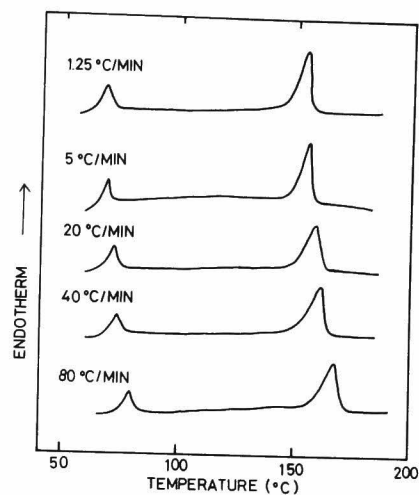


Figure 5. Effect of cooling rate on DSC thermograms of sample A-8 (63 mol% VdF).

Figures 4 and 5 show effect of heating rate and annealing process, respectively, on the apparent melting temperature of sample A-8 (63 VdF content) in DSC measurement. As seen from the figures, both T_m and T_m' are independent of the heating rate and annealing process. These results indicate that the T_m' peak is common origin in TrFE-VdF copolymers. Only difference is that the peak position of both T_m and T_m' peaks shift to upper temperature side with increasing heating rate and decreasing cooling rate. In the case of TrFE-VdF system, a solid phase transition seems to be related to T_m' transition, because T_m' is observed at a comparatively lower temperature, and the temperature difference between T_m and T_m' is large.

5-4-2 CRYSTAL FORM

Poly(trifluoroethylene) (PTrFE) is classified as a high crystalline polymer similar to other fluorinated ethylene polymers as described in chapter 4. The crystal form of PTrFE is not established yet. However, there are some reports claiming that the crystal form is hexagonal and main chain takes helical conformation in crystal.^{22,23} On the other hand, poly(vinylidene fluoride) (PVdF) exhibits three crystal forms²⁴⁻³¹; the α -crystal form (form II) has a trans-gauche-trans-gauche' (TGTG') conformation, and the β -crystal form (form I) has a planar zigzag conformation. The γ -crystal form (form III) is closely similar to the β -form crystal.²⁹ It was indicated that the β -crystal form of PVdF has a spontaneous polarization and a possibility of ferroelectricity.³⁰

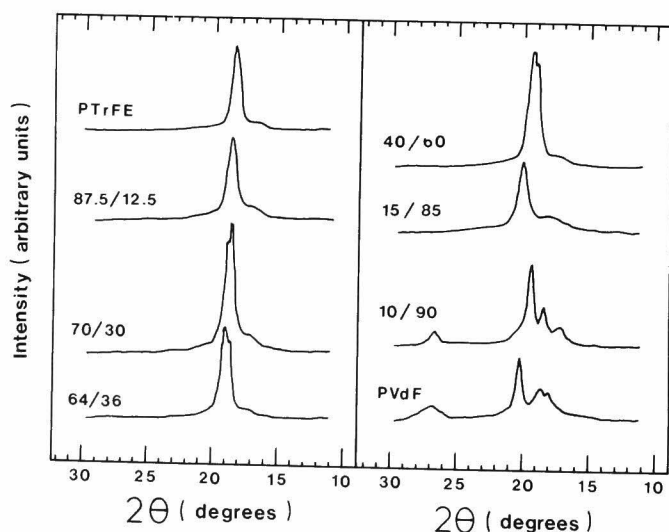


Figure 6. X-ray diffraction profiles of TrFE-VdF copolymers.

Figure 6 shows x-ray diffraction profiles of TrFE-VdF copolymers. As seen from the figure, the diffraction profiles are observed clearly in whole range of polymer composition. These results support the above consideration that the TrFE-VdF copolymer are in crystalline state in whole range of polymer composition. As seen from the figure, the x-ray diffraction profile changes largely between sample 85 and 90 mol-% VdF content. Sample A-12 shows typical profile of α -crystal form of PVdF, showing four strong diffractions.²⁵ The x-ray diffraction profile of sample A-10 resemble to that of PVdF, except for the diffraction angles. The x-ray diffraction profiles of A-1 to A-9 (0 to 85 mol-% VdF content) are quite resemble to each other, and only one strong diffraction is observed. The β -form PVdF shows one strong diffraction at $2\theta = 21.0^\circ$ in x-ray measurement.²⁵ The x-ray diffraction fiber pattern of the 1 : 1 TrFE-VdF copolymer is very poor. This indicates that the copolymer copolymer crystal is very disordered. The head-to-head and tactic defects in polymer chain seem to cause the crystalline defects as mentioned in chapter 4. However, some weak peak diffractions are observed in copolymer, corresponding to those of the β -form PVdF crystal.

A similar crystal form changes of the TrFE-VdF copolymers are also observed in infrared measurement. Figure 7 shows the infrared spectra of the TrFE-VdF copolymers in the region of 600 to 1100 cm^{-1} . Infrared spectrum of sample A-12 shows typical pattern of α -form PVdF.^{30, 31} Sample A-10 also shows a pattern

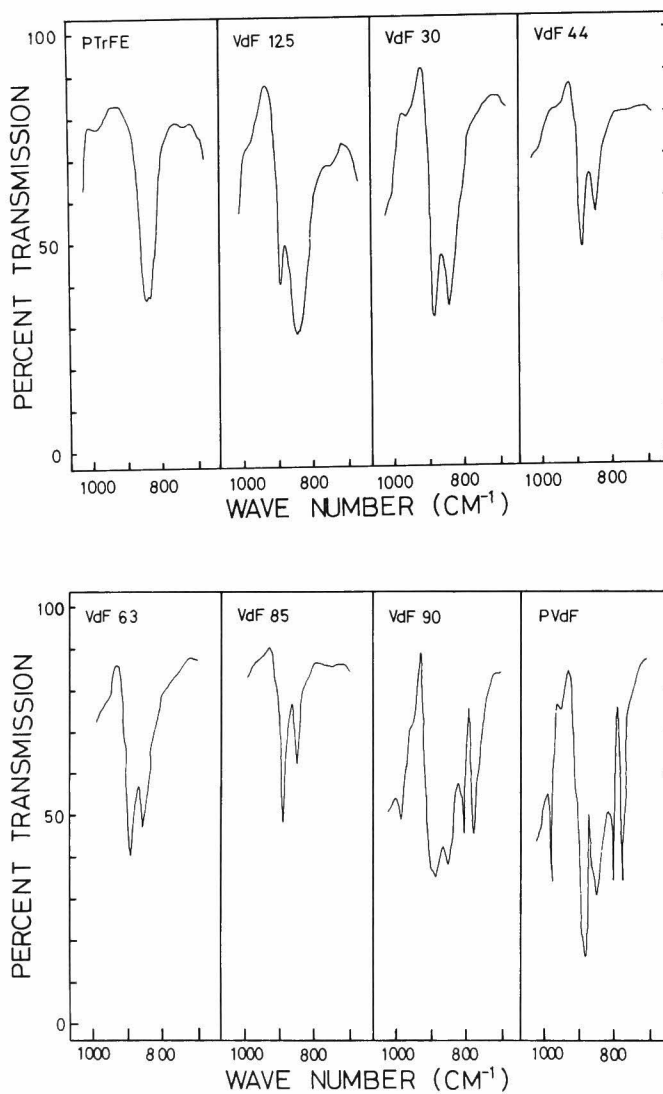


Figure 7. Infrared spectra of TrFE-VdF copolymers in the region from 650 to 1050 cm⁻¹.

of α -form crystal, showing five absorption peaks in the regions of 600 to 1100 cm^{-1} . However, the peak intensity ratios of each peaks are different between sample A-10 and A-12. As seen from Figure 7, the infrared spectrum pattern change largely between sample A-9 and A-10. In sample A-9, only two peaks (885 and 852 cm^{-1}) are observed. The spectrum pattern of this sample is closely similar to that of β -form crystal.^{30,31} Therefore, it is seen that the crystal of the TrFE-VdF copolymers change from α - to β -form between 85 to 90 mol-% VdF content. This result agrees well with the study of x-ray measurements. As seen in Figure 7, the infrared spectra profiles of sample A-2 to A-9 are resemble to each other, and shows a characteristic profiles of β -form crystal. Therefore, it is considered that the TrFE-VdF copolymers take trans or trans-like conformation in crystal in wide range of polymer composition (12.5 to 85 mol-% VdF content). The only difference is that the intensity of absorption peak at 880 cm^{-1} decrease with decreasing VdF content. As seen in Figure 7, the absorption peak in 840 cm^{-1} of 12.5 mol-% VdF copolymer splits into two parts. In sample A-1 (PTrFE), only one peak is observed at about 840 cm^{-1} , and this peak also splits into two parts same as to that of 12.5 mol-% VdF copolymer.

According to the energy calculation of atactic PTrFE crystal by Kolda and Lando,²³ the trans conformation of polymer chain is stable, if the percentage of the head-to-head defects is above 20 %. A high-resolution ^{19}F NMR and simulation studies (described

in chapter 2) indicated that the polymer chain of PTrFE (prepared by radical polymerization method at 22°C) contained about 25 % head-to-head defects. Therefore, it is considered that the probability, that the PTrFE molecules take trans conformation in crystal, is large. According to the electron diffraction study by Gal'perlin and Strogalin,²² the polymer chain of PTrFE takes helical conformation torsioned from trans conformation in crystal.

In conclusion of this section, the crystal form of the TrFE-VdF copolymers can be classified into three parts: (1) TGTG'-conformation (α -form) in PVdF and 90 mol-% VdF copolymer; (2) trans or trans-like conformation (β - or β -like form) in 12.5 to 85 mol-% VdF copolymers; (3) helical conformations in PTrFE. The α - and β -form crystal of PVdF can be transformed into each other by appropriate thermal treatment.²⁴ However, the 1 : 1

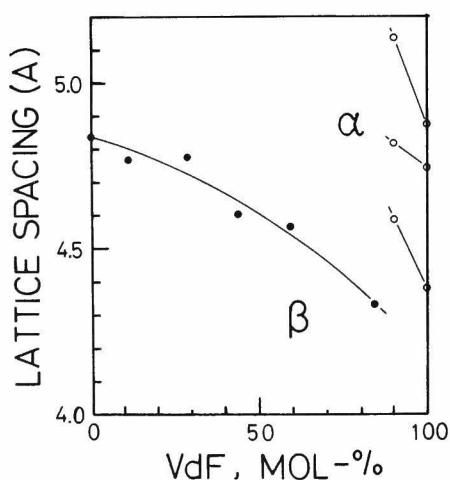


Figure 8. Change of inter-molecular distance (d-space) for TrFE-VdF copolymers.

TrFE-VdF copolymer always shows the β -crystal form and does not transformed into the α -form crystal by any thermal treatments.

Lando and Doll^{2 5} reported that the TrFE-VdF copolymer (83 mol-% VdF content) does not take α -form but β -form in crystal, studying by x-ray diffraction method, and they considered that the rotational barrier between CF_2 and CFH group (in TrFE unit), or CF_2 and CF_2 group (head-to-head structure between TrFE and VdF) prevented to take TGTG' conformation in crystal. Similar change of crystal morphology was also observed in the TFE-VdF copolymers.^{2 5}

Figure 7 shows change of average intermolecular distance (d-space) with polymer composition. In the figure, the symbol α represents TGTG' conformation in crystal; the symbol β represents trans or trans-like conformation in crystal. The length of d-space (the distance of intermolecular in crystal) decreases almost linearly with increasing VdF content, independent of polymer morphology. This result indicates that the TrFE and VdF units dissolve each other in crystal; i.e., the TrFE-VdF copolymer system cocrystallize isomorphically. Usually, much of isomorphism system shows a continuous linear relationship between melting temperature and polymer composition.¹ However, a limited number of copolymer systems are reported in which the isomorphism replacement took place independent of the melting temperature versus polymer composition curve.⁷

This conclusion is also supported by the molecular dimension

of TrFE and VdF units. According to Natta and coworkers,⁹ isomorphism occurs when the dimensions of the isomorphous molecules are slightly different. The van der Waals of fluorine (1.35 Å) is a slightly different from that of hydrogen (1.25 Å), and that C-H and C-F bond distance are not very different (1.10 and 1.35 Å. respectively).^{3,2} So the difference of molecular dimension between TrFE and VdF units is thought to be very little.

In the TrFE-VdF copolymer system, the melting temperature versus polymer composition curve takes minimum point at 90 mol-% VdF content. This point corresponds to the change point of crystal form (α - to β -form).

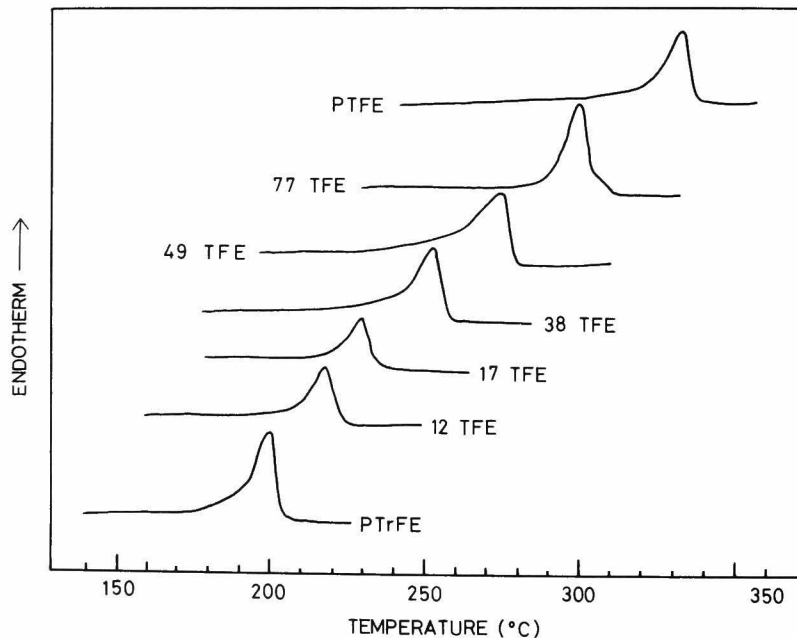


Figure 9. DSC thermograms of TrFE-TFE copolymers.

5-5 TrFE-TFE COPOLYMERS

The DSC endotherms peaks of the TrFE-TFE copolymers were observed clearly and sharply in whole range of polymer composition, as shown in Figure 9. This indicates that the TrFE-TFE copolymers are in crystalline state in whole range of polymer composition. In Figure 1, the change of T_m with polymer composition for the TrFE-TFE copolymer system is shown. As is obvious from the figure, the T_m versus polymer composition curve does not take a minimum point at intermediate polymer composition, but change linearly. This result indicates the existence of isomorphism in the TrFE-TFE copolymer crystal.

Figure 10 shows the x-ray diffraction profiles of PTrFE, 51 : 49 TrFE-TFE copolymers and PTFE. The x-ray diffraction profiles observed clearly and sharply not only in homopolymers but also in copolymer. This results supports the above con-

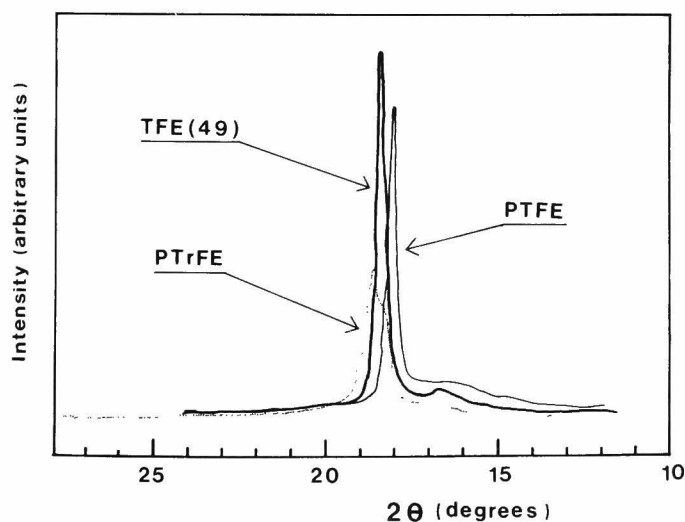


Figure 10. X-ray diffraction profiles of TrFE-TFE copolymers.

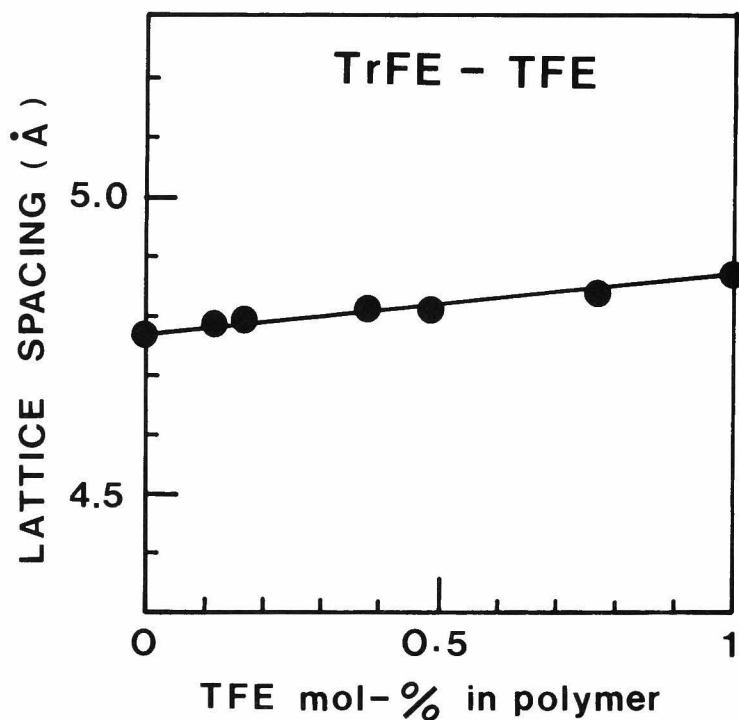


Figure 11. Change of intermolecular distance in crystal (d-space) with polymer composition for TrFE-TFE copolymers.

sideration that the TrFE-TFE copolymers are in crystalline state in whole range of polymer composition. Figure 11 shows the change of intermolecular distance (d-space) with polymer composition. As seen from the figure, the intermolecular distance of PTrFE increases linearly with increasing TFE content. This results also indicates the existence of isomorphism in copolymer crystal.

According to Natta and coworkers,⁹ the main conditions for isomorphism are chemical similarity of molecules; i.e., equal bonding distance between the atoms, and similar van der Waals distance of the atoms or molecules. And in isomorphism system, the copolymers crystallized with lattice constants in between the two homopolymers. As mentioned previous section, the van der Waals radius of fluorine (1.35 Å) was slightly different from that of hydrogen (1.25 Å), and that C-H and C-F bond distance were not very difference (1.10 and 1.35 Å, respectively),³² the difference of the molecular dimension between TrFE and TFE units was thought to be very little, as well as between VF and VDF, and between VDF and TrFE. The both VF-VDF copolymers and the VDF-TrFE copolymers show isomorphism, as mentioned above.

The PTFE crystal takes hexagonal lattice in chain twist by 180 °C at each CF_2 group, between 19 to 30 °C.³³ On the other hand, the crystal form of PTrFE is not established yet. However, there are some reports claiming that the crystal form is hexagonal, as well as PTFE, and main chain takes helical conformation.^{22, 23}

5-6 TrFE-CTFE COPOLYMERS

The change of melting temperature T_m with polymer composition for the TrFE-CTFE copolymers is shown in Figure 1. The T_m versus composition curve takes minimum point at 25 mol% CTFE content. Figure 12 shows x-ray diffraction profiles of the

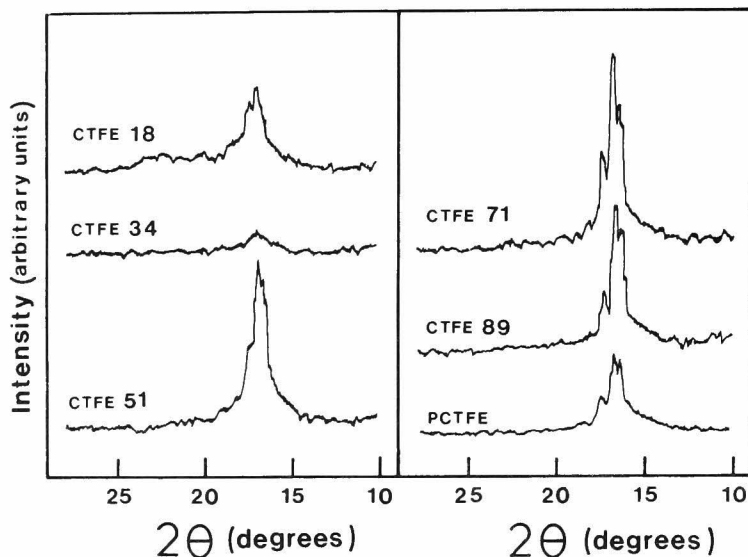


Figure 12. X-ray diffraction profiles for TrFE-CTFE copolymers.

TrFE-CTFE copolymers. The crystal form of poly(chlorotrifluoroethylene) (PCTFE) is hexagonal,^{3 4} similar to PTrFE and PTFE. As seen from Figure 12, the intensities of each diffraction peaks of homopolymer (PTrFE and PCTFE) decrease with increasing comonomer concentration. These results indicate that the degree of crystallinities of homopolymers decrease with copolymerization. Especially, the 34 mol% CTFE copolymers shows a marked reduction of the crystallinity. Therefore, it is seen that the TrFE-CTFE copolymer system does not shows a isomorphism replacement.

5-7 TrFE-HFP COPOLYMERS

The change of melting temperature T_m with polymer composition for TrFE-HFP copolymers is seen in Figure 1. The introduction of HFP units into PTrFE homopolymer seems to cause the reduction of the crystallinity. In sample D-3 and D-4 (9 mol% and 28 mol% CTFE, respectively), T_m does not observed in the DSC measurement. These polymers is rubbery state. According to the literature,³⁵ poly(hexafluoropropylene) is a amorphous polymer.

5-8 THEORY OF ISOMORPHISM

The kinetic theory of random copolymer crystallization suggested by Helfand and Lauritzen is applied to the isomorphism crystal.¹⁷ Consider a random copolymer of A and B with a fraction X_B of B units, and a fraction of $X_A (=1 - X_B)$ of A units. Both homopolymers A and B are in semicrystalline polymers. The molecular dimensions of A and B units are similar to each other, and the copolymers of A and B can cocrystallized isomorphically: i.e., the copolymers are in semicrystalline state in whole range of polymer composition, and each co-unit incorates into the crystal of homopolymers.

Actually, a real copolymer crystal contains a fraction X_B^C of B units in crystal, and a fraction X_A^C of A units in crystal. However, they do not achieve an equilibrium concentration $X_A^{C(eq)}$ and $X_B^{C(eq)}$. The copolymer chain contains the excess enthalpy

ΔH^{ex} due to the interaction between A and B units. In addition, the copolymer crystal contains the excess free energy ϵ due to the crystalline defects which are created by the inclusion of A units in B crystal or the inclusion of B units in A crystal. When the dimensional difference between A and B units is very small, ϵ takes on a small value. According to equilibrium statistical mechanics, the fraction $x_A^{c(eq)}$ of A units in the crystalline region is given by^{17,18}

$$x_A^{c(eq)} = \frac{x_A \exp(-\epsilon\beta)}{(1 - x_A) + x_A \exp(-\epsilon\beta)} \quad (1)$$

where

$$\epsilon\beta = \frac{1}{RT} \quad (2)$$

where R is the gas constant.

The free energy of the copolymers A and B are different from that of polymer blending of homopolymers A and B. Denoting the free energy of random copolymer of A and B, which exhibits the isomorphism replacement, as G, the condition of equilibrium at given temperature T is expressed as

$$G = G_O - T\Delta S_m \quad (3)$$

where G_O is the free energy of the blending of homopolymers A and B, and ΔS_m is the mixing entropy. G_O is given by

$$G_0 = X_A G_{A0} + X_B G_{B0} \quad (4)$$

where G_{A0} and G_{B0} are the free energy of homopolymers A and B, respectively. $-T\Delta S_m$ is given by

$$-T\Delta S_m = R(X_A \ln X_A + X_B \ln X_B) \quad (5)$$

When the copolymer system contains the excess free enthalpy ΔH^{ex} , G is given by

$$G = G_0 - T\Delta S_m + \Delta H^{ex} \quad (6)$$

According to the quasi-chemical model by Guggenheim,^{36, 37} the excess enthalpy is given by

$$\Delta H^{ex} = ZNX_A X_B \omega \quad (7)$$

where Z is the co-ordination number, N is the Avogadro number, and ω is given by

$$\omega = \omega_{12} - (\omega_{11} + \omega_{22})/2 \quad (8)$$

where ω_{11} , ω_{12} and ω_{22} are the interaction energies between A and A, A and B, and B and B, respectively. Equation 7 is rewritten as

$$\Delta H^{ex} = RTX_A X_B K \quad (9)$$

where K is

$$K = \frac{ZN\omega}{RT} \quad (10)$$

combination of eq 5, 6 and 9 yields

$$G = G_0 + RT(X_A \ln X_A + X_B \ln X_B + X_A X_B K) \quad (11)$$

According to the thermodynamics,^{2,9} dG is given by

$$dG = G_A dX_A + G_B dX_B \quad (12)$$

where G_A and G_B are the free energies per mol. of both A and B units in copolymer, respectively. Then, the free energy of copolymer G is given by

$$G = G_A X_A + G_B X_B \quad (13)$$

combination of $X_A = 1 - X_B$, $dX_A = -dX_B$, eq 11 and 12 yields

$$G_A = G - X_B (dG/dX_B) \quad (14)$$

$$G_B = G - X_A (dG/dX_B) \quad (15)$$

combination of equation 4, 11 and 14 leads to

$$G_A = G_{A0} + RT[\ln X_A + K(2X_A - 1)] \quad (16)$$

In the same manner as G_A , the free energy G_A^C of A units in crystalline region is given by

$$G_A^C = G_{A0}^C + RT[\ln X_A^C + K(2X_A^C - 1)] + \epsilon \quad (17)$$

where ϵ is the excess free energy due to the crystalline defects created by the inclusion of B units in A crystal. Combination of equation 16 and 17 yields

$$\Delta G_A^C = \Delta G_{A0}^C + RT[\ln(X_A^C/X_A) + 2K(X_A^C - X_A) + \epsilon/RT] \quad (18)$$

where $\Delta G_A^C = G_A^C - G_A$ is the free energy difference between the crystal and the melt of the copolymer, and $\Delta G_{A0}^C = G_{A0}^C - G_{A0}$ is that of homopolymer A. Near the melting temperature T_m , ΔG_{A0}^C is given by

$$\Delta G_{A0}^C = \Delta H_u^A (1 - T_m/T_m^A) \quad (19)$$

where ΔH_u^A is the heat of fusion of homopolymer A, T_m^A is the melting temperature of homopolymer A, and T_m is the melting temperature of copolymer. Setting $\Delta G_A = 0$ and combination of equation 18 and 19 yield

$$1/T_m^A - 1/T_m = (R/\Delta H_u^A) [\ln (X_A^C/X_A) + 2K(X_A^C - X_A) + \epsilon/RT_m] \quad (20)$$

In the same manner as B units in A crystal, the following equation is also obtained for A units in B crystal

$$1/T_m - 1/T_m^B = (R/\Delta H_u^B) [\ln (X_B^C/X_B) + 2K(X_B^C - X_B) + \epsilon/RT_m] \quad (21)$$

Copolymer crystallization which exhibits isomorphism replacement can be represented by equation 20 and 21. When the interaction energy between A and B units are very small ($\omega \rightarrow 0$), equation 20 and 21 are

$$1/T_m - 1/T_m^A = (R/\Delta H_u^A) [\ln (X_A^C/X_A) + \epsilon/RT_m] \quad (22)$$

$$1/T_m - 1/T_m^B = (R/\Delta H_u^B) [\ln (X_B^C/X_B) + \epsilon/RT_m] \quad (23)$$

As X_A^C and X_B^C approach to the equilibrium concentration $X_A^{C(eq)}$ and $X_B^{C(eq)}$, equation 22 and 23 are reduced to the appropriate free energy of fusion¹⁷

$$1/T_m - 1/T_m^A = (R/\Delta H_u^A) \ln [1 - X_A + X_A \exp(-\epsilon/RT_m)] \quad (24)$$

$$1/T_m - 1/T_m^B = (R/\Delta H_u^B) \ln[1 - X_B + X_B \exp(-\epsilon/RT_m)] \quad (25)$$

Setting $\epsilon=0$ in equation 24 and 25 yield

$$1/T_m - 1/T_m^A = (R/\Delta H_u^A) \ln(X_A^C/X_A) \quad (26)$$

$$1/T_m - 1/T_m^B = (R/\Delta H_u^B) \ln(X_B^C/X_B) \quad (27)$$

when X_A and X_B approach to 1, equation 26 and 27 are reduced to the Flory's equation¹⁵

$$1/T_m - 1/T_m^A = -(R/\Delta H_u^A) \ln X_A \quad (28)$$

$$1/T_m - 1/T_m^B = -(R/\Delta H_u^B) \ln X_B \quad (29)$$

Incorporation of equation 20 and 21 into the expression³⁸

$G-2\sigma_e/\ell=0$ yields the melting temperature $T_m(\ell)$ of the lamellar crystal

$$T_m(\ell) = T_m \left[1 - \frac{2\sigma_e}{\Delta H_u} + \frac{RT}{\Delta H_u} [\ln(X_A^C/X_A) + 2K(X_A^C - X_A) + \epsilon/RT_m] \right] \quad (30)$$

$$T_m(\ell) = T_m \left[1 - \frac{2\sigma_e}{\Delta H_u} + \frac{RT}{\Delta H_u} [\ln(X_B^C/X_B) + 2k(X_B^C - X_B) + \epsilon/RT_m] \right] \quad (31)$$

5-9 MELTING TEMPERATURE VERSUS POLYMER COMPOSITION

When the molecular dimensional difference between A and B is very little, equation 28 and 29 can be used. As mentioned above, dimensional difference between TFE and TrFE is very little. Then, Melting temperatures of the TrFE-TFE copolymers and x_{TrFE}^C were calculated using equation 28 and 29. The heat of fusion employed were 1300 cal/mol for PTrFE^{3,9} and 1370 cal/mol for PTFE.^{4,0} Figure 13 shows change of calculated and observed T_m with polymer composition. As seen from the figure, they agree fairly well.

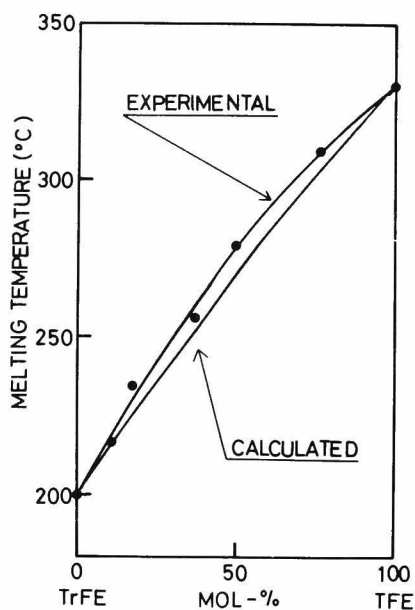


Figure 14. Change of calculated and observed melting temperature T_m with polymer composition, for the TrFE-TFE copolymer system.

Figure 14 shows relationship between X_{TrFE} and $X_{\text{TrFE}}^{\text{C}}$ for the TrFE-TFE copolymer system. In this condition, the relations $X_{\text{TrFE}}^{\text{C}} > X_{\text{TrFE}}$ and $X_{\text{TFE}}^{\text{C}} < X_{\text{TFE}}$ are found. These indicated that the TrFE units have tendency to enter the crystal region compared with TrFE-units.

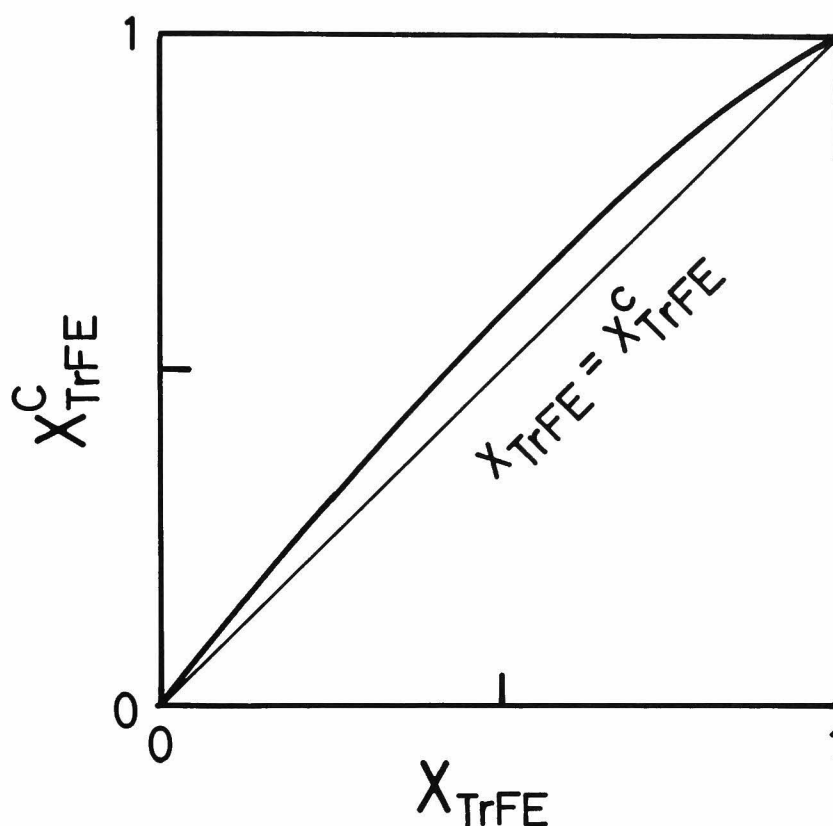


Figure 14. Relationship between the overall fraction of TrFE units X_{TrFE} and that of TrFE units in crystalline region $X_{\text{TrFE}}^{\text{C}}$ for the TrFE-TFE copolymers.

REFERENCES

1. O. B. Edger and R. Hill, J. Polym. Sci., 8, 1 (1952).
2. F. Cramer and R. G. Beaman, J. Polym. Sci., 21, 237 (1956).
3. A. J. Yu and R. D. Evans, J. Amer. Chem. Soc., 20, 5361 (1959).
4. A. J. Yu and R. D. Evans, J. Polym. Sci., 42, 249 (1960).
5. M. Levine and S. C. Temin, J. Polym. Sci., 49, 241 (1961).
6. G. Natta, P. Corradini, D. Sianesi and D. Morero, J. Polym. Sci., 51, 527 (1961).
7. T. C. Tranter, J. Polym. Sci. Part A, 2, 4289 (1964).
8. A. Bell, J. G. Smith and C. J. Kibler, J. Polym. Sci., Part A, 3, 19 (1965).
9. G. Natta, G. Allegra, I. M. Bassi, D. Sianesi, G. Caporiccio and E. Torti, J. Polym. Sci., Part A, 3, 4263 (1965).
10. G. J. Howard and S. Knutton, Polymer, 9, 527 (1968).
11. G. Natta, G. Allegra, I. W. Bassi, C. Carlini E. Chiellini and G. Montagnoli, Macromolecules, 2, 311 (1969).
12. F. R. Prince and E. M. Pearce, Macromolecules, 4, 347 (1971).
13. F. R. Prince and R. J. Fredericks, Macromolecules, 5, 168 (1972).
14. F. R. Prince, E. A. Turi and E. M. Pearce, J. Polym. Sci., Part A-1, 10, 465 (1972).
15. P. J. Flory, "Principle of Polymer Chemistry", Cornell University Press: Ithace, 1953.

16. I. C. Sanchez and R. K. Eby, J. Pes. Natl. Bur. Stand., 77A, 353 (1973).
17. E. Helfand and J. I. Lauritzen Macromolecules, 6, 631 (1973).
18. I. C. Sanchez and R. K. Eby, Macromolecules, 8, 638 (1975).
19. T. Yagi and M. Tatamoto, Submitted to Polym. J.
20. J. P. Bell, P. E. Slade, and J. H. Dumbleton, J. Polym. Sci., Part A-2, 6, 1773 (1968).
21. J. P. Bell, and J. H. Dumbleton, J. Polym. Sci., Part A-2, 7, 1033 (1969).
22. E. L. Galperin, Yu. V. Stroglain, Vysokomolekul. Soedin., 7, 16 (1965); Polym. Sci. (USSR) (English transl.), 7, 15 (1965).
23. R. R. Kolda and J. B. Lando, J. Macromol., Sci., Phys., B11, (1), 21 (1975).
24. Ye. L. Galperin, Yu. V. Strogalin, and M. P. Mlenik, Vsokomol. Soedin., 7, 933 (1965).
25. J. B. Lando, H. G. Olf, and A. Peter, J. Polym. Sci., Part A-1, 4, 941 (1966).
26. J. B. Lando, and W. W. Doll, J. Macromol. Sci., Phys., 2, 205 (1968).
27. W. W. Doll, and J. B. Lando, J. Macromol. Sci., Phys., 2, 309 (1970).
28. R. Hasegawa, Y. Tanabe, M. Kobayashi, and H. Tadokoro, J. Polym. Sci. , Part A-2, 8, 1073 (1970).
29. R. Hasegawa, Y. Takahashi, T. Chatani, and H. Tadokoro, Polym. J., 3, 600 (1972).

30. S. Enomoto, Y. Kawai, and M. Sugita, J. Polym. Sci., Part A-2, 6, 861 (1968).
31. M. Kobayashi, K. Tashiro, and H. Tadokoro, Macromolecules, 8, 158 (1975).
32. L. Pauling, "The Nature of Chemical Bond", Cornell Univ. Press, Ithaca, N. Y., (1961).
33. E. S. Clark and L. T. Muus, Z. Krist., 117, 119 (1962).
34. Z. Mencik, J. Polym. Sci., Polym. Phys. Ed., 11, 1585 (1973).
35. D. W. Brown and L. A. Wall, J. Polym. Sci., Part A-2, 7, 601 (1969).
36. G. S. Rushbrooke, "Introduction to Statistical Mechanics", Oxford, 1951.
37. P. Gordon, "Principle of Phase Diagrams in Material Systems", McGraw-Hill, 1968.
38. I. C. Sanchez and E. A. DiMarzio, Macromolecules, 4, 677 (1971).
39. T. Yagi, Submitted to Polym. J..
40. H.W. Strakeather, Jr., and R.H. Boyd, J. Phys. Chem., 64, 410 (1960).

CHAPTER 6

TRANSITIONS AND RELAXATIONS OF POLY(TRIFLUOROETHYLENE)

6-1 INTRODUCTION

In chapter 2, we have reported the preparation and microstructure of poly(trifluoroethylene) [PTrFE, $-(\text{CF}_2\text{-CFH})_n-$] by a high resolution fluorine-19 NMR spectrometer. It was found that the amounts of abnormal head-to-head, tail-to-tail and tail-to-head linkages in polymer chain were very large.¹ In chapter 4, we have also reported the crystallization behavior of PTrFE. This chapter is concerned with the nature of molecular motions in PTrFE polymers.

It has been widely recognized that the mechanical and dielectric relaxation studies are available for characterization of both semicrystalline and amorphous polymers. It would be of great interest, therefore, to study the relaxation mechanism of fluorinated-ethylene polymers, since these polymers are semicrystalline and the chemical structure of their repeating units is very simple, having no side group or small special group in main chain.

Recently, Choy and coworkers² reported the relaxation of PTrFE for the first time. It was noted that PTrFE exhibits two transitions. They concluded that the upper transition was associated with large scale motion of the main chain and the lower transition was attributed to the limited motion of a few segments of the frozen main chain. However, the spectrum was not analyzed in detail. There exist still some problems as to the nature of transitions and relaxations in PTrFE because of

its complicated solid state structure. For example, attempts to describe the crystallinity dependence on the transition peaks have not been successful.

PTrFE is classified as a highly crystalline polymer similar to other fluorinated-ethylene polymers. But, the crystal form of PTrFE has not been established yet. However, there are some reports claiming that the crystal form is hexagonal and main chain takes helical conformation in crystal.^{3, 4}

The purpose of this chapter is concerned with the transition behavior and motions in PTrFE molecules, by mechanical and dielectric measurements in the temperature range of -150 to 100 °C. This study deals with the influence of crystallinity, molecular weight, cold drawing and copolymerization on the mechanical properties, and frequency dependence of mechanical and dielectric properties of PTrFE polymers.

6-2 EXPERIMENTAL

The preparation and microstructure of PTrFE were described in chapter 1. The physical properties of the samples used in this study are tabulated in Table I. Sample A-2 is the copolymer with vinylidene fluoride (VdF). The detail process of copolymerization was described in chapter 2.

The specimen used for mechanical relaxation measurement were films of about 0.06 to 0.3 mm thickness molded by heat pressed technique. Three specimen with different crystallinities

Table I. Physical properties of samples.

Sample code	$[\eta]^a$ (dl/g)	R_c^b (°C/min)	s_p^c	x_c^d (%)	T_m^e (°C)
A-1-1	5.9	50	1.9905	53	199.4
A-1-2	5.9	ice water quenched		49	198.0
A-1-3	5.9	0.3		73	203.4
A-1H	2.2	50	1.9930	56	201.3
A-2	4.7	50	1.9657		185.0
A-1D ^f					

^aIntrinsic viscosity in dimethylformamide at 30 °C.

^bCooling rate in molding process.

^cSpecific gravity at 23 °C.

^dDegree of crystallinity estimated by x-ray diffraction method.

^eMelting temperature measured by DSC.

^fObtained by cold drawing of sample A-1-1.

were prepared by changing time and temperature of annealing or quenching. The details of the fabrication procedures are given in the third column of Table I. The degrees of crystallinity were estimated by x-ray diffraction method.

Sample A-1D was obtained by drawing sample A-1-1 at room temperature and then annealed at 80 °C for 5 hours under strain. The draw ratio was about 400%. The mechanical relaxation measurements were carried out by means of spectrometer (Iwamoto Seisakusho VES-2) and viscoelastometer (Toyo-Bauldwin Vibron DDV-2) over the temperature range of -120 to 100 °C at various frequencies up to 110 Hz and heating rate of about 0.5 °C/min.

The specimen used for dielectric measurement was heat pressed circular-sheet of 1.03 mm in thickness and 50 mm in diameter. The cooling rate in molding procedure was about 50 °C/min. Aluminum was evaporated on the specimen surface in high vacuum. Dielectric measurement was carried out by means of a transformer bridge (Ando-Denki TR-10) at various frequencies up to 300 kHz and over the temperature range of -150 to 100 °C.

The degree of the crystallinity was estimated by wide-angle x-ray diffraction method, by means of a Rigaku-Denki diffractometer.

The melting temperature was measured by a differential scanning calorimeter (Perkin-Elmer DSC-2) at a heating rate of 10 °C/min. Aluminum pan was used as specimen container and each specimen weight was about 10 mg.

6-3 EXPERIMENTAL

6-3-1 MECHANICAL RELAXATIONS

The dynamic mechanical data in the temperature regions of -150 to 100 °C and at fixed frequency of 35 Hz for each material investigated here are plotted in Figure 1-4. Figure 1 shows temperature dependence of dynamic tensile modulus, E' , and loss tangent, $\tan \delta$, for three samples of PTrFE at different crystallinities. Two transitions were observed as $\tan \delta$ peaks at near 50 °C (designated α) and -20 °C (designated β). Figures 2, 3 and 4 show the effect of molecular weight, cold drawing, and copolymerization with vinylidene fluoride (VdF) on the mechanical properties of PTrFE, respectively.

6-3-2 DIELECTRIC RELAXATIONS

Figures 5 and 6 show the temperature dependence of dielectric constant, ϵ' , and dielectric loss, ϵ'' , in the temperature region of -150 to 100 °C and at indicated different frequencies. Intermediate frequencies are omitted for clearness. Two distinct peaks, α and β , are also observed in the order of decreasing temperature, corresponding to mechanical relaxation data. A rapid increase in ϵ'' observed at high temperature and low frequency is thought to be due to the predominant ionic conductance. Figure 7 shows the transition map of PTrFE, which illustrates the logarithm of frequency versus reciprocal absolute temperature of loss maximum in mechanical and dielectric measurements.

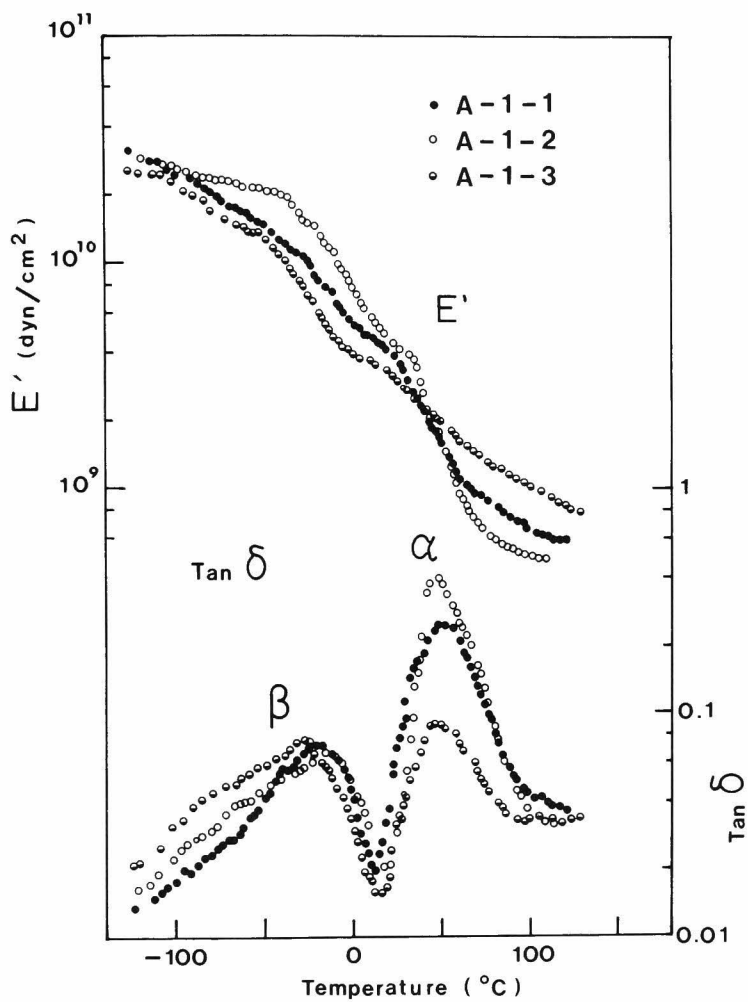


Figure 1. Temperature dependence of dynamic tensile modulus, E' , and loss tangent, $\tan \delta$, for three samples of different crystallinity, measured at 35 Hz: sample A-1-1 (●), A-1-2 (○), and A-1-3 (◐).

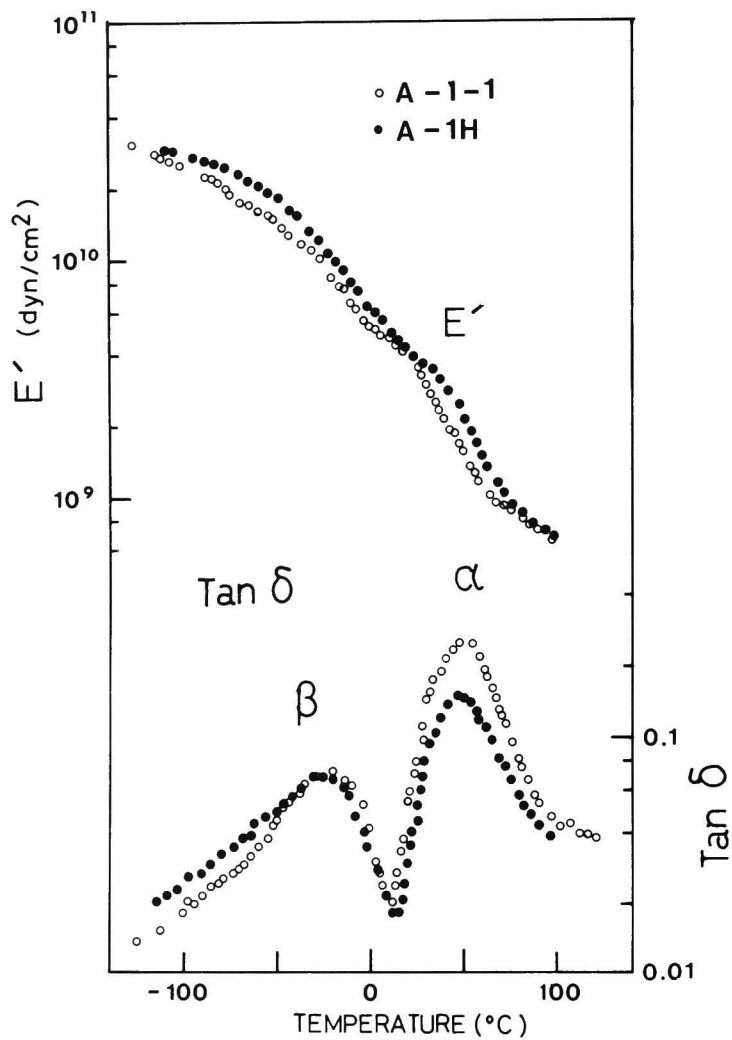


Figure 2. Effect of molecular weight on dynamic mechanical properties of PTrFE measured at 35 Hz: sample A-2 (●), and A-1-1 (○).

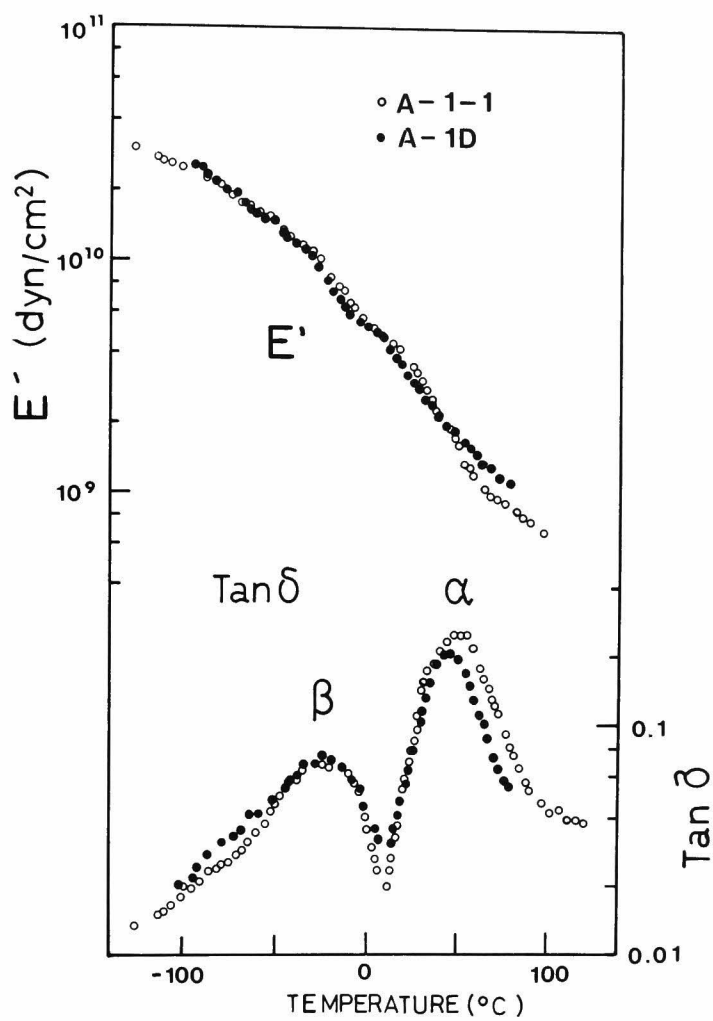


Figure 3. Effect of cold drawing on dynamic mechanical properties of PTrFE measured at 35 Hz: sample A-1D (●) and A-1-1 (○).

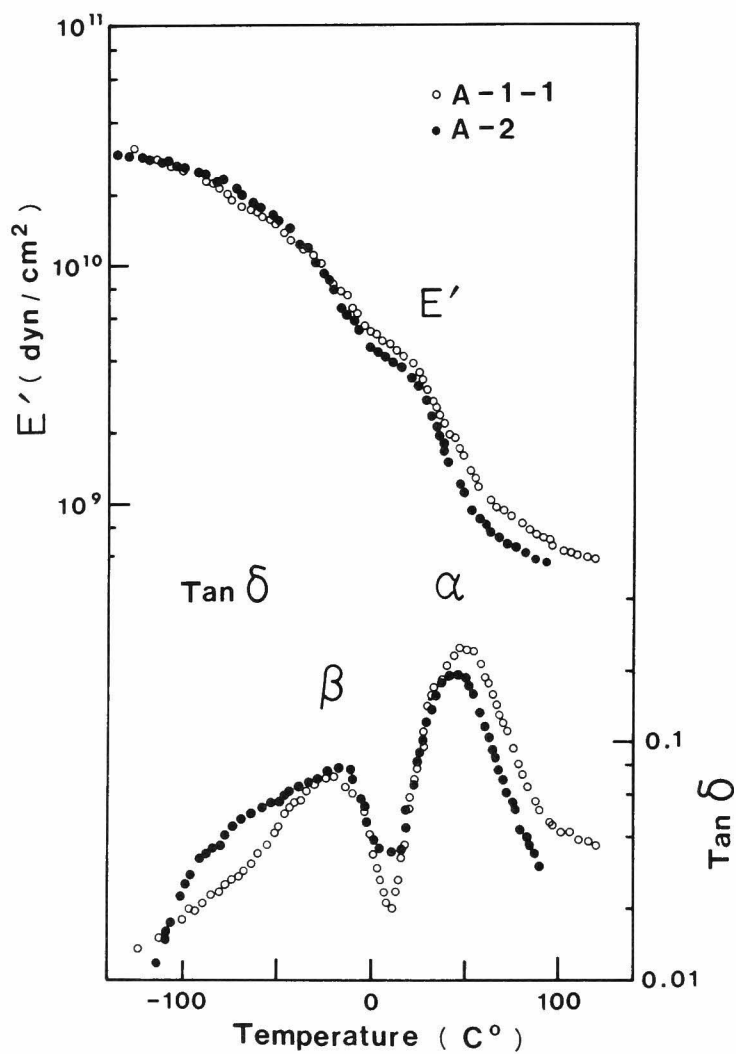


Figure 4. Effect of copolymerization with VdF-monomer on dynamic mechanical properties of PTrFE measured at 35 Hz: sample A-2 (●) and A-1-1 (○).

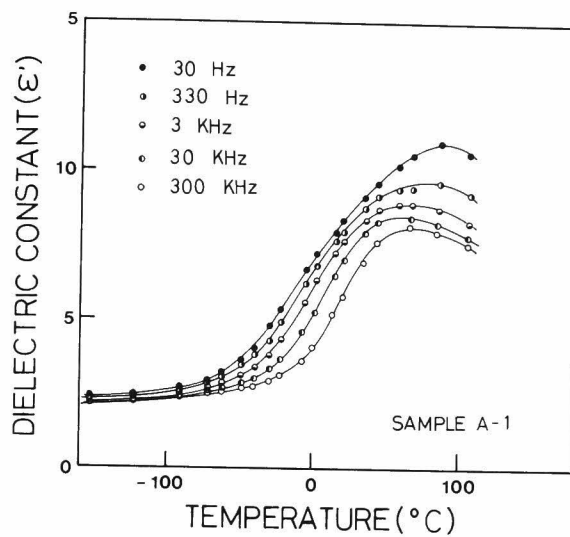


Figure 5. Temperature dependence of dielectric constant ϵ' for PTrFE (sample A-1-1).

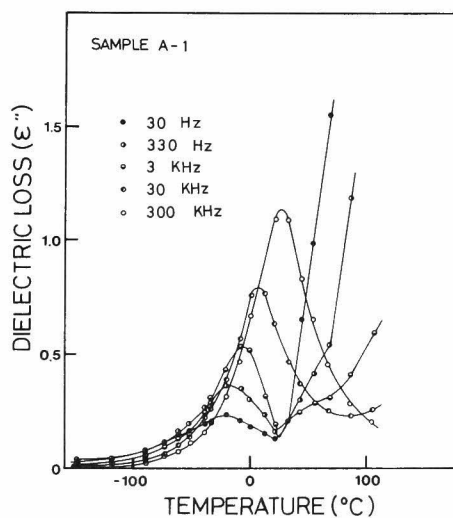


Figure 6. Temperature dependence of dielectric loss ϵ'' for PTrFE (sample A-1-1).

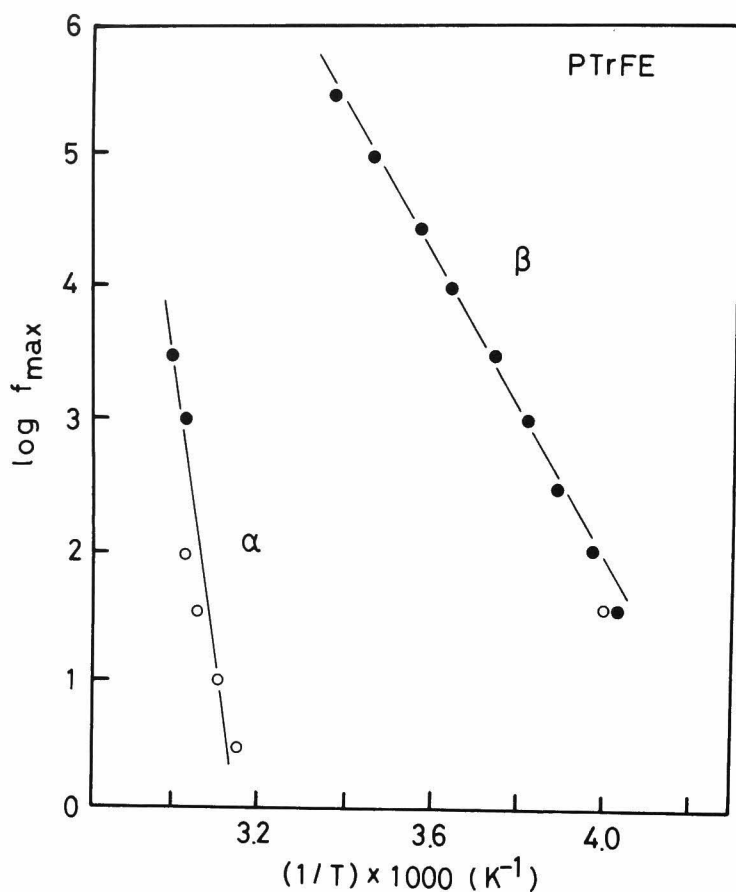


Figure 7. Loss maximum frequency f_{\max} plotted against reciprocal absolute temperature for PTrFE (sample A-1-1). Closed and open circles represent dielectric and mechanical loss, respectively.

6-4 DISCUSSION

6-4-1 α -TRANSITION

As seen from Figure 1, the magnitude of the α -transition peak is about 1.8 times larger than that of the β -transition peak for the sample A-1-1. and the peak form of the α -transition is sharp and symmetrical. Figure 8 shows the dependence of the maximum value of $\tan \delta$ of each transition peak on the degree of

crystallinity. As seen from the figure, the magnitude of the α -transition peak shows a tendency to increase with decreasing the crystallinity of sample. This result indicates that the α -transition reflects molecular motion in amorphous region. On the other hand, the maximum temperature of the β -transition peak is independent of the degree of crystallinity. It is seen that the large drop of E' is observed in the α -transition region. Among three samples of PTrFE, the drop of E' of low-crystallinity sample (sample A-1-2) is notable compared with high-crystallinity sample (sample A-1-3).

Unfortunately, significant specific heat change, indicating the glass-to-rubber transition, could not be observed even in liquid-nitrogen quenched sample of PTrFE (maybe the degree of crystallinity is lower than that of sample A-1-2) by DSC measurement. According to Schuman and coworkers⁵, the

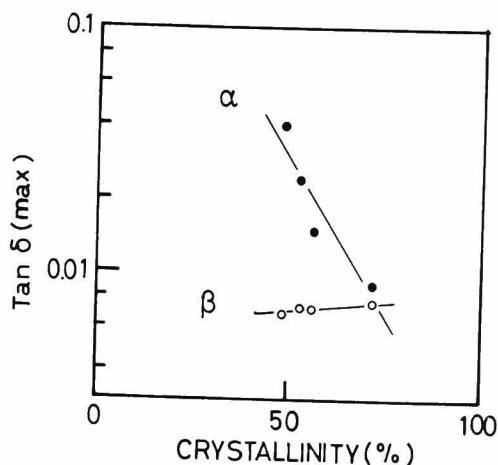


Figure 8. Temperature dependence of maximum value of $\tan \delta$ of the α and β transition peaks in PTrFE.

glass-to-rubber transition of PTrFE occurs at 31 °C, determining by differential thermal analysis measurement. Furthermore, Lee and coworker⁶ found a change in slope of heat capacity in PTrFE at 40 °C, and they took this point as glass-to-rubber transition temperature, T_g. By applying good empirical rule (T_g/T_m) = 2/3, T_g is calculated as 41 °C (T_m is taken as 199.4 °C from Table I). Therefore, it is speculated that T_g of PTrFE may exist between 30 to 40 °C. This conclusion is also supported by the chemical structure of PTrFE. The glass-to-rubber transition of both polar and unsymmetrical polymers, generally shifts to a upper temperature, than the symmetrical ones. For example, poly(chlorotrifluoroethylene) [PCTFE, -(CF₂-CFCl-)_n-] is polar and unsymmetrical polymer, and the difference of the chemical structure from PTrFE is that only chlorine atoms is substituted by a hydrogen atom. T_g of PCTFE polymer is around 52 °C.⁷

As seen from Figure 1, T_g lies on the foot of the α-transition peak and the temperature difference between T_g and the α-transition peak is about 10 to 20 °C. Therefore, the α-transition is reasonably related to glass-to-rubber transition.

The α-transition peak is also observed in dielectric study, as shown in Figure 5 and 6. Because of ionic conductance, well-defined α-transition peak could not be observed except for a few data. Plot of the logarithm of the frequency

versus the reciprocal absolute temperature of loss maximum for the α -transition, obtained by dielectric and mechanical measurement, was given in Figure 7. The curve of $\log f_{\max}$ versus $1/T$ is linear in the limited temperature range of 45 to 75°C. It is difficult to decide whether the α -transition satisfies the WLF equation^{8,9} or not, because employed data are very few. It is generally said that the WLF equation has been able to satisfy the glass-to-rubber transition for noncrystalline polymers. In highly crystalline polymers, the glass-to-rubber transition may occur without holding the WLF theory, because the molecular motion in amorphous region is generally restricted by the crystalline regions. PTrFE can be classified as highly crystalline polymer, as seen from fifth column of Table I.

The activation energy of the α -transition, $\Delta H(\alpha)$, was obtained from a plot of $\log f_{\max}$ versus $1/T$ by use of the following equation

$$\Delta H = -2.303R \, d(\log f_{\max})/(1/T) \quad (1)$$

where R is the gas constant and T is the absolute temperature. The value of $\Delta H(\alpha)$ was found to be about 56 Kcal/mol over the limited temperature range of 43 to 75°C. The ΔH value of primary dispersion in PCTFE is 57 Kcal/mol;¹⁰ this value is closely similar to that PTrFE.

Thus, from these results and discussion, we have assigned the α -transition to the micro-Brownian motion of main chain in amorphous region.

6-4-2 β -TRANSITION

The β -transition peak is observed at $-20\text{ }^{\circ}\text{C}$ by mechanical relaxation technique at 35 Hz, and this peak is lying below T_g . The peak form of the β -transition is broad and unsymmetric.

It is generally said that most linear polymers exhibit one or more secondary transitions below T_g . These transitions are usually assigned to the relaxation of particular molecular motion, such as the movement of the side groups, end groups or small groups within the main chain. As seen from Figure 5, the magnitude of the β -transition peak of PTrFE is not sensibly affected by the degree of crystallinity, at least in the crystallinity range investigated here, compared with the α -transition peak. The peak intensity of the β -transition increases slightly with increasing the crystallinity, showing inverse tendency to the α -transition. Therefore, it is speculated that the β -transition relates not only to the amorphous region but also the crystalline region. Therefore, the β -transition is divided into both components associated with crystal and amorphous regions. These are overlapping. Maximum point of the β -transition peak shifts a little to the upper temperature side with decreasing crystallinity of samples.

It may be noted here that the β -transition peak of these samples is not sensibly affected by the molecular weight, cold drawing and copolymerization with VdF, as seen from Figures 2, 3, and 4. Figure 2 shows the effect of molecular weight on dynamic mechanical properties of PTrFE at fixed frequency of

35 Hz. As seen from the figure, the molecular weight, hence the content of the end groups, does not affect the $\tan \delta$ versus temperature curve. Since PTrFE has no side chain (with the exception of a small number of branches), the process should not be attributed to the end groups but the main chain motions.

As mentioned above, the $\tan \delta$ versus temperature curve of the β -transition peak is unsymmetrical. According to Hoffman and coworkers¹¹ the unsymmetrical loss curve observed in the semicrystalline polymers below T_g is due to the superposition of two relaxation mechanisms, one arises in the crystalline region and the other is associated with the amorphous region. In such a case, the relaxation loss curve is not sensibly affected by the degree of crystallinity. This fact also supports the above speculation that the β -transition of PTrFE relates to the molecular motion in both crystalline and amorphous regions.

Many polymers exhibit the relaxations related with the crystal region in the lower temperature side of T_g . Usually, these are attributed to the local molecular motion of main chains in crystal lattice. And in this molecular motion the crystal structure is not affected by the transition. Hoffman and coworkers¹¹ observed such a relaxation in PCTFE, and attributed it to the chain twisting of "chain end" in crystal lattice. As mentioned above, the "chain end" groups of PTrFE molecular do not affect the β -transition.

Therefore, it is considered that other kinds of defects cause the crystalline relaxation in the β -transition region.

According to Galperin³ and Lando⁴, the crystal structure of PTrFE is very disordered, studying by electron and x-ray diffraction methods. The ^{19}F NMR results¹² indicate that the abnormal head-to-head, tail-to-tail and tail-to-head linkages are predominant in PTrFE molecule. It is considered that these defects remain in crystal lattice as holes, because the van der Waals radius of fluorine is larger in some extent than that of hydrogen, and the C-F bond distance is also to some degree longer than the C-H bond distance. Therefore, the crystal of PTrFE is thought to contain many crystalline defects. Although the evidence is not so complete as one might as wish, these defects are thought to cause the crystal relaxation in the β -transition region largely.

In broad-line NMR measurement of PTrFE,¹³ a narrow line component appears at about -60°C and narrows largely in the temperature region of the β -transition. This indicates the onset of the local molecular motion in amorphous region. The β -transition peak is also clearly observed in dielectric relaxation measurements, as seen in Figures 5 and 6. Plot of the logarithm of the frequency versus reciprocal absolute temperature of loss maximum for the β -transition is seen in Figure 7. The curve of $\log f_{\text{max}}$ versus $1/T$ is linear (Arrhenius type). The activation energy of the β -transition,

$\Delta H(\beta)$, was calculated as 28 Kcal/mol, using eq 1. This value seems to be considerably large compared with those of other linear polymers for secondary transition. The activation energy of the halogenated-ethylene polymers in the secondary transition region is usually 10 to 20 Kcal/mol: for example, $\Delta H(\beta)$ is 18 Kcal/mol for polytetrafluoroethylene [PTFE, $-(CF_2-CF_2-)_n-$]¹⁴; 16.8 Kcal/mol for PCTFE¹¹; 12 Kcal/mol for PVdF; 15 Kcal/mol for polyvinyl chloride [PVC, $-(CH_2-CHCl-)_n-$]¹⁶. Therefore, it is speculated that the comparatively large scale molecular motion, corresponding this high value of $\Delta H(\beta)$ of PTrFE should arise in this β -transition region.

As seen from Figure 5, the dielectric constant, ϵ' , increases rapidly in the β -transition region and shows very large value of ϵ' at room temperature (i.e. below T_g); $\epsilon' = 7.5$ at 22 °C and 1 KHz. The dipole moment, μ , of the repeating unit of PTrFE is very large similar to that of other fluorinated-ethylene polymers; μ is 1.63 Debye for the repeating unit of PTrFE. The details of the estimation of μ will be discussed in the following section. It is generally said, the large value of ϵ' found in solid polymer is closely related to the large-scale dipole motion in amorphous region. Therefore, it is difficult to consider that the limited molecular motion of main chain, such as vibrational motions about their equilibrium position, results in high value of ϵ' at room temperature. The comparatively large scale molecular

motion for the local molecular motion is thought to occur in the β -transition region enough to orient the dipole in electric field, which is different from the cooperative micro-Brownian motion of main chain responsible for the α -transition. In same manner as ϵ' , the dynamic tensile modulus of PTrFE also changes largely in the β -transition region, as seen from Figures 1, 2, and 3. Therefore, we would like to consider that the comparatively large scale molecular motion for the local molecular motion may occur in amorphous region in the temperature region of the β -transition.

Another type of PTrFE was prepared at about -50°C using a alkylboron as an initiator, so that the amount of head-to-tail structure is proportional to the polymerization temperature. However, the high molecular weight polymer was not obtained enough to give the film strong enough to measure the mechanical properties. Therefore, we can not estimate experimentally whether the β -transition is cooperative type or not.

From the above results and discussion, we have tentatively assigned that the β -transition of PTrFE is related to local molecular motion in both amorphous and crystal regions, associated with the comparatively large scale molecular motion for the local molecular motion in amorphous region and with the molecular motion due to the crystal defects in crystal region.

6-4-3 EFFECT OF COLD DRAWING

The temperature dependence of mechanical relaxation of cold drawn PTrFE (sample A-1D) is shown in Figure 3. By cold drawing process, the intensity of the α -transition peak decreases a little and the maximum temperature of peak shifts to the low temperature side, while that of the β -transition peak remains unchanged. It is speculated that the decrease of intensity of the α -transition peak is due to the increase of the crystallinity of sample by cold drawing process. Sometimes, a new transition peak is observed by drawing process due to the orientation of polymer chain in amorphous region¹⁷⁻¹⁸. However, such a peak could not be observed in the cold drawn PTrFE polymer.

6-4-4 EFFECT OF COPOLYMERIZATION

Figure 4 shows the mechanical relaxation data of TrFE-VdF 87.5 : 12.5 copolymer (sample A-2). In such a polymer composition, the shape of $\tan \delta$ versus temperature curve does not change sensibly and resemble to that of PTrFE of sample A-1-1. The differences are that the α -transition peak is slightly displaced at the low temperature side, whereas its intensity decreases a little, and the β -transition peak is also slightly displaced at the upper temperature side, whereas its intensity remains unchanged. As seen from the figure, a new peak due to the copolymerization modification does not

observed in $\tan \delta$ versus temperature curve like a PVC.¹⁹

6-4-5 FURTHER COMMENTS ON TRANSITIONS OF PTrFE

As mentioned above, two transitions (α and β) were observed in PTrFE polymers. The tendency of $\tan \delta$ versus temperature curve, observed in the mechanical relaxation study, closely resembles to those of the other fluorinated-ethylene polymers, such as PCTFE,²⁰ and polyvinyl fluoride [PVF, $-(\text{CFH}-\text{CH}_2-)_n-$].²¹ These polymers exhibit the crystal transition at the high temperature side in the high crystallinity samples or single-crystal mats. However, such a peak was not observed in PTrFE even in high crystallinity sample (A-1-1).

6-4-6 DIPOLE MOMENT OF REPEATING UNIT OF PTrFE

The chemical structure of repeating unit of PTrFE is similar to trifluoroethane. However, the dipole moment μ of trifluoroethane has not been reported in the literature yet. Table II tabulated the bond moment of C-H and C-F, and the dipole moment of fluorinated methanes.¹⁵ It is seen that the effective dipole moment of $-\text{CF}_2-$ group is similar to that of CF_2H_2 , $-\text{CFH}-$ to CFH_3 , and $-\text{CH}_2-$ to CH_4 . Therefore, it is considered that μ of the repeating unit is 1.96 Debye for PVdF and 1.79 Debye for PVF.

Although it seems oversimplified the dipole moment of the repeating unit of PTrFE was calculated by assuming a vectorial sum of the bond moments. There are three conformations in the

Table II. Dipole moment of the fluorinated methanes; inductive effect of fluorine substitution on the bond moment. Data are taken from ref. 15.

Compound	Bond moment (Debye)		Total moment of molecule (Debye)
	C-H - +	C-F + -	
CH ₄	0	-	0
CFH ₃	0	1.81	1.79
CF ₂ H ₂	0.23	1.45	1.96
CF ₃ H	0.32	1.22	1.64

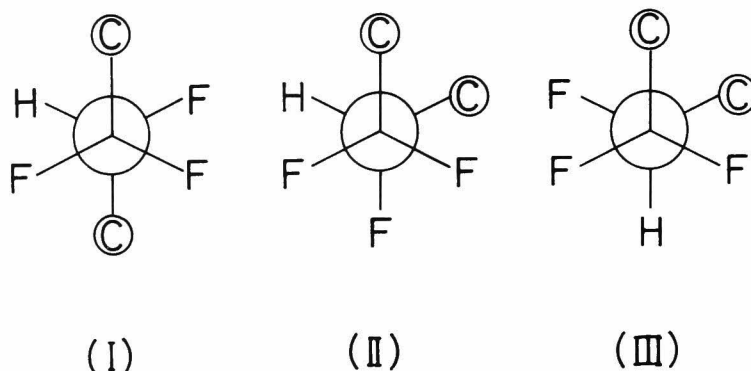


Figure 9. Three conformations of the repeating units of PTrFE. The conformation (I) and (III) are less polar, and conformation (II) is more polar.

repeating unit of PTrFE, as shown in Figure 9. The value of the C-F bond moment is taken as 1.81 Debye for -CFH- group and 1.45 Debye for $\text{-CF}_2\text{-}$ group, from Table II. It was calculated that μ of the repeating unit of PTrFE was 1.63 Debye for conformations (I) and (III), and 3.25 Debye for conformation (II). The conformations (I) and (III) are less polar and (II) is more polar. Among these three conformations, the steric hindrance of conformation (II) seems to be larger than of the other conformations. According to the results of the conformational analysis of atactic PTrFE by Colda and Lando⁴, the trans-conformation is more stable than TGTG'-conformation. Therefore, the effective dipole moment of repeating unit of PTrFE is thought to be approximately 1.63 Debye in practice. As is obvious from Table II, this value is similar to that of trifluoromethane.

6-4-7 ANALYSIS OF DIELECTRIC PROPERTIES IN β -TRANSITION

Figure 10 shows the frequency dependence of ϵ'' for PTrFE of sample A-1-1 at various temperatures. The curves of ϵ'' versus frequency seems to fit Cole-Cole equation.²² Figure 11 shows the temperature dependence of the Cole-Cole's parameter β and magnitude of dielectric relaxation $T\Delta\epsilon$ ($\Delta\epsilon = \epsilon_0 - \epsilon_\infty$). T is the absolute temperature. ϵ_0 is the static dielectric constant and ϵ_∞ is the dielectric constant at very high frequency at which the orientation of any dipole does not take

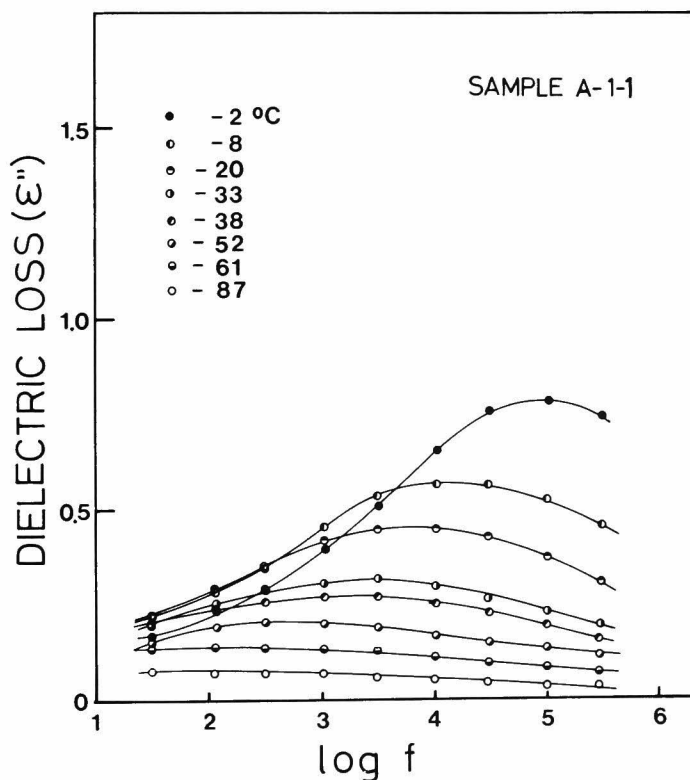


Figure 10. Frequency f dependence of dielectric loss ϵ'' for PTrFE (sample A-1-1) at various temperature.

place. The numerical values of both β and $\Delta\epsilon$ were estimated by Cole-Cole plot. In Figure 11, $T\Delta\epsilon$ was adopted instead of $\Delta\epsilon$ in order to remove the influence of temperature on $\Delta\epsilon$. As is seen from the figure, the value of β increases linearly with increasing temperature. This result indicates that the distribution of relaxation times increases gradually with increasing temperature. The value of $T\Delta\epsilon$ also increases slowly with

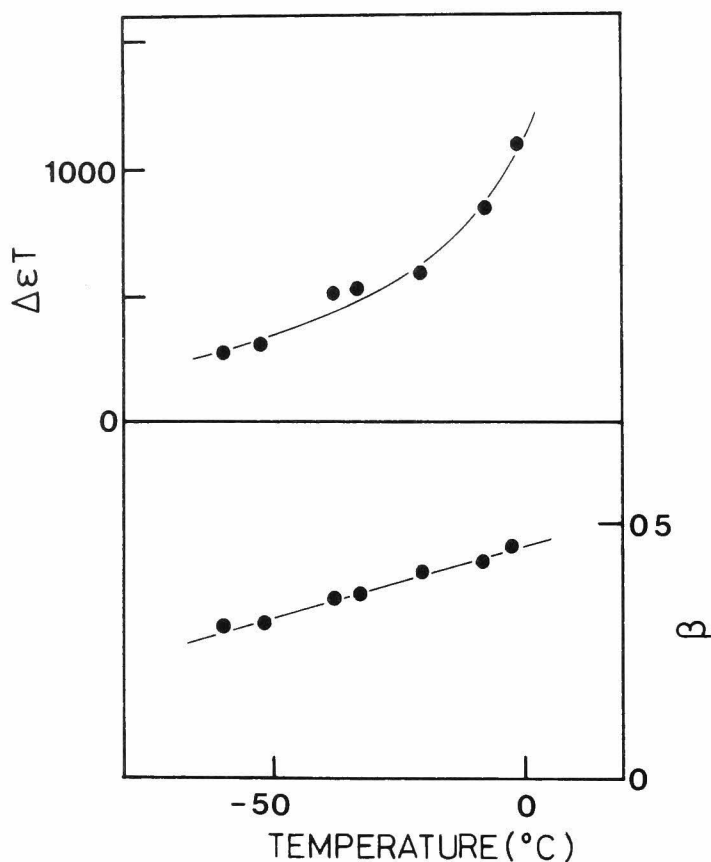


Figure 11. Variations with temperature of the Cole-Cole distribution parameter β and the magnitude of relaxation $\Delta\epsilon T$ in the β -transition region for PTrFE.

increasing temperature in the region of -50 to 0°C. These temperature regions are considered to correspond to the β -transition region of PTrFE.

For evaluation of the dipole moment of polymer molecules, the Frölich-Kirkwood theory^{2,3} is usually used. According to their theory, the dielectric permittivity is expressed by

$$\Delta\epsilon = \epsilon_0 - \epsilon_\infty = \frac{3\epsilon_0}{2\epsilon_0 + \epsilon_\infty} \frac{4\pi N}{3kT} \left(\frac{\epsilon_0 + 2}{3}\right)^2 g_r \mu_0^2 \quad (2)$$

where N is the concentration of the repeating unit, μ_0 the dipole moment, g_r the Kirkwood reduction factor which is expressed as an average of the spacial orientation, k the Boltzmann constant, and T the absolute temperature. The value of ϵ_0 and ϵ_∞ were estimated by Cole-Cole plot. The value of μ_0 is taken as 1.63 Debye for the repeating unit of PTrFE. The g_r is calculated by assuming that μ_0 arises mainly from the dipole orientation in amorphous region. Therefore, N is given as follow:

$$N = N_A X_a / M_0 V_s \quad (3)$$

where N_A is the Avogadro's number, M_0 the molecular weight of repeating unit, V_s the specific volume, and X_a the weight fraction of amorphous region. The values of V_s and X_a are taken from Table I. The calculated values of $\mu^2 (= g_r \mu_0^2)$ and g_r are tabulated in Table III together with ϵ_0 , ϵ_∞ , and $\Delta\epsilon$. From these results, it is speculated that the free dipole rotation of PTrFE molecules does not occur in the β -transition region, since the g_r value takes small value in these temperature region.

Table III. Values of the Kirkwood reduction factor, g_r , of PTrFE in the temperature region of the β -transition.

Temperature (°C)	ϵ_∞	ϵ_0	$\Delta\epsilon$	$\bar{\mu}^2$	g_r
-60	2.54	3.65	1.11	0.44	0.16
-38	2.55	4.70	2.15	0.89	0.34
-20	2.80	5.55	3.20	1.06	0.40
-2	3.05	7.15	4.10	2.02	0.76

REFERENCES

1. T. Yagi, Polym. J., 11, No. 5, 353 (1979).
2. C.L. Choy, T.K. Tse, S.M. Tsui and B.S. Hsu, Polymer, 16, 501 (1975).
3. E.L. Galperin and Yu. V. Strogalin, Vysokomolekul. Soedin., 7, 16 (1965); Polymer Sci. (USSR) (English transl.), 7, 16 (1965).
4. R.R. Kolda and J.B. Lando, J. Macromol. Sci., Phys., B11, (1), 21 (1975).
5. P.D. Schuman, E.C. Stumpand and G. Westmoreland, J. Macromol. Sci., B1(4), 815 (1967).
6. W.K. Lee and C.L. Choy, J. Polym. Sci., Polym. Phys. Ed., 13, 619 (1975).
7. J.D. Hoffman and J.J. Week, J. Chem. Phys., 37, 1723 (1962).
8. W.L. Williams, F.F. Landel and J.D. Ferry, J. Amer. Chem. Soc., 77, 3701 (1955).
9. J.D. Ferry, "Viscoelastic Properties of Polymers", Wiley, New York, 1961.
10. T. Nakajima and S. Saito, J. Polym. Sci., 31, 423 (1958).
11. J.D. Hoffman, G. Williams and E. Passaglia, J. Polym. Sci., Part C, 14, 173 (1966).
12. T. Yagi and M. Tatemoto, Polym. J., 11, No 6, 429 (1979).
13. W.P. Slichter, J. Polym. Sci., 24, 173 (1957).
14. N.G. MacCrum, B.E. Read and G. Williams, "Anelastic and Dielectric Effects in Polymeric Solids", John and Wiley,

1967.

15. P. Hedvig, "Dielectric Spectroscopy of Polymers" Adam Hilger, 1977.
16. Y. Ishida, Kolloid-Z, 168, 29 (1960).
17. K. Kawasaki and Y. Wada, Japan J. Appl. Phys., 6, 100 (1967).
18. F. Krum and F.H. Müller, Kolloid-Z., 164, 81 (1959).
19. G. Pezzin, G. Ajroldi and C. Garbuglio, J. Appl. Polym. Sci., 11, 2553 (1967).
20. J.M. Crissman and E. Passaglia, J. Polym. Sci., Part C, 14, 237 (1966).
21. N. Kawasaki and T. Hashimoto, J. Polym. Sci., A2, 9, 2095 (1971).
22. K.S. Cole and R.H. Cole, J. Chem. Phys., 9, 314 (1941).
23. H. Frölich, "Theory of Dielectrics", Oxford Univ. Press, 1958.

CHAPTER 7

TRANSITIONS AND RELAXATIONS OF VINYLIDENE
FLUORIDE - TRIFLUOROETHYLENE COPOLYMERS

7-1 INTRODUCTION

In chapter 6, the transitions and relaxations of polytrifluoroethylene [PTrFE, $-(CF_2-CFH-)_n-$] by mechanical and dielectric measurements were described.¹ It was found that PTrFE exhibited two transitions with peaks at 50°C and -20°C in mechanical relaxation measurement at 35 Hz; the upper-transition was assigned to micro-Brownian motion of main chain in the amorphous region, and lower-transition was assigned to local molecular motion in both the amorphous and crystalline regions. The glass transition temperature of PTrFE is around 40°C.¹⁻³

The relaxation mechanism of polyvinylidene fluoride [PVdF, $-CF_2-CH_2-)_n-$] has been studied in detail by mechanical⁴⁻⁶, dielectric^{5,7-15}, and NMR¹⁶⁻¹⁸ methods. PVdF polymer exhibited three transitions with peaks at 50°C (designated as α), -35°C (designated as β), and -80°C (designated as γ). According to these studies the α -transition was assigned to molecular motion in crystalline region including lamellar surface and crystalline the defects; the β -transition was assigned to micro-Brownian motion in the amorphous region; the γ -transition was assigned to local molecular motion in the amorphous region. The glass transition temperature of PVdF is around -40°C.¹¹⁻¹⁹

The purpose of this chapter is concerned with the determination of transition behavior and molecular motion in trifluoroethylene(TrFE)-vinylidene fluoride(VdF) copolymers, by mechanical and dielectric measurements in the temperature range from -150°C to 100°C.

7-2 EXPERIMENTAL

The preparations of samples were described in chapter 1, and crystallization parameters were described in chapter 5. Table I shows the physical properties of the TrFE and VdF copolymer.

Mechanical relaxation measurements were carried out by means of the viscoelastometer (Toyo-Bowldwine Vibron DDV-2 and Iwamoto Seisakusho Spectrometer VES-2) over a temperature range from -120 to 100°C and a frequency range from 3 to 110 Hz, at a heating rate of about 0.5°C/min. The specimens used for mechanical relaxation measurements were films about 0.05 to 0.5mm thickness molded by heat-pressed method. In sample A-5 (TrFE-VdF 56 : 44), three different crystallinity specimens were prepared by changing time and temperature of annealing or quenching. The details of the fabrication procedures are given in Table I.

Dielectric measurements were carried out by means of a transformer bridge (Ando-Denki TR-10C) at frequencies from 30 Hz to 300 KHz and over a temperature range from -150 to 100 °C. The specimens used for dielectric measurements were heat-pressed circular-sheet of 1.0 to 1.3mm thick and 50mm diameter. Aluminium was evaporated on the specimen surface in high vacuum.

The linear thermal expansion was measured by use of a quartz-tube dilatometer. The cylindrical specimen for linear thermal expansion was of about 10mm high and 7mm diameter, and

which was annealed for 30 hours at 100 °C in order to remove the strain.

Table I. Physical properties of the TrFE-VdF copolymers.

Sample code	VdF content (mol-%)	[η] (dl/g)	R ^a (°C/min)	sp ^b	X _C ^c (%)
A-1	0	5.9	50	1.9905	53
A-2	12.5		50	1.9657	
A-3	30	3.6	50	1.9385	
A-4	36	2.1	50	1.9296	
A-5-1	44	1.8	50	1.8927	64
A-5-2	44	1.8	ice water quenched		57
A-5-3	44	1.8	0.3		76
A-6	54	4.7	50	1.8943	
A-7	60	5.1	50	1.8859	
A-8	63	2.3	50	1.8806	
A-9	85	2.7	50	1.8663	
A-10	90		50	1.8206	
A-11	98	3.8	50	1.7852	
A-12	100	2.0	50	1.7560	

^aCooling rate in molding process.

^bSpecific gravity measured at 23 °C.

^cDegree of the crystallinity obtained by wide-angle x-ray diffraction measurement.

7-3 VdF-RICH COPOLYMERS

Figure 1 shows temperature dependence of dynamic tensile modulus, E' , and loss tangent, $\tan \delta$, for the VdF-rich copolymers (sample A-9 and A-10) and Poly(vinylidene fluoride) (PVdF) (sample A-12). The α -transition peaks in PVdF becomes clearly and sharply with increasing TrFE content in the copolymer, and its peak position shifts to lower temperature side. On the contrary, the peak intensity decreases with increasing TrFE content. The shape of the β -transition peak in PVdF also change sharply with increasing TrFE content, and its position shifts to high temperature side. The intensity of the β - and γ -transition peaks decrease largely with increasing TrFE content. The dynamic tensile modulus E' of the VdF-rich copolymer is higher than that of PVdF.

It is generally said, the introduction of second component usually disturbs the crystal lattice. Therefore, the VdF-rich copolymer contains many crystalline defects. According to the literature¹¹, the α -transition in PVdF is related to the molecular motions of both crystalline defects and lamellar surface. Since the degrees of the crystallinity does not decrease largely with increasing VdF content, the effect of the crystalline defects onto the α -transition seems to be little. The increase of E' with increasing VdF content seems to be related to the conformational change of crystal form α - to β -form.

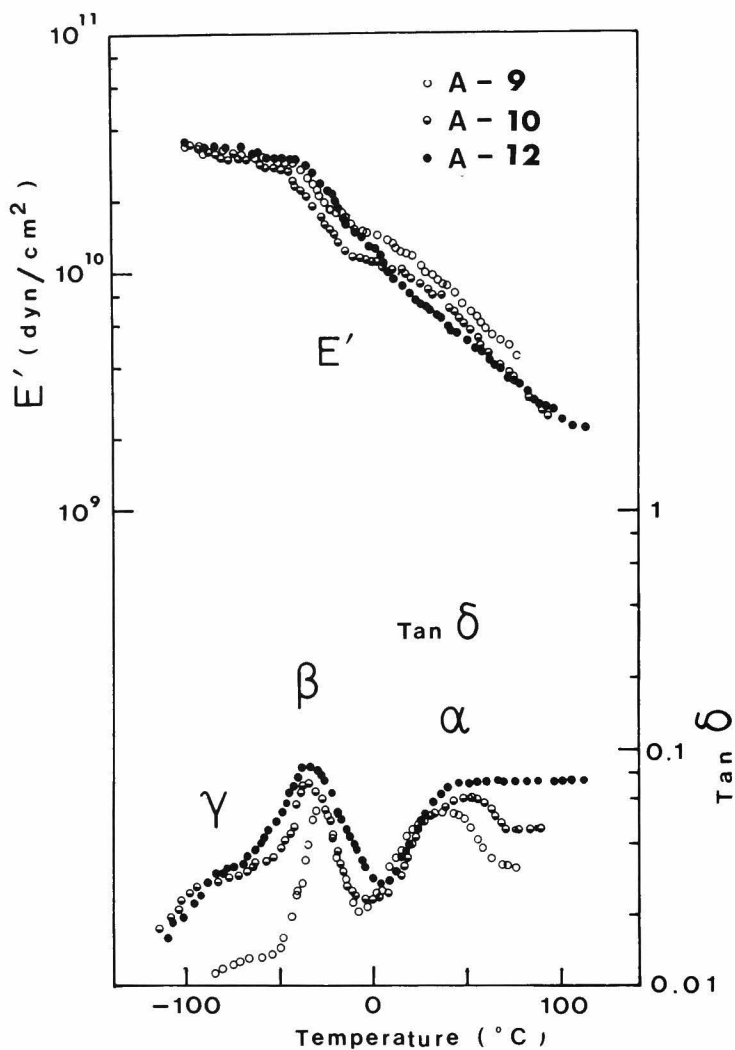


Figure 1. Temperature dependence of dynamic tensile modulus, E' , and loss tangent, $\tan \delta$, for VdF-rich copolymers (sample A-9 and A-10), and PVdF (sample A-12) measured at 35 Hz.

Figure 2 shows temperature dependence of dielectric constant ϵ' and dielectric loss ϵ'' of the VdF-rich copolymers and PVdF at 30 Hz. The measurements were carried out in the frequency of 30 Hz to 300 KHz. The data of other frequencies were omitted from the figures for clearness. As is seen from the figure, three transition peaks were observed clearly in PVdF, corresponding to mechanical data. It is seen that the α -transition peak is sensible to dielectric measurement compared to the mechanical measurement. The α -transition peaks of sample A-10 (90 mol% PdF) and sample A-9 (85 mol% VdF) were not observed in the limitation of the measurement.

The dielectric constant of PVdF increases with increasing TrFE content, in the whole range of temperature measured here. As mentioned above, the polymer chain in sample A-9 takes trans or trans-like conformation in crystal. Therefore, it is also considered that the polymer chain in amorphous region also takes trans or trans-like conformation in large parts. The effective dipole moment of trans conformation is advantage compared to the TGTG' conformation.

Figure 3 shows the $1/T$ versus f_{\max} curves of these copolymers in the β -transition region. The shape of each curves is resemble to each other, and of WLF type.^{20,21} As seen from the figure, the curve of PVdF shifts to upper temperature side with increasing TrFE content.

The second melting temperature T_m' can not be observed in

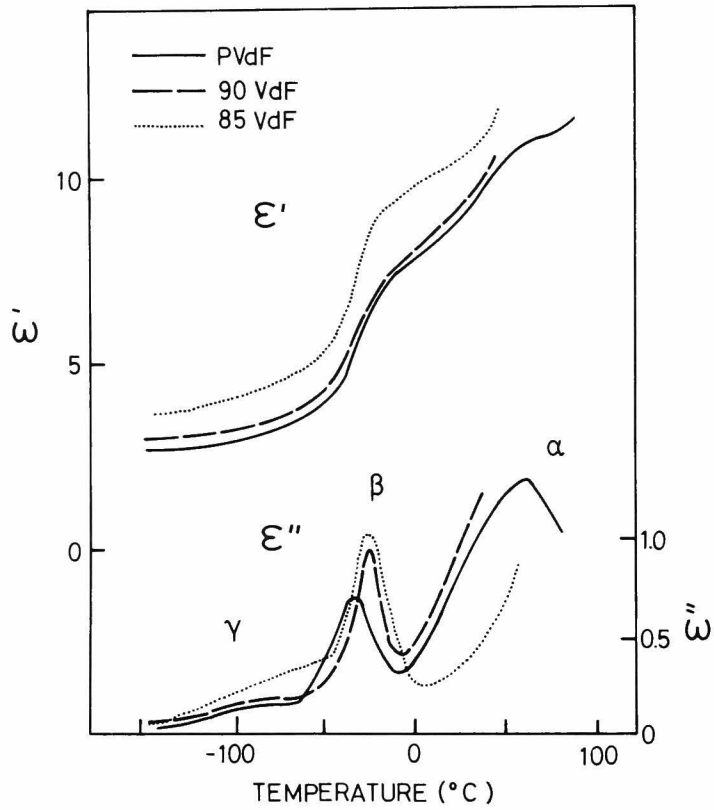


Figure 2. Temperature dependence of dielectric constant ϵ' and dielectric loss ϵ'' for TrFE-rich copolymers (sample A-9 and A-10), and PVdF (sample A-12) measured at 30 Hz.

mechanical and dielectric measurements. It is obvious that the origin of T_m' is quite different from that of the α -transition observed in PVdF and VdF-rich copolymers, since the temperature difference between T_m' and the α -transition is very large.

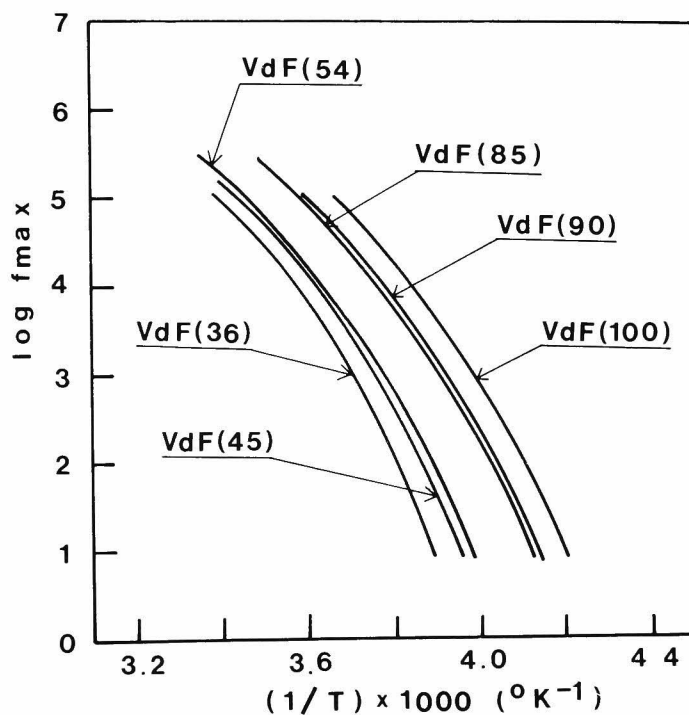


Figure 3. Dispersion map of TrFE-VdF copolymer and PVdF, illustrated by the logarithm frequency versus reciprocal absolute temperature at loss maximum in the β -transition region.

7-4 1 : 1 COPOLYMERS

Figure 4, 5, and 6 show temperature dependence of E' and $\tan \delta$ for the 1 : 1 copolymers (sample A-3, A-4, A-5, A-6, and A-7) in the temperature region of -120 to 100 °C and at 35 Hz. As seen from the figures, the mechanical data of these copolymers are resemble to each other, except for upper temperature side peak observed in sample A-7. This peak seems to relate to the T_m' transition. In this section, we have studied the mechanical relaxation of sample A-5 (44 mol% VdF content copolymer) mainly.

The temperature dependences of E' and $\tan \delta$ for three samples of 56 : 44 TrFE-VdF copolymer at different crystallinity are shown in Figure 5. In the temperature region from -120 to 100 °C, three transition regions have been observed with peaks at 40 °C (designated as β_1), -20 °C (designated as β_2), and -70 °C (designated as γ), respectively, at 35 Hz. These three transitions show crystallinity dependence and the magnitude of each peak decreases with increasing the crystallinity. This result indicates that these three transitions are related to molecular motion in amorphous region. The maximum temperature of the β_1 and β_2 transition peaks are independent of the degree of the crystallinity. It is also seen from the figure that the large drop of E' occurs in both β_1 and β_2 transition regions.

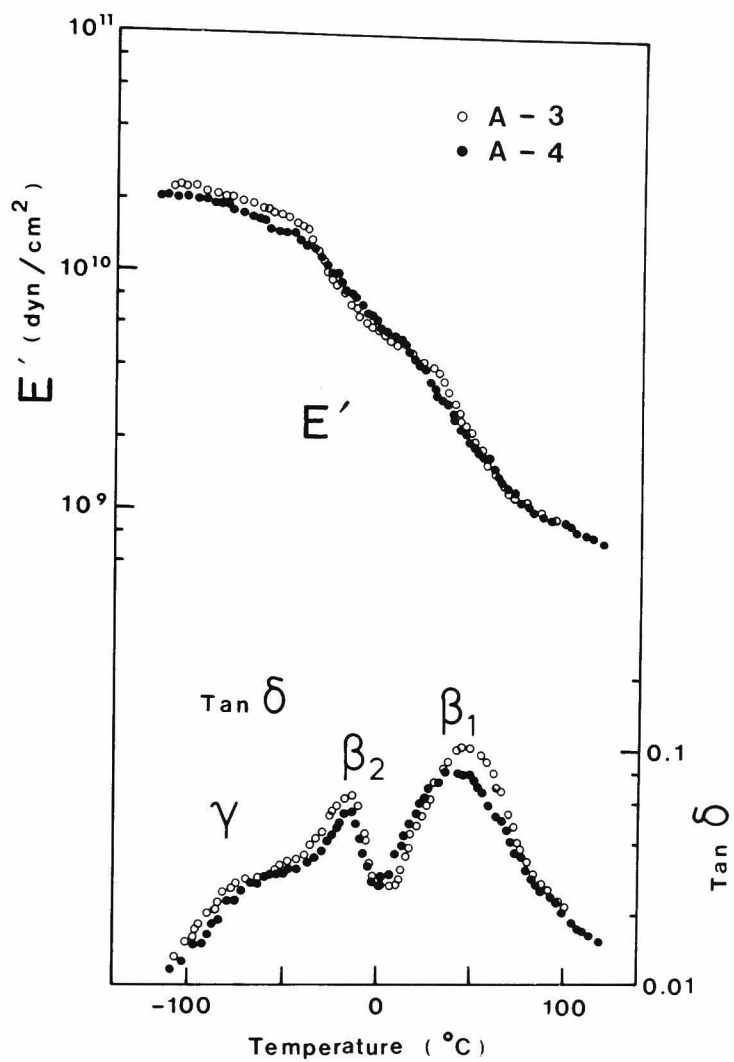


Figure 4. Temperature dependence of dynamic tensile modulus E' and loss tangent $\tan \delta$ for the 1 : 1 TrFE-VdF copolymers (sample A-3 and A-4) measured at 35 Hz.

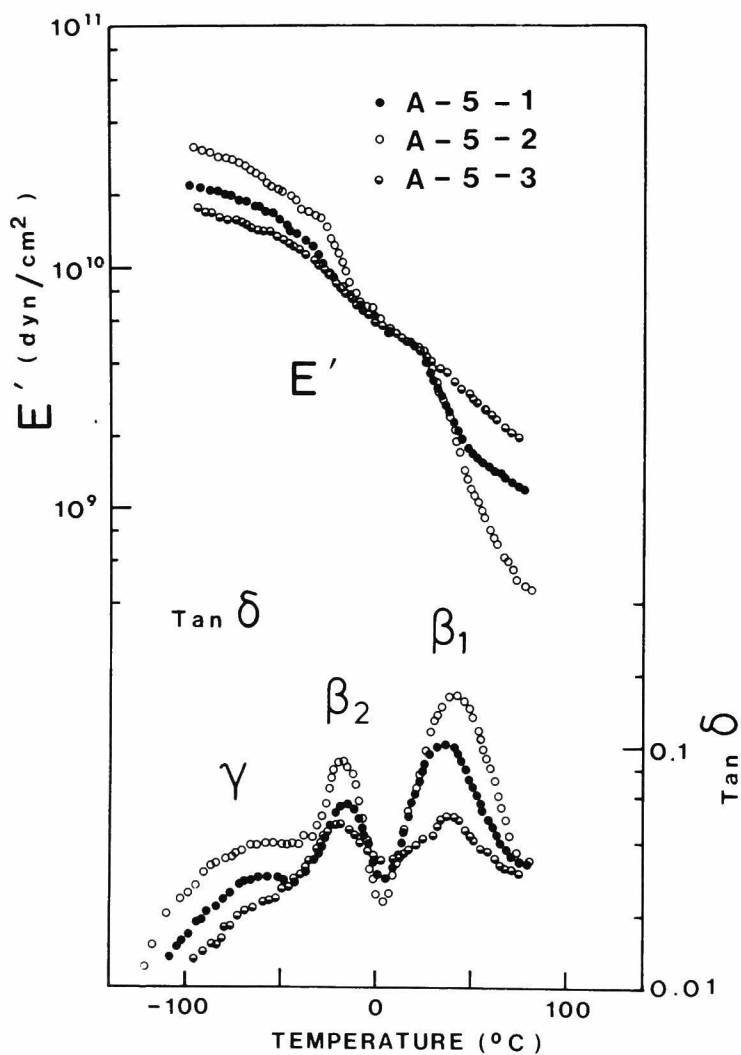


Figure 5. Temperature dependence of dynamic tensile modulus E' and loss tangent $\tan \delta$ for three samples of the 1 : 1 TrFE-VdF copolymer (sample A-5) at different crystallinity, measured at 35 Hz.

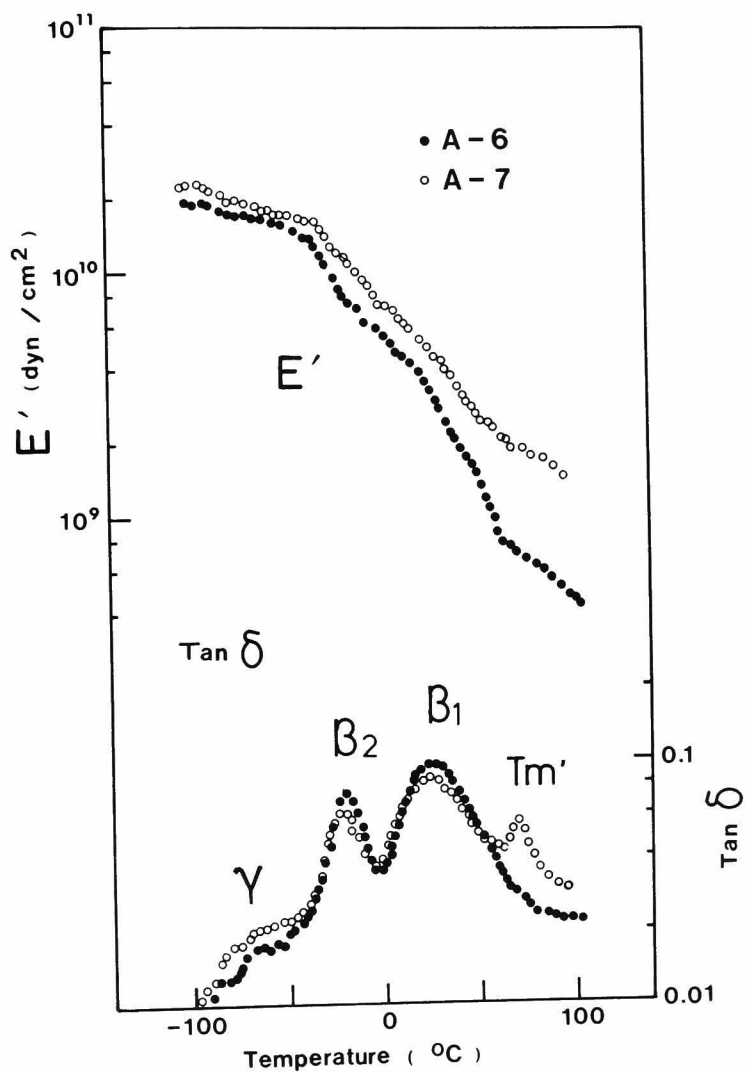


Figure 6. Temperature dependence of dynamic tensile modulus E' and loss tangent $\tan \delta$ for the 1 : 1 TrFE-VdF copolymers (sample A-6 and A-7), measured at 35 Hz.

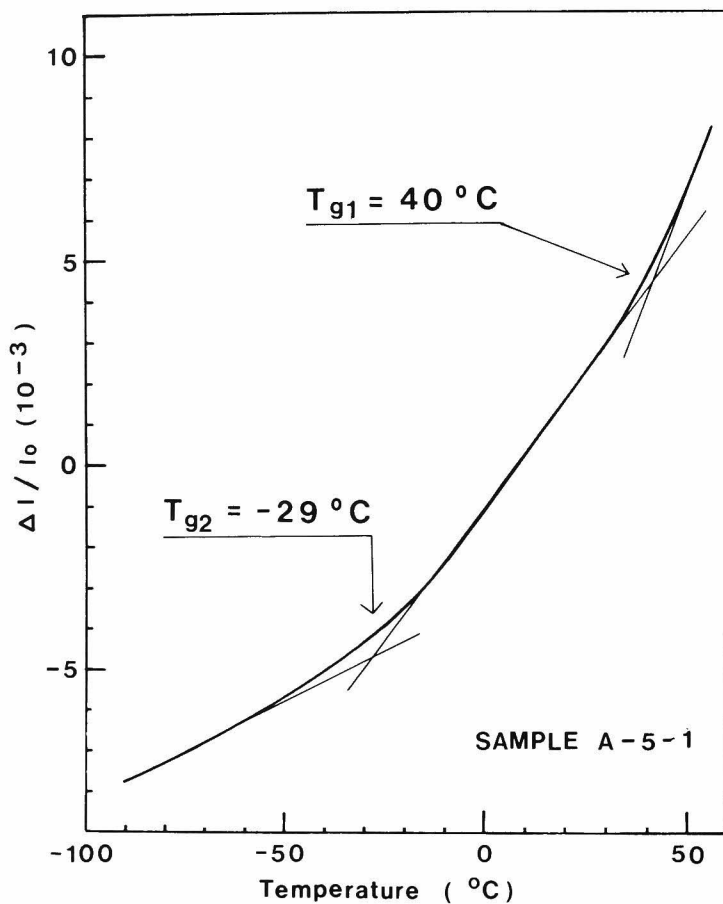


Figure 7. Linear thermal expansion of 44 mol% VdF content copolymer (sample A-5).

Figure 7 shows thermal expansion data of the 44 mol% VdF copolymer (sample A-5). Two break points were observed; one at 40°C and the other at -29°C . Hence, this result indicates the presence of two glass-to-rubber transitions. They are designated as T_{g1} (upper break) T_{g2} (lower break), respectively. It is seen from the figure that the β_1 and β_2 -transitions relate to T_{g1} and T_{g2} , respectively.

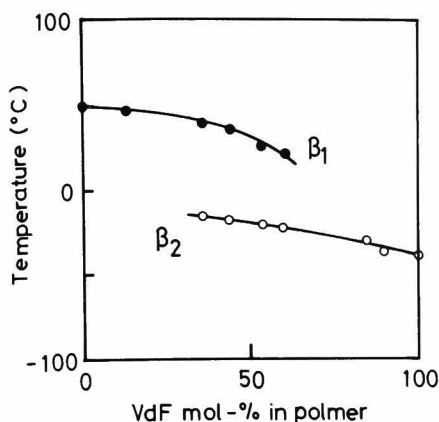


Figure 8. Change of transition temperatures of both β_1 - and β_2 -transitions with polymer composition.

Figure 8 shows the change of transition temperature of both β_1 and β_2 -transitions with polymer composition. As seen from the figure, the β -transition observed in PVdF, which is related to micro-Brownian motion in amorphous region, changes to the β_2 -transition of the 1 : 1 TrFE-VdF copolymer with increasing TrFE content. On the other hand, the β_1 -transition observed in PTrFE, which is related to micro-Brownian motion in amorphous region, changes to the β_1 -transition of the 1 : 1 copolymer with increasing VdF content. Therefore, it is reasonable to consider that T_{g1} closely related to glass transition in PTrFE, and T_{g2} to that of PVdF.

As mentioned above, the monomer reactivity ratios (r_1 and r_2) and the high resolution ^{19}F NMR studies indicated that the TrFE-VdF copolymers give a random structure. We would like to

consider the microstructure of the 1 : 1 TrFE-VdF copolymer in following: in segments of some limited degree of length, there are two parts, one rich in TrFE-units and the other rich in VdF-units, because both monomer units do not arrange in polymer chain alternately or block-like. Furthermore, it must be noted here that the difference in molecular dimension between TrFE and VdF units is thought to be very little, as mentioned above. Therefore, it is speculated that the small amount of VdF-units in TrFE-rich sequence or that of TrFE-units in VdF-rich sequence may not affect to molecular motions largely. Thus, we have assigned that T_{g1} is related to the amorphous region rich in TrFE-units; T_{g2} to amorphous region rich in VdF-units. Such double T_g were observed in many semicrystalline polymers.^{22, 23, 24}

These β_1 and β_2 transitions of TrFE-VdF copolymers were also observed in broad-line NMR measurements.²⁵ Judging from the derivative curves for copolymers, the solid to liquid transition seems to occur at the β_1 -transition.

Figures 9 and 10 show the frequency dependence of ϵ' and ϵ'' of 44 mol% VdF copolymer in the frequency region of 30 Hz to 300 KHz and at indicated temperatures in the figures. Two distinct peaks, β_2 and γ , corresponding to mechanical relaxation study, are also observed as seen in Figure 5. The β_1 -transition peak was not observed in the limitation of the measurement.

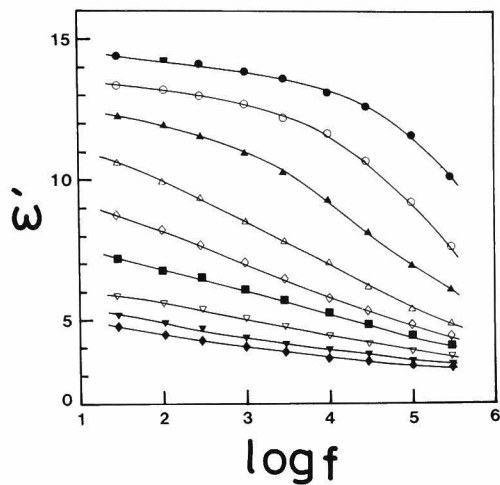


Figure 9. Frequency dependence of dielectric constant ϵ' of 44 mol% VdF copolymer (sample A-5) in the frequency region from 30 Hz to 300 kHz: ●, 22.0 °C; ○, 11.0 °C; ▲, -2.0 °C; △, -12.5 °C; ◇, -20.0 °C; ■, -27.5 °C; ▽, -40.5 °C; ▼, -53.0 °C; and ◆, -63.0 °C.

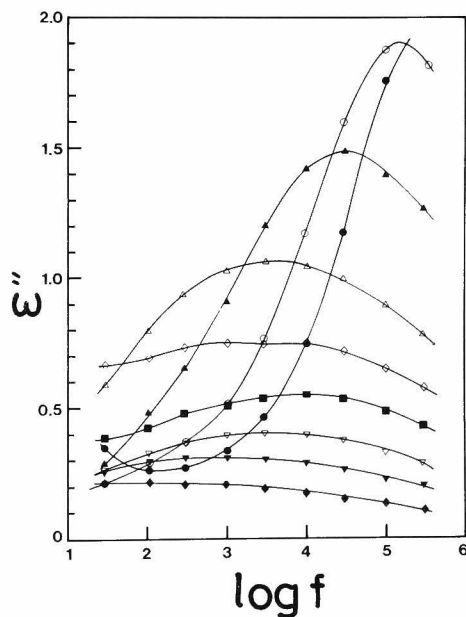


Figure 10. Frequency dependence of dielectric loss ϵ'' of 44 mol% VdF copolymer (sample A-5) in the frequency region from 30 Hz to 300 kHz: ●, 22. °C; ○, 11.0 °C; ▲, -2.0 °C; △, -12.5 °C; ◇, -20.0 °C; ■, -27.5 °C; ▽, -40.5 °C; ▼, -53.0 °C; and ◆, -63.0 °C.

Figure 11 shows the dispersion map of 44 mol% VdF content copolymer, which illustrates the logarithm frequency versus the reciprocal absolute temperature at loss maximum in both dielectric and mechanical measurements. As seen from the figure, the curve of $\log f_{\max}$ versus $1/T$ of the β_2 -transition is of WLF type.^{20,21} However, it is difficult to decide whether the β_1 -transition satisfies the WLF equation or not, because the employed data are very few. The activation energy ΔH was obtained from a plot of $\log f_{\max}$ versus $1/T$ by use of following equation

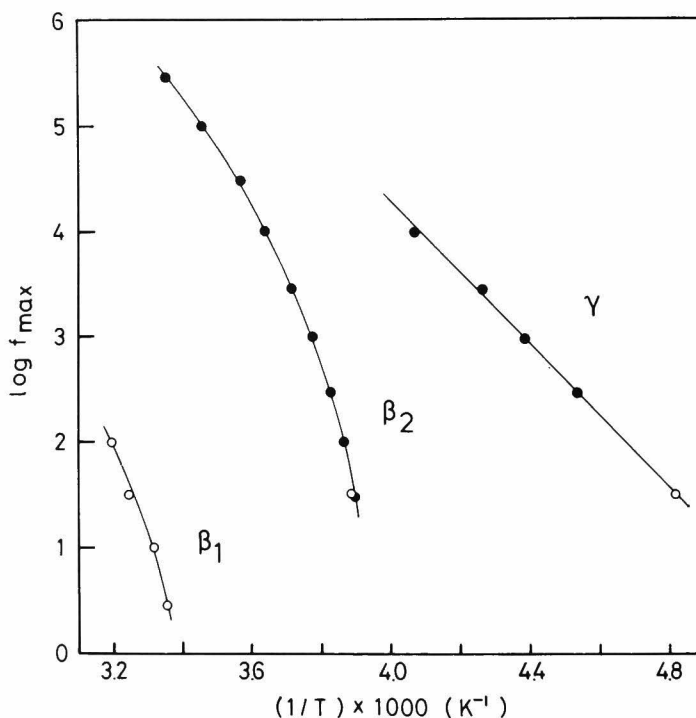


Figure 11. Dispersion map of 44 mol% VdF copolymer (sample A-5), illustrated by the logarithm frequency versus reciprocal absolute temperature at loss maximum in both dielectric (●) and mechanical (○) measurements.

$$\Delta H = -2.303R \, d(\log f_{\max})/d(1/T) \quad (1)$$

where R is the gaseous constant and T the absolute temperature. The ΔH of the β_1 , β_2 and γ transitions as a function of temperature are shown in Figure 12. For example, the ΔH of the β_1 -transition is about 38 Kcal/mol at 30°C, and that of the β_2 -transition is about 37 Kcal/mol at -5°C. These values are closely similar to the activation energies of both PTrFE and PVdF in glass-to-rubber transition regions: the ΔH of PTrFE in glass-to-rubber transition region is about 57 Kcal/mol at 40°C,¹ and that of PVdF is about 28 Kcal/mol at 25°C.

The plots of the logarithm of frequency versus reciprocal absolute temperature of the 1 : 1 TrFE-VdF copolymers (sample A-4, A-5, and A-6) in the β_2 -transition region are also shown in Figure 3. The slope of these curves are similar to that of PVdF. These results also provide that the β_2 -transition is related to glass-to-rubber transition of PVdF largely.

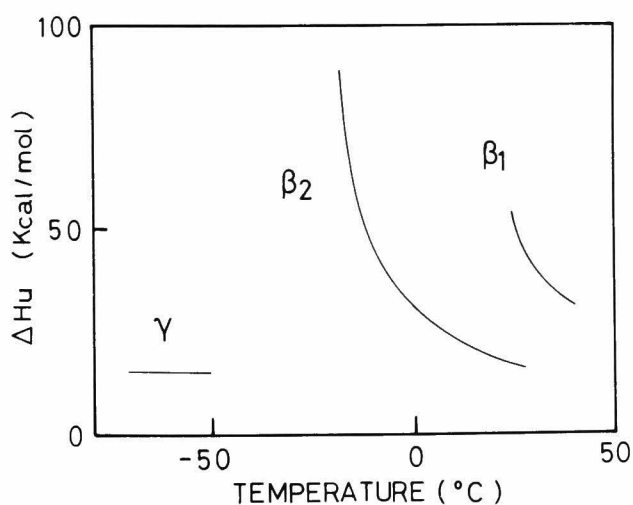


Figure 12. Temperature dependence of activation energy ΔH for the β_1 , β_2 , and γ relaxations of 44 mol% VdF copolymers (sample A-5).

According to WLF theory,²⁰ ΔH is related to the freezing temperature T_c of molecular motion by

$$\Delta H = 2.303 R C_1 C_2 T^2 / (C_2 + T + T_c) \quad (2)$$

where R is the gaseous constant and C_1 and C_2 are constant. Figure 13 shows a plot of $1/\sqrt{\Delta H}$ versus $1/T$ for the β_2 -transition of 44 mol% VdF copolymer. The data shows linear relationship in the temperature range of -12 to 25°C (satisfying the WLF theory).

From these results and discussion, we have assigned that the β_1 -transition is related to the micro-Brownian motion of main chain in the amorphous region which is rich in TrFE units; the β_2 -transition is assigned to the micro-Brownian motion of main chain in the amorphous region rich in VdF units.

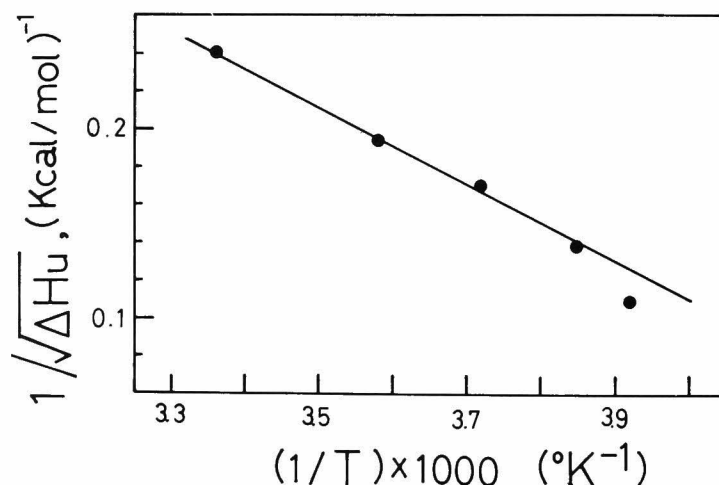


Figure 13. Plot of $1/\sqrt{\Delta H}$ versus $1/T$ for the β_2 -transition of 44 mol% VdF copolymer (sample A-5).

The γ transition of 44 : 56 TrFE-VdF copolymer can be observed in both mechanical and dielectric measurements, as seen in Figures 5 and 10. The γ transition is also affected by the crystallinity of sample, similar to the β_1 and β_2 transitions, and the magnitude of its peak decreases with increasing the crystallinity. The γ transition is observed below the lower glass-to-rubber transition temperature, T_{g2} , of -29°C . Therefore, we have assigned the γ transition as local molecular motion in amorphous region. A plot of the logarithm of the frequency versus reciprocal absolute temperature of the loss maximum for the γ transition in 54 : 46 TrFE-VdF copolymer was also shown in Figure 18. The curve is linear in the temperature region of -50 to -65°C . The activation energy ΔH is found to be about 15 Kcal/mol. This transition is thought to be similar to the local molecular motion in PVdF, because the γ -transition in PVdF also is related to amorphous region and the ΔH is very small ($\Delta H = 14$ Kcal/mol)^{2,6} similar to those of TrFE-VdF copolymers. On the other hand, local molecular motion of PTrFE is related to both the crystal and the amorphous region, and the ΔH is very large (28 Kcal/mol)¹.

As mentioned, the TrFE-VdF copolymers are in crystalline state in whole range of polymer composition. Many semicrystalline polymers exhibit the crystal transition in high temperature side. However such a peak was not observed in the highest crystalline sample of 44 mol% VdF copolymer.

7-5 TRANSITION MAP

Figure 14 shows changes of transition temperature with polymer composition. The primary and secondary melting temperatures (T_m and T_m') are determined by DSC measurement, and the other transition temperatures are determined by mechanical relaxation measurements at 35 Hz.

The primary dispersion observed in both PTrFE and PVdF homopolymers change to the β_1 and β_2 dispersion in the 1 : 1 TrFE-VdF copolymer. As seen in the figure, the α -dispersion in PVdF (attributed to crystalline dispersion) also seems to change to the β_1 dispersion in the copolymer. However, the β_1 dispersion in copolymer does not show the characteristic feature of crystalline dispersion. According to Boyer,²⁴ the α -transition in PVdF is not attributed to molecular motion in crystal region but to amorphous region. He claimed that PVdF has double glass-to-rubber transitions, and considered this transition point as secondary glass-to-rubber transition. However, various studies supported that the α -transition in PVdF is attributed to the molecular motion in crystal region.^{4,8,10,11} If the α -transition in PVdF is attributed to the glass-to-rubber transition, our experimental results that double glass-to-rubber transitions exist in the 1 : 1 TrFE-VdF copolymer will be explained well.

On the other hand, the α -dispersion in PTrFE (attributed to secondary dispersion) also seems to change to the β_2 -transi-

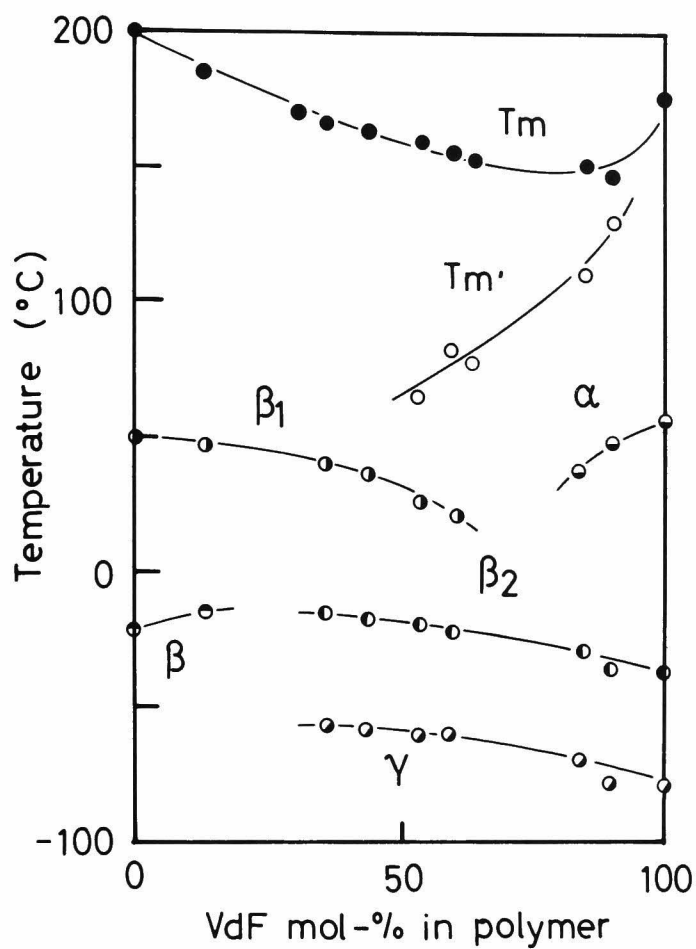


Figure 14. Change of transition temperatures with polymer composition. The primary and secondary melting temperatures (T_m and T_m') are determined by DSC measurement. Other transition temperatures are determined by mechanical relaxation measurement at 35 Hz.

tion in copolymers as seen in Figure 14. However, the β_2 -transition in copolymer does not show the characteristic feature of the γ -transition of PTrFE. For example, secondary dispersion in PTrFE does not show crystallinity dependence, and shows an asymmetric $\tan \delta$ versus temperature curve.

In summary, even if the influence of the crystalline dispersion in PVdF homopolymer to the β_1 dispersion in copolymer exists, it seems to be very small. And in the same manner as the β_1 dispersion, the influence of secondary dispersion in PTrFE homopolymer to the β_2 dispersion in copolymer seems to be very little.

REFERENCES

1. T. Yagi, Polym. J., in press.
2. P. D. Schuman, E. C. Stumpant and G. Westmoreland, J. Macromol. Sci., B1(4), 815 (1967).
3. W. K. Lee and C. L. Choy, J. Polym. Sci., Polym. Phys. Ed., 13, 619 (1975).
4. H. Kakutani, J. Polym. Sci., Part A-2, 8, 1177 (1970).
5. N. K. Kalfoglou, and H. L. Williams, J. Appl. Polym. Sci., 17, 3367 (1973).
6. E. J. Parry, and D. Tabor, Polymer, 14, 623 (1973).
7. S. P. Kabin, S. G. Malkevich, G. P. Mikhailov, B. I. Sazhin and A. L. V. Chereshevich, Vysokomol. Soedin., 3, 618 (1961).
8. Y. Ishida, M. Watanabe and K. Yamafuji, Kolloid-Z. Polym., 211, 48 (1964).
9. A. Peterlin and J. Elwell, J. Mater. Sci., 2, 1 (1967).
10. H. Sasabe and S. Saito, Rept. Progr. Polym. Phys. Japan, 11, 379 (1968).
11. S. Yano, J. Polym. Sci., Part A-2, 8, 1057 (1970).
12. K. Nakagawa and Y. Ishida, J. Polym. Sci., Polym. Phys. Ed., 11, 1503 (1973).
13. S. Uemura, J. Polym. Sci., Polym. Phys. Ed., 12, 1177 (1973).
14. S. Osaki and Y. Ishida, J. Polym. Sci., Polym. Phys. Ed., 12, 1727 (1974).
15. S. Yano, K. Tadano, K. Aoki, and N. Koizumi, J. Polym. Sci., Polym. Phys. Ed., 12, 1875 (1974).

16. W. P. Slichter, J. Polym. Sci., 24, 173 (1957).
17. V. J. McBrierty, D. C. Douglass, and T. A. Weber, J. Polym. Sci., Polym. Phys. Ed., 14, 1271 (1976).
18. V. J. McBrierty, and D. C. Daglass, Macromolecules, 10, 855 (1977).
19. L. E. Nielsen, Mechanical Properties of Polymers, Reinhold Publishing Corp., New York, 1962.
20. W. L. Williams, F. F. Landel and J. D. Ferry, J. Amer. Chem. Soc., 77, 3701 (1955).
21. J. D. Ferry, "Viscoelastic Properties of Polymers", Wiley, New York, 1961.
22. Y. Wada, and Y. Hotta, J. Polym. Sci., Part C, 23, 583 (1968).
23. R. F. Boyer, J. Macromol. Sci., Phys., B8, 503 (1973).
24. R. F. Boyer, J. Polym. Sci., Symposium, 50, 189 (1975).
25. T. Yagi, unpublished data.
26. P. Hedvig, "Dielectric Spectroscopy of Polymers", Adam Hilger, 1977.

CHAPTER 8

DIELECTRIC PROPERTIES OF TRIFLUOROETHYLENE COPOLYMERS

8-1 INTRODUCTION

Poly(vinylidene fluoride) (PVdF) is distinguished among the crystalline polymers by such a high dielectric constant as $\epsilon' = 8.5$, at 1 KHz and 22 °C. Recently, this material has drawn attention as a new transducer material because of their interesting piezoelectricity and pyroelectricity properties.¹⁻¹² There are many reports which are claiming that these properties are closely correlated with the existence of an oriented dipole structure in crystal.¹⁻⁷ It was indicated that the β -crystal form of PVdF has a spontaneous polarization and a possibility of ferroelectricity.¹ Poly(trifluoroethylene) (PTrFE) is also a high ϵ' material ($\epsilon' = 7.5$, at 1 KHz and 22 °C) in the same manner as PVdF.¹³ It would be of interesting, therefore, to examine the dielectric and piezoelectric properties of the trifluoroethylene (TrFE) - vinylidene fluoride (VdF) copolymers. Since the TrFE-VdF copolymers are in crystalline state in whole range of polymer composition and the dipole moments of their repeating units are very large, as described in chapter 6.

The purpose of this chapter is concerned with the determination of, first, the dielectric properties of the TrFE copolymers with VdF, tetrafluoroethylene (TFE) and chlorotrifluoroethylene (CTFE), and of, second, the piezoelectric properties of the TrFE-VdF copolymers. The dielectric properties of the TrFE-VdF copolymers will be discussed in terms of (1) the

magnitude of dipole moments of repeating units, (2) the position and direction of dipole with respect to the chain backbone, (3) the freedom of the dipole rotation, and (4) the crystal form; i.e., a possibility of a spontaneous polarization in crystal.

8-2 EXPERIMENTALS

The preparation of these copolymers were described in chapter 1. The microstructures and the physical properties were described in chapter 3 and 5, respectively. Sample codes are listed in Table I, II, III and IV of chapter 5.

The specimens used for dielectric measurement were heat pressed in circular-sheets of 1.0 to 1.3 mm in thickness and 50 mm in diameter. The cooling rate in the molding process was about 50 °C/min. Aluminum was evaporated on the specimen surface in high vacuum. Dielectric measurements were carried out by a transformer bridge (Ando-Denki TR-10) at various frequencies up to 300 KHz and over a temperature range from -150 to 100 °C.

The piezoelectric properties were measured by use of Piezoelectron (Toyo-Seiki).

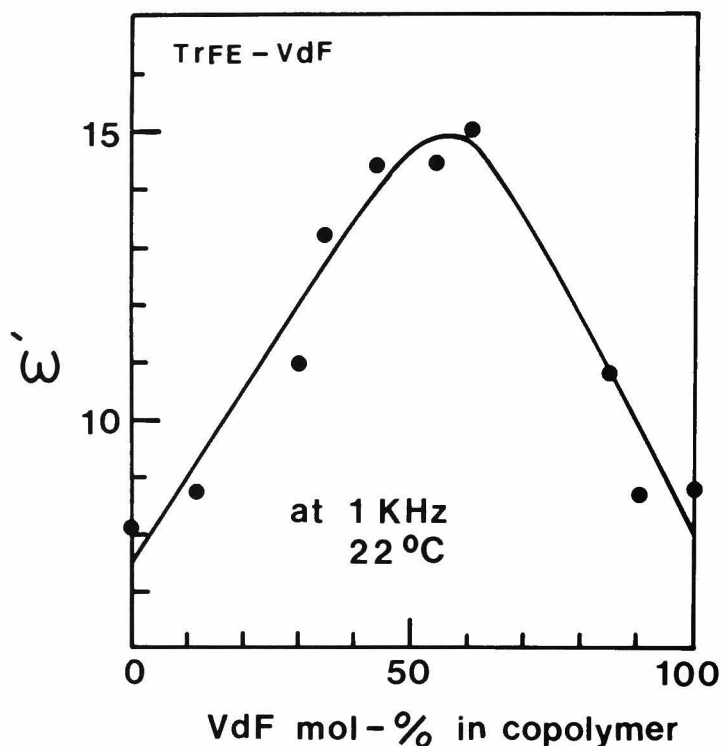


Figure 1. Change of dielectric constant ϵ' with polymer composition, at 1 kHz and 22 °C.

8-3 DIELECTRIC PROPERTIES OF TrFE-VdF COPOLYMERS

Figure 1 shows change of dielectric constant ϵ' with polymer composition at 1 KHz and at 22°C. As seen from the figure, ϵ' shows a maximum at 55 mol% VdF content. The numerical value of ϵ' is about 15.0 (1 KHz and 22°C) and approximately 1.7 times higher than those of both PTrFE and PVdF homopolymers.

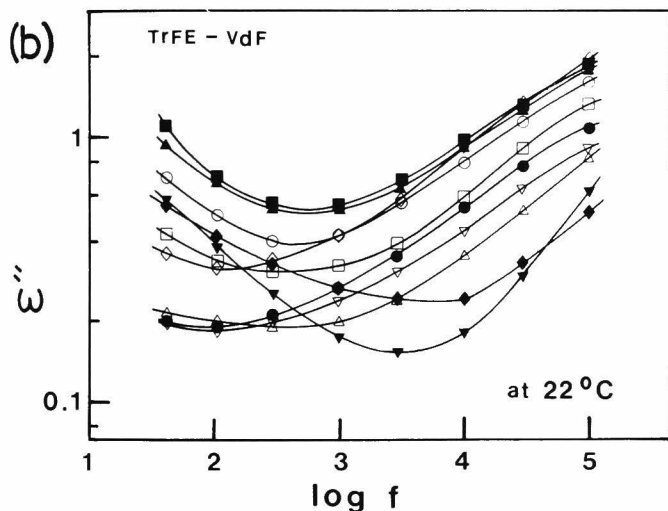
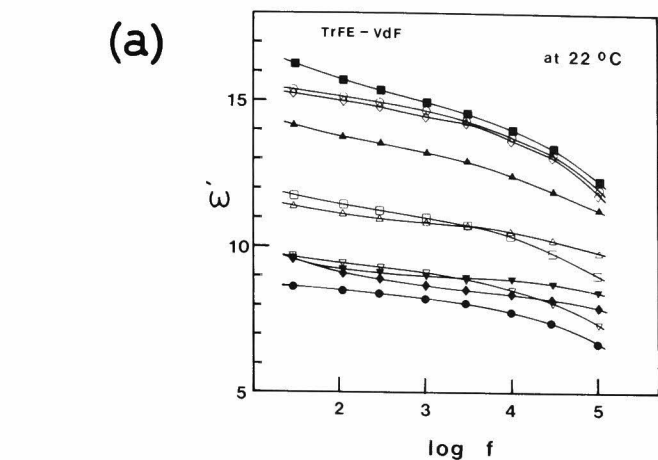


Figure 2. Frequency dependence of ϵ' (a) and ϵ'' (b) of the TrFE-VdF copolymer, at 22 °C.

Figures 2a and 2b show frequency dependence of ϵ' and ϵ'' of the TrFE-VdF copolymers, at 22 °C. As seen from the figure, the 1 : 1 TrFE-VdF copolymers shows always higher value compared with other samples, in the whole range of frequency investigated here. The amplitude of ϵ' of each samples decreases slowly with increasing frequency. The minimum value of ϵ'' appears in the region from 100 Hz to 10 kHz.

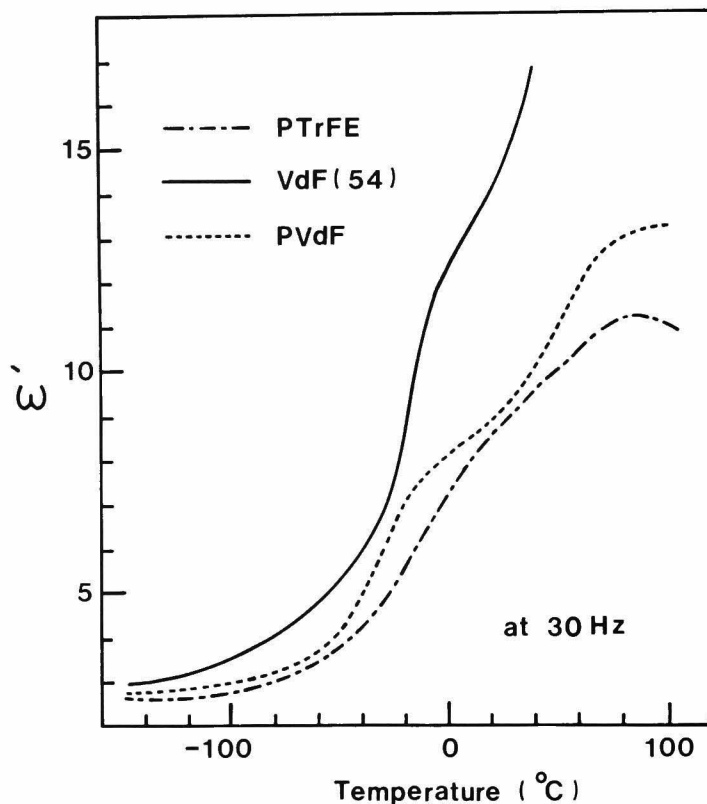


Figure 3. Change of dielectric constant ϵ' of PTrFE, 1 : 1 TrFE-VdF copolymer, and PVdF with temperature, at 30 Hz.

Figure 3 shows a temperature dependence of ϵ' of PTrFE (sample A-1), the 54 mol% VdF copolymer (sample A-5), and PVdF (sample A-12). It is also seen from the figure, that ϵ' of copolymer always shows high value compared with that of both homopolymers in the whole temperature region investigated here. The 1 : 1 TrFE-VdF copolymer is characterized at high value of ϵ' .

It was mentioned that the high value of dielectric constant of semicrystalline polymer depends on (1) the magnitude of dipole moment of repeating units, (2) the position and direction of dipole with respect to the chain backbone, (3) freedom of the dipole rotation in the electric field, and (4) the crystal form of polymer, i.e., a possibility of a spontaneous polarization in crystal. These terms are discussed in following.

8-3-1 MAGNITUDE OF DIPOLE MOMENT

The effective dipole moment for the repeating unit of PTrFE is 1.63 Debye for trans and gauche (+) conformation, and 3.25 Debye for gauche (-) conformation.¹³ On the other hand, that of PVdF is 1.96 Debye.¹³ These values seem to be very large compared with other monomeric units.

8-3-2 POSITION AND DIRECTION OF DIPOLE

It was generally said that the microstructure of the polymer chain had direct effects upon the dielectric properties of the polymeric material. In polar polymer, the existence of head-to-head structure of repeating units will affect the dielectric properties largely. For example, PVdF has about 8 % head-to-head structures in the polymer chain,¹⁴ and this material shows a high dielectric constant ($\epsilon' = 8.5$ at 1 KHz and 22 °C). On the other hand, ϵ' of ethylene (E)-tetrafluoroethylene (TFE) copolymer is very little ($\epsilon' = 2.6$ at 1 KHz

and 22 °C).¹⁵ The microstructure of E-TFE copolymer is equivalent to PVdF having 100 % head-to-head structure, since both E and TFE monomers copolymerized alternaitngly.¹⁶ It is considered that in the case of the E-TFE copolymer system the effective dipole moments are canceled each other in the polymer chain. Therefore, it is predicted that ϵ' changes largely in accordance with the position and direction of dipole moments.

A high resolution ¹⁹F NMR study indicated that the main feature of the 1 : 1 TrFE-VdF copolymer is $-\text{CF}_2-\text{CH}_2-\text{CF}_2-\text{CFH}-\text{CF}_2-$. This microstructure arises from the head-to-tail structure of TrFE-VdF (and/or VdF-TrFE) sequence. Here, it is defined that the CF_2 -position of both TrFE ($\text{CF}_2=\text{CFH}$) and VdF ($\text{CF}_2=\text{CH}_2$) is head-position, and the other position (CFH or CF_2) is tail-position. As described in chapter 3, the head-to-tail structures of TrFE-VdF (and/or VdF-TrFE) sequences is rather abundant. The content of this microstructure shows maximum at middle point of polymer composition, and this point corresponds to maximum point of dielectric constant.

8-3-3 FREEDOM OF DIPOLE ROTATION

It was mentioned that the dielectric properties should be in practice more sensible to the dipole motion in amorphous region than crystalline region in the electric field. The large scale molecular motion in amorphous region is also necessary to observe high ϵ' value. The value of ϵ' changes

largely between below and above glass transition temperature. In the 1 : 1 TrFE-VdF copolymer, the lower-to-rubber transition is observed below room temperature, as mentioned above ($T_{g2} = -29\text{ }^{\circ}\text{C}$).

The dielectric rotation is correlated with the magnitude of dielectric relaxation. The magnitude of dielectric relaxation, $\Delta\epsilon$, is given by

$$\Delta\epsilon = \epsilon_0 - \epsilon_{\infty} \quad (1)$$

where ϵ_0 is the static dielectric constant and ϵ_{∞} is the dielectric constant at very high frequency at which the orientation of any dipoles are not taken place. The value of $\Delta\epsilon$ can be obtained from the Cole-Cole plot,¹⁷ or be obtained from the area under a plot of ϵ'' versus $\ln f$, by the following equation.¹⁸

$$\epsilon_0 - \epsilon_{\infty} = \frac{2}{\pi} \int_{-\infty}^{\infty} \epsilon'' d(\ln f) \quad (2)$$

For evaluation of the dipole moment of polymer molecules, the Frölich-Kirkwood theory¹⁹ is usually used. According to their theory, the dielectric permittivity is expressed as

$$\Delta\epsilon = \epsilon_0 - \epsilon_{\infty} = \frac{3\epsilon_0}{2\epsilon_0 + \epsilon_{\infty}} \frac{4\pi N}{3kT} \left(\frac{\epsilon_{\infty} + 2}{3} \right) g_r \mu_0^2 \quad (3)$$

where N is the concentration of the repeating unit, μ_0 the dipole moment, g_r the Kirkwood reduction factor which is expressed as an average of the special orientation, k the

Boltzmann constant, and T the absolute temperature. The values of ϵ_0 and ϵ_∞ were estimated by the Cole-Cole plot. The values of g_r of TrFE-VdF copolymer is calculated by assuming that $\Delta\epsilon$ arises mainly from the dipole orientation, in VdF-rich amorphous phase and at the β_2 transition region. Therefore, N is given by

$$N = N_A f_A X_A / M_O V_S \quad (4)$$

where N_A is the Avogadro's number, M_O the molecular weight of repeating unit, V_S the specific volume, f_A the weight fraction of amorphous region, and X_A the molar fraction of VdF in copolymer. The values of V_S and f_A are taken from Table I. The calculated values of g_r and $g_r \times \mu_0^2 (= \mu^2)$ are tableted in Table II, together with the values of ϵ_0 , ϵ_∞ , and $\Delta\epsilon$. From these results, it is speculated that the free rotation of dipole moment of VdF-unit may occur in the β_1 -transition region.

8-3-4 CRYSTAL FORM

As mentioned above, the crystal form of the 1 : 1 TrFE-VdF copolymer is closely similar to that of β -form of PVdF, and the main chain of the copolymer takes trans conformation in crystal. This means that the unit cell of the copolymer crystal has a permanent dipole and this has a possibility of spontaneous polarization. According to Nakamura and Wada,³⁰ the β -form PVdF crystal has a spontaneous polarization and

this material is classified as a ferroelectric polymers. It will be considered that the TrFE-VdF copolymer also has a ferroelectric nature similar to the β -form PVdF crystal. In addition, the trans conformation of main chain also seems to hold locally in amorphous region. This structure also consider to contribute to dielectric properites of this copolymers largely.

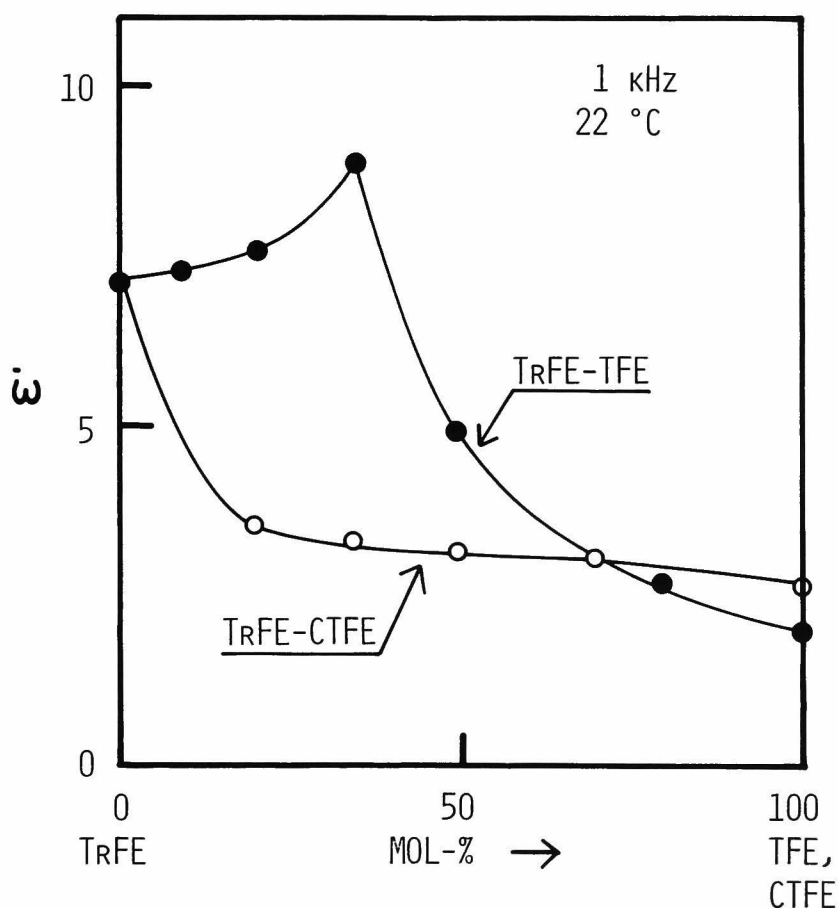


Figure 4. Change of dielectric constant ϵ' with polymer composition for the TrFE-TFE and TrFE-CTFE copolymers, at 1 kHz and 22 °C.

8-5 DIELECTRIC PROPERTIES OF TrFE-TFE AND TrFE-CTFE COPOLYMERS

Figure 4 shows change of dielectric constant ϵ' with polymer composition for the TrFE-TFE and TrFE-CTFE copolymers, at 1 kHz and 22 °C. As seen from the figure, the ϵ' versus

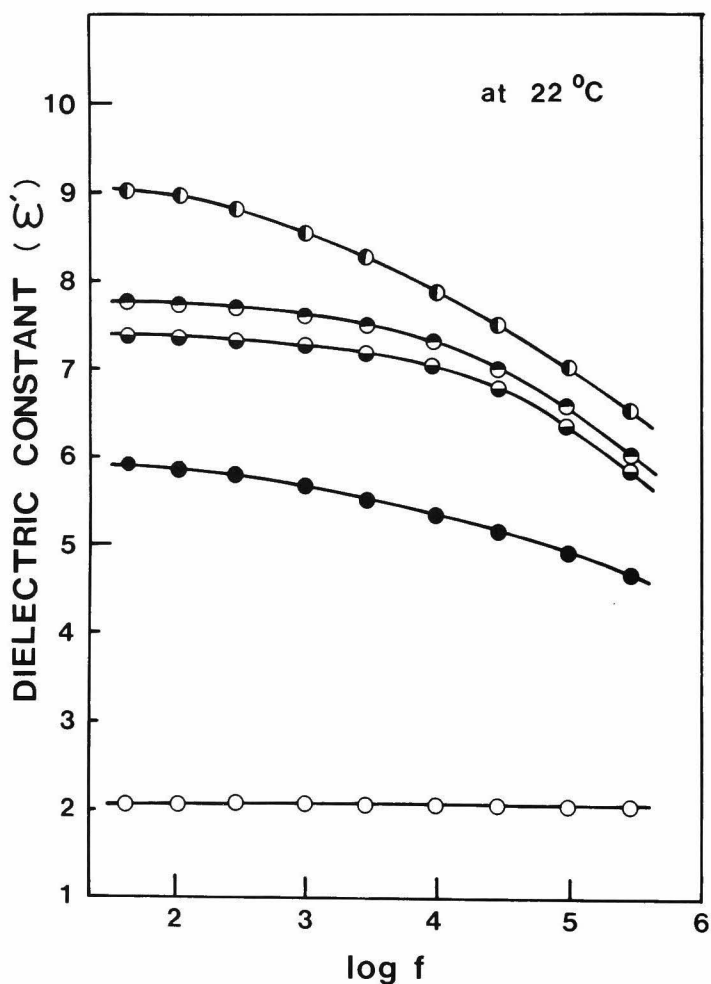


Figure 5. Change of dielectric constant ϵ' with frequency f for the TrFE-TFE copolymer system: ○ , 38 mol% TFE; ● , 17 mol% TFE; ● , 12 mol% TFE; ● , 49 mol% TFE and ○ , PTFE.

polymer composition curve of the TrFE-TFE copolymer system takes maximum at 38 mol% TFE, in the same manner as the TrFE-VdF copolymer system.

Figure 5 and 6 show change of dielectric constant ϵ' and loss ϵ'' with frequency f for the TrFE-TFE copolymers. As seen from the figure, the 38 mol% TFE copolymer exhibits the highest ϵ' value in the whole range of frequency investigated here.

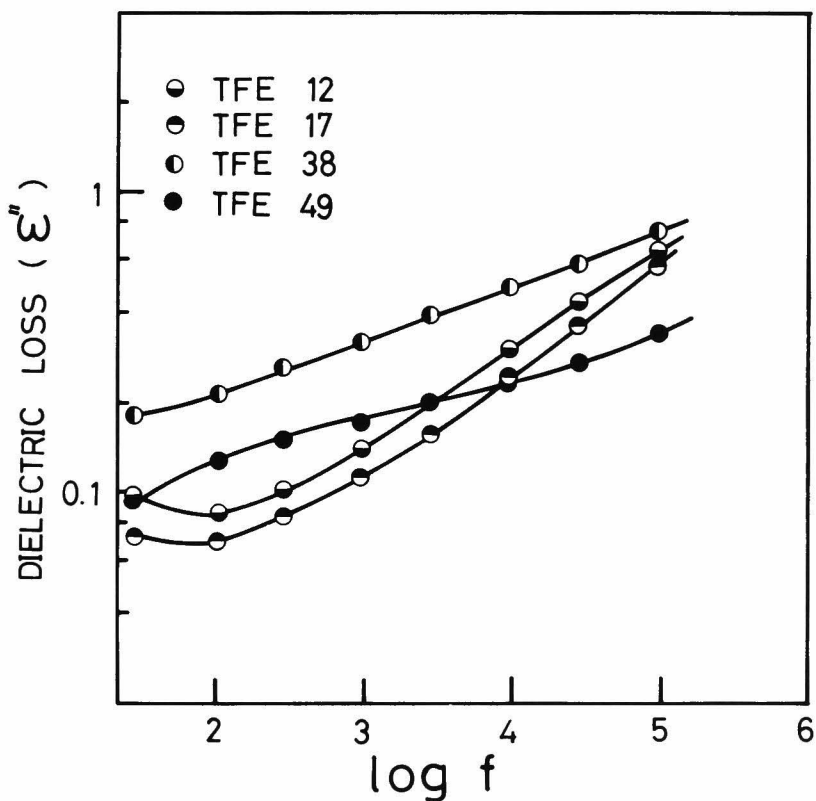


Figure 6. Change of dielectric loss ϵ'' with frequency for the TrFE-TFE copolymers.

The ϵ' versus polymer composition curves of the TrFE-CTFE copolymer system changes monotonously, as shown in Figure 4. Figure 7 and 8 show change of ϵ' and ϵ'' with frequency for the TrFE-CTFE copolymers.

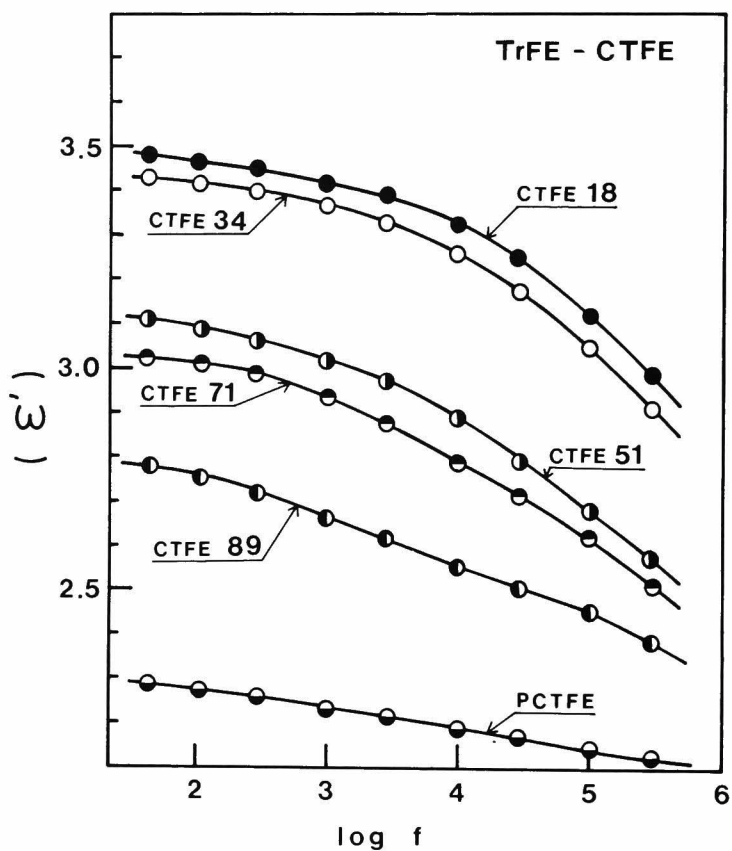


Figure 7. Change of ϵ' with frequency f for the TrFE-CTFE copolymers.

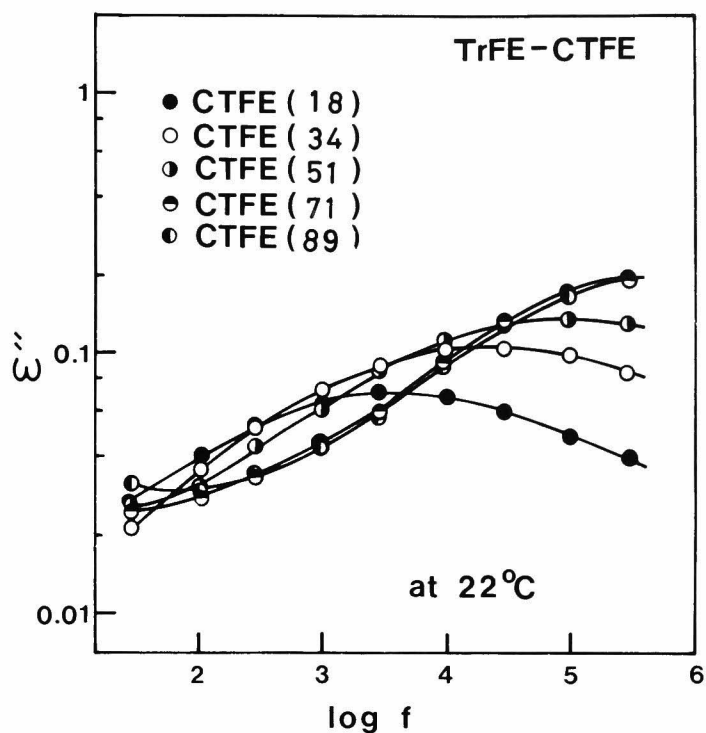


Figure 8. Change of $\tan \delta$ with frequency f for the TrFE-CTFE copolymers.

8-5 PIEZOELECTRICITY OF TrFE-VdF COPOLYMERS

Recently, it is found that the TrFE-VdF copolymer electret exhibits the high piezoelectricity.²⁰⁻²³ Figure 9 shows change of the d_{31} constant with polymer composition for the TrFE-VdF copolymer electrets in both unstretched and stretched (x5) films.

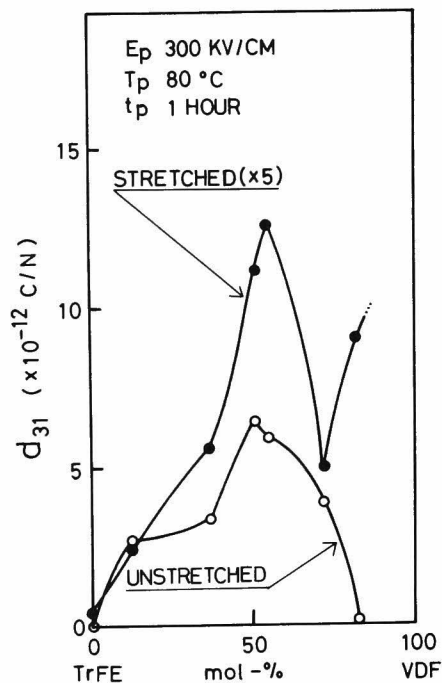


Figure 9. Change of the piezoelectricity with polymer composition for the TrFE-VdF copolymers electret.

In this measurement, the casting films from dimethylformamide are used. As is seen from the figure, the d_{31} constant takes maximum value at 50-55 mol% VdF content in both stretched and unstretched samples. The curve of the d_{31} constant versus polymer composition shows similar tendency to that of the ϵ' versus polymer composition. In addition, the high value of d_{31} constant was observed not only in stretched sample but in unstretched one, in the 1 : 1 TrFE-VdF copolymer. Usually,

Table I. Piezoelectric properties of the 45 : 55 TrFE-VdF copolymer electret films at room temperature: E_p , 300 KV/cm, T_p , 80 °C, and t_p , 1 hour. The films were prepared by melt-casting method.

	unstretched		stretched	
	crystal form	d_{31} (pC/N)	crystal form	d_{31} (pC/N)
PVdF ^a	α	0.4	β	20
TrFE-VdF (44:55)	β	7.0	β	28

^aData taken from ref. 5, 8 and 9.

high value of piezoelectricity of polymeric material was observed only in stretched sample. The increasing of the d_{31} constant of the TrFE-VdF copolymer with increasing VdF content in the region of VdF-rich polymer composition seems to relate to the changing of the crystal form from α to β . Piezoelectric properties of the 45 : 55 TrFE-VdF copolymer electret films at room temperature are tabulated in Table I, together with those of PVdF electret. The films are prepared with melt-casting method. The copolymer electret of stretched film exhibits a very high value of the d_{31} constant, in the same manner as the β -form PVdF electret. At present time, the β -form PVdF electret exhibits the highest value of the piezoelectric constant as the polymeric material.¹⁻¹²

REFERENCES

1. K. Nakamura, and Y. Wada, J. Polym. Sci., Part A-2, 9, 161 (1971).
2. G. Pfister, M. Abkowitz, and R. G. Crystal. J. Appl. Phys., 44, 2064 (1973).
3. G. Pfister, and M. Abkowitz, J. Appl. Phys., 45, 1001 (1974).
4. H. Ohigashi, J. Appl. Phys., 47, 949 (1976).
5. Y. Wada, and R. Hayakawa, Japan J. Appl. Phys., 15, 2041 (1976).
6. M. Tamura, S. Hagiwara, S. Matsumoto, and N. Ono, J. Appl. Phys., 48, 513 (1977).
7. H. Lee, R. E. Salomon, and M. M. Labes, Macromolecules, 11, 171 (1978).
8. N. Murayama, J. Polym. Sci., Polym. Phys. Ed., 13, 929 (1975).
9. N. Murayama, T. Oikawa, T. Kato, and K. Nakamura, J. Polym. Sci., Polym. Phys. Ed., 13, 1033 (1975).
10. R. E. Salomon, B. K. Oh, and M. M. Labes, J. Appl. Phys., 47, 1710 (1976).
11. R. E. Salomon, H. Lee, C. S. Bak, and M. M. Labes, J. Appl. Phys., 47, 4206 (1976).
12. K. Takahashi, H. Lee, R. E. Salomon, and M. M. Labes, J. Appl. Phys., 48, 4694 (1977).
13. T. Yagi, Polym. J., to be published.
14. C. W. Willson, III, J. Polym. Sci., 56, S12 (1962).
15. Du Pont, "Tefzel Technical Information".

16. M. Modena, C. Garbuglio, and M. Ragazzini, J. Polym. Sci., Part B, 10, 153 (1972).
17. K. S. Cole, and R. H. Cole, J. Chem. Phys., 9, 314 (1941).
18. T. Nakajima, and S. Saito, J. Polym. Sci., 31, 423 (1958).
19. H. Frölich, "Theory of Dielectrics", Oxford Univ. Press, 1958.
20. Y. Higashihata, T. Yagi and J. Sako, paper presented at the 26th Spring Meeting of the Japan Society of Applied Physics and the Related Societies, Tokyo, 1979.
21. M. Uchidoi, T. Iwamoto, K. Iwama and M. Tamura, paper presented at the 26th Spring Meeting of Japan Society of Applied Physics and the Related Societies, Tokyo, 1979.
22. T. Yamada, T. Ueda and T. Kitayama, paper presented at the 26th Spring Meeting of the Japan Society of Applied Physics and the Related Societies, Tokyo, 1979.
23. T. Yagi, Y. Higashihata, J. Sako and M. Tatamoto, paper presented at the 14th B Sectional Meeting, the 142 organic materials for Science of Information Committee, the Japan Society for the Promotion of Science, Tokyo, Japan, 1979.

GENERAL CONCLUSION

In chapter 1, polymerization of trifluoroethylene (TrFE), and copolymerizations of trifluoroethylene (TrFE) with vinylidene fluoride (VdF), tetrafluoroethylene (TFE), chlorotrifluoroethylene (CTFE) and hexafluoropropylene (HFP) were described. The polymerizations were carried out in bulk polymerization method at 22 °C using peroxide (3,5,6-trichloroperfluorohexanoyl peroxide) as an initiator. The monomer reactivity ratios (r_A and r_B) were obtained by use of the Fineman and Ross method: $r_A(\text{TrFE}) = 0.5$ and $r_B(\text{VdF}) = 0.7$ for TrFE-VdF copolymer system; $r_A(\text{TrFE}) = 0.75$ and $r_B(\text{TFE}) = 0.95$ for TrFE-TFE copolymer system; $r_A(\text{TrFE}) = 0.5$ and $r_B(\text{CTFE}) = 2.0$ for TrFE-CTFE copolymer system; and $r_A(\text{TrFE}) = 20.0$ and $r_B(\text{HFP}) = 0.01$ for TrFE-HFP copolymer system.

In chapter 2, microstructure of polytrifluoroethylene (PTrFE) chain was described. With the high-resolution fluorine-19 NMR study of PTrFE and the Monte Carlo simulation of the same polymerization system, the amount of the backward-added monomer-units and their distribution in polymer chain were estimated. The distribution is represented by the reactivity ratios of head- and tail-position of unsymmetrical monomer to each propagating polymer radicals. The assignment of absorption peaks in ^{19}F NMR spectrum of PTrFE was made on an empirical basis, and four possible microstructures, containing 5 carbon atoms along the polymer chain with $-\text{CF}_2-$ group as the central group, were figured out.

It was found that the percentage of backward-added TrFE-

monomer in PTrFE chain polymerized at 22 °C was 50%. Denoting CFH-position and CF₂-position in TrFE (CFH=CF₂) by B and A, respectively, the reactivity ratio of B and A to the ---CF₂· propagating radical was estimated as B/A = 1/0.75 and that to the ---CFH· radical was 1/1.33. These results indicated that the TrFE-monomer was polymerized at random state with respect to the head- and tail-positions: i.e., there was no difference between head- and tail-positions in the adding reaction.

In addition, poly(vinylidene fluoride) (PVdF) chain was also studied, in same manner as PTrFE. It was found that the percentage of backward-added VdF-monomer in the PVdF chain polymerized at 22°C was 7%, and the reactivity ratio of B (CH₂-position) and A (CF₂-position) to the ---CF₂· radical was estimated at 1/0.02 and that to the ---CH₂· was 1/0.05. These results indicated that the VdF-monomer reacted to radicals from the tail-position in high regularity independent of radical sorts.

In chapter 3, microstructures of TrFE-copolymers with VdF, TFE, CTFE, and HFP were described. The normalized monomer-diad and -triad fractions as a function of polymer composition were obtained by use of the comonomer sequence distribution theory. It was indicated that the TrFE-VdF, TrFE-TFE and TrFE-CTFE copolymer system were in random copolymer structures. The microstructures of the TrFE-VdF copolymers were also examined by use of ¹⁹F NMR. The peaks assignments of NMR spectra were made on an empirical basis. The normalized monomer-diad fractions were

also obtained from the analysis of NMR data, and they agreed well with calculated ones. This result indicated the accuracy of the monomer reactivity ratios. It was also found that the amount of head-to-tail (H-T) structure in the TrFE-TrFE sequence was very small, and that in VdF-VdF sequence was very large. However, the amount of H-T structure in TrFE-VdF or VdF-TrFE sequences was rather abundant. This result indicated that the TrFE-monomer reacted to the $---CH_2CF_2\cdot$ propagating radical from tail-position with a considerably high probability. In most cases, the TrFE monomer reacts to radicals with no distinct difference between head- and tail-position.

In chapter 4, crystallization behaviors of PTrFE were described. The electron micrograph showed the lamellar spherulites character. The equilibrium melting temperature of PTrFE was found to be 213°C from the plot of crystallization temperature versus observed melting temperature; i.e., the Hoffman and Weeks plot. The heat of fusion and the entropy of fusion were found to be 1300 kcal/mol and 2.75 eu/mol, respectively, from the analysis of polymer-diluent melting data. The surface free energy of lamella of PTrFE crystal was found to be about 1.2 kcal/mol from the melting temperature - lamellar thickness data obtained from the small angle x-ray diffraction method. The crystallization kinetic was studied by calorimetric method. The Avrami exponent was found to be about 2.7. The surface free energy of lamella, calculated by the crystallization rate,

was about 0.79 kcal/mol. This value seems to give fairly good agreement with the above result by the small angle x-ray diffraction method.

In chapter 5, the crystallization behaviors of TrFE-co-polymers with VdF, TFE, CTFE and HFP were described. Among these copolymers, the TrFE-VdF and TrFE-TFE copolymers system were in crystalline state in whole range of polymer composition, and these copolymer systems showed isomorphism replacement. Especially, the linear relationship between melting temperature and polymer composition was observed in the TrFE-TFE copolymer system. This isomorphism replacement was treated theoretically and agreed well with experimental result.

In the TrFE-VdF copolymers, the change of crystal form from α form to β form was observed between 85 to 90 mol% VdF content. Double endotherm peaks T_m and T_m' were observed in the DSC measurement of the TrFE-VdF copolymers. It was found that the upper peak was related to the crystal melting and the lower peak was the molecular motion in crystal region.

In chapter 6, the transition behavior of PTrFE was described. The studies were carried out (1) by mechanical relaxation measurements, dealing with the influence of crystallinity, molecular weight, cold drawing and copolymerization with VdF, and (2) by dielectric relaxation measurement at various frequencies up to 300 KHz, and in the temperature range of -150 to 100°C. In PTrFE, two transitions have been observed with peaks at 50°C

(designated as α) and -20°C (designated as β) by mechanical relaxation measurement at 35 Hz. It was found that the α -transition was related to micro-Brownian motion of main chain in amorphous region, and the β -transition was related to local molecular motion in both amorphous and crystalline regions.

In chapter 7, the transitions and relaxations of the TrFE-VdF copolymers were described. In the thermal expansion measurement of the 1 : 1 TrFE-VdF copolymer, two peaks were observed, indicating two glass-to-rubber transitions. These two transitions were also observed in mechanical relaxation study with peaks at 40°C (designated as β_1) and -20°C (designated as β_2), measured at 35 Hz. The β_1 -transition was tentatively assigned to the micro-Brownian motion of main chain in the amorphous region which was rich in TrFE-units; the β_2 -transition was assigned to the micro-Brownian motion of main chain in the amorphous region, rich in VdF-units.

In chapter 8, dielectric properties of TrFE-copolymers with VdF, TFE and CTFE were described. The dielectric constant ϵ' of the TrFE-VdF and TrFE-TFE copolymer did not change linearly with polymer composition, but took maximum at the middle point of polymer composition. Especially, the value of ϵ' of the 1 : 1 TrFE-VdF copolymer was about 15 (1 kHz and 22°C), and about 1.8 times larger than that of PVdF. PVdF has been distinguished among the crystalline polymers by a high ϵ' as $\epsilon' = 8.5$ (1 kHz and 22°C). The 1 : 1 TrFE-VdF copolymer

electret exhibited very high piezoelectricity. The d_{31} constant of this material is 28×10^{-12} C/N, being nearly equal to that of the β -form PVdF electret. At present time, the β -form PVdF exhibits the highest value of piezoelectric constant as the polymeric material.

Further works are needed to understand the nature of the piezoelectricity of the TrFE-VdF copolymer. It is generally said that the values of piezoelectricity depend greatly on conditions of preparation of films and conditions of measurement. For the practical application of this copolymer electret, it is important to examine reproducibility and long-time durability. The study on the temperature dependence of the piezoelectric property is also important in both fundamental and practical aspects. In addition, the examination of the pyroelectricity of the TrFE-VdF copolymer must be carried out.

LIST OF PAPERS

- PAPER 1 "Studies on Microstructure of Poly(trifluoroethylene) Chain by Fluorine-19 NMR and Monte Carlo Simulation", Polym. J., 11, 353 (1979).
- PAPER 2 "A Fluorine-19 NMR Study of the Microstructure of Vinylidene Fluoride-Trifluoroethylene Copolymers", Polym. J., 11, 429 (1979); Co-author: Masayoshi Tatemoto.
- PAPER 3 "Transitions and Relaxations in Poly(trifluoroethylene)", Polym. J., 11, No. 9, (1979), in press.
- PAPER 4 "Transition Behavior and Dielectric Properties in Trifluoroethylene and Vinylidene Fluoride Copolymers", Submitted to Polym. J.; Co-author: Masayoshi Tatemoto and Junichi Sako.
- PAPER 5 "Crystallization Behavior of Poly(trifluoroethylene)", Submitted to Polym. J..
- PAPER 6 "Isomorphism in Trifluoroethylene Copolymers", Submitted to Polym. J.; Co-author Masayoshi Tatemoto.

COMPARISON OF CHAPTER WITH PAPER

CHAPTER 1	PAPER 1, PAPER 2 AND PAPER 6
CHAPTER 2	PAPER 1
CHAPTER 3	PAPER 2
CHAPTER 4	PAPER 5
CHAPTER 5	PAPER 4 AND PAPER 6
CHAPTER 6	PAPER 3
CHAPTER 7	PAPER 4
CHAPTER 8	PAPER 4

LIST OF PRESENTATIONS

1. "Synthesis and Characterization of Trifluoroethylene - Vinylidene Fluoride Copolymer", the 8th International Symposium on Fluorine Chemistry, Kyoto, Japan, August, 1976; Co-worker: Junichi Sako and Masayoshi Tatamoto.
2. "Dielectric Properties Trifluoroethylene-Vinylidene Fluoride Copolymers", the 8th International Symposium on Fluorine Chemistry, Kyoto, Japan, August, 1976; Co-worker: Junichi Sako and Masayoshi Tatamoto.
3. "Structure and Properties of Vinylidene Fluoride - Trifluoroethylene Copolymers", the 14th B Sectional Meeting, the 142 organic Materials Committee for Science of Information, the Japan Society for the Promotion of Science, Tokyo, Japan, May, 1979; Co-worker: Yoshihide Higashihata, Junichi Sako and Masayoshi Tatamoto.
4. "Crystallization Behavior of Trifluoroethylene Copolymers", the 9th International Symposium on Fluorine Chemistry, Avignon, France, September, 1979.

ACKNOWLEDGEMENT

u
The present thesis is based on the studies carried out by the author at the Applications Research Department, Chemical Division, Daikin Kogyo Co., Ltd., Osaka, Japan, from 1975 to 1979, under the auspices of Professor Akio Nakajima, the Department of Polymer Science, Faculty of Engineering, Kyoto University.

The author wishes to express his sincere gratitude to Professor Akio Nakajima, Dr. Yoshihiko Kubouchi, Daikin Kogyo Co., Ltd., and Dr. Yutaka Kometani, Daikin Kogyo Co., Ltd., for their invaluable guidance and suggestions with constant encouragement.

He wishes to express his sincere thanks to Mr. Masayoshi Tatemoto, Daikin Kogyo Co., Ltd., for his valuable suggestions, comments and co-operation. He also wants to express his thanks to Mr. Kimio Kubota, Mr. Akira Yamada, Mr. Takaomi Satokawa, Mr. Syun Koizumi, Mr. Junichi Sako, Mr. Syoji Kawachi, Mr. Shinichi Nakagawa and Takuro Kawamura, for thier valuable suggestions and comments. He also wants to express to his gratitude to Professor Naokazu Koizumi, the Chemical Research Institute, Kyoto University, for his valuable suggestions and comments on chapters 6, 7 and 8.

Thanks are also due to Messr. Masahiro Okuda,

Sada-atsu Yamaguchi, Kiyohiko Ihara and Yoshihide Higashihata,
and to other members of the Applications Research Department
and the Research Department, Daikin Kogyo Co., Ltd., for
their valuable discussions and co-operations.

